

ASPECTS OF PHASE SEPARATION IN
AN EXPERIMENTAL MIXER-SETTLER
USING TWO SOLVENT EXTRACTION SYSTEMS

By

NORBERT L. ECKERT

B.A.Sc, The University of British Columbia, 1984

A THESIS SUBMITTED IN PARTIAL FULFILLMENT OF
THE REQUIREMENTS FOR THE DEGREE OF
MASTER OF APPLIED SCIENCE

in

THE FACULTY OF GRADUATE STUDIES
(Department of Chemical Engineering)

We accept this thesis as conforming
to the required standard

THE UNIVERSITY OF BRITISH COLUMBIA

1987

© Norbert L. Eckert, 1987

In presenting this thesis in partial fulfilment of the requirements for an advanced degree at the University of British Columbia, I agree that the Library shall make it freely available for reference and study. I further agree that permission for extensive copying of this thesis for scholarly purposes may be granted by the head of my department or by his or her representatives. It is understood that copying or publication of this thesis for financial gain shall not be allowed without my written permission.

Department of Chemical Engineering

The University of British Columbia
1956 Main Mall
Vancouver, Canada
V6T 1Y3

Date Oct 14 / 1987

ABSTRACT

An experimental investigation was undertaken to study the factors affecting phase separation in a specially constructed, laboratory scale mixer-settler. Two phase systems were used:

1. A laboratory prepared HSLIX64N-copper phase system, similar to that used in commercial copper solvent extraction processes.
2. A phase system obtained directly from the uranium extraction circuit of the Key Lake Mining Corporation, Sask., millsite.

A settler scale-up criterion relating dispersion band thickness to specific settler flow of dispersed phase, was found to have considerable merit. Besides being dependent on specific settler flow, the dispersion band thickness was found to be a function of the phase ratio (for system 2 only), dispersion introduction level (for system 2 only), and temperature. Mixing intensity had no appreciable effect with either system.

Microscopic examination of the dispersion produced with system 2 revealed the existence of double dispersions; that is, drops within drops.

A photomicroscopic technique was used to undertake a drop size investigation of the dispersion produced with system 2. Drop size was found to be independent of dispersion throughput, a weak function of impellor speed and a relatively strong function of

the phase ratio.

With the exception of organic continuous operation with system 1, it was possible, based on the holdup and drop size profile within the dispersion band, to distinguish two horizontal sublayers within the dispersion band. In the "even concentration sublayer", comprising the majority of the dispersion band, the holdup and average drop size is nearly constant throughout. In the "dense concentration sublayer", both the holdup and the average drop size increase sharply as the coalescence front is approached.

Table of Contents

ABSTRACT	ii
LIST OF TABLES	vii
LIST OF FIGURES	viii
ACKNOWLEDGEMENT	xi
CHAPTER 1 - INTRODUCTION	1
1.1 General	1
1.2 Research objectives	4
CHAPTER 2 - BACKGROUND	7
2.1 General settler operation	7
2.2 Settler scale up	10
2.3 Separation mechanism in a deep layer settler	14
2.4 Entrainment and phase continuity	18
2.5 Effect of mixer operation on settler performance	21
2.6 Temperature	23
2.7 Surface effects	24
2.8 Effect of mass transfer on coalescence	25
2.9 Installation of horizontal plates	26
CHAPTER 3 - DESCRIPTION OF TYPICAL PROCESSES	28
3.1 Introduction	28
3.2 Description of KLMC solvent extraction process	28
3.3 Description of NCCM copper extraction plant	37
CHAPTER 4 - EXPERIMENTAL PHASE SYSTEMS	42
CHAPTER 5 - EXPERIMENTAL APPARATUS	43
5.1 Introduction	43
5.2 Mixer-settler	43
5.3 Interphase regulator	53
5.4 Storage vessels	53
5.5 Pumps	55

5.6 Temperature regulation	55
5.7 Flow metering and regulation	56
5.8 Panel board	57
5.9 Safety considerations	57
CHAPTER 6 - EXPERIMENTAL PROCEDURE	59
6.1 Properties of the phases	59
6.2 Mixer-settler start-up procedure	59
6.3 Time for dispersion band to reach steady state	62
6.4 Sampling for dispersion band holdup	65
6.5 Determination of dispersion drop size	66
6.6 Orientation of microscope	69
CHAPTER 7 - RESULTS AND DISCUSSION	72
7.1 General observations of mixer-settler operation	72
7.1.1 Dispersion band appearance	72
7.1.2 Crud	76
7.1.3 Operation at desired phase continuity	78
7.1.4 Drift in physical behavior of phases	80
7.1.5 Effect of introduction level on ΔH	81
7.2 Q_d/A - ΔH relationship	88
7.2.1 Case 1 - HSLIX64N-copper system (org. cont.)	89
7.2.2 Case 2 - HSLIX64N-copper system (org. cont.)	93
7.2.3 Case 3 - Key Lake system (org. cont.)	95
7.2.4 Q_d/A - ΔH data at Key Lake, Sask.	97
7.3 Effect of operating temperature	99
7.4 Effect of impellor speed	101
7.5 Dispersion band holdup profiles	105
7.6 Dispersion drop size distribution	110
7.6.1 General observations	110
7.6.2 Double and triple dispersions	114
7.6.3 Effect of O/A ratio and Q_d on mixer drop size	118

7.6.4 Effect of impellor speed on mean drop size	122
7.6.5 Drop size profile within dispersion band	124
7.7 Theoretical terminal velocity	129
CHAPTER 8 - SUMMARY AND CONCLUSIONS	136
NOMENCLATURE	141
REFERENCES	143
APPENDIX I-PLOTS OF CHAPTER 7	148
APPENDIX II-CHARACTERISTIC CURVE STATISTICAL ANALYSIS	166
APPENDIX III - ERROR ANALYSIS; GENERAL COMMENTS	177

LIST OF TABLES

TABLE	DESCRIPTION	PAGE
1	Key Lake pregnant solution composition.	30
2	Key Lake typical product analysis.	35
3	Dimensions of NCCM solvent extraction process mixer-settlers.	41
4	Summary of equipment specifications and ranges in capability.	45
5	Physical properties of the experimental phases.	60
6	Effect of dispersion introduction level on dispersion band thickness (system: HSLIX64N-copper; temperature: 24°C).	83
7	Effect of dispersion introduction level on dispersion band thickness (system: Key Lake; temperature: 35°C).	84

LIST OF FIGURES

FIG.	DESCRIPTION	PAGE
1	Wedge and deep-layer dispersion bands.	8
2	Theoretical dispersion band holdup profiles.	15
3	Flow diagram of KLMC solvent extraction process.	31
4	KLMC mixer-settler design and dimensions.	36
5	Flow diagram of NCCM solvent extraction process.	38
6	Schematic arrangement of experimental apparatus.	44
7	Photograph of mixer-settler Gore-tex seal.	47
8	Dimensions of experimental mixer-settler.	48
9	Impellor geometry.	50
10	Photograph of mixing chamber.	51
11	Interphase regulator.	54
12	Photograph of panel board.	58
13	Photograph of mixer-settler operation with Key Lake phase system.	63
14	Time for dispersion band thickness to achieve steady-state after introduction of dispersion into settler (HSLIX64N-copper phase system).	64
15	Design of glass-walled cell used for determination of dispersion drop size.	67
16	Photograph of arrangement of microscope and cell.	71
17	Effect of dispersion introduction level for Key Lake phase system for cases identified in Table 7.	85

18	Dispersion band thickness versus specific settler flow of dispersed phase (effect of O/A ratio and settler area), HSLIX64N-copper system, organic continuous operation, 24°C, 300rpm.	90
19	Dispersion band thickness versus specific settler flow of dispersed phase (effect of O/A ratio and settler area), HSLIX64N-copper system, aqueous continuous operation, 24°C, 300rpm.	94
20	Dispersion band thickness versus specific settler flow of dispersed phase (effect of O/A ratio and settler area), Key Lake phase system, organic continuous operation, 35°C, 300rpm.	96
21	Dispersion band thickness versus specific settler flow of dispersed phase (effect of operating temperature), HSLIX64N-copper phase system, organic continuous operation, 300rpm.	100
22	Dispersion band thickness versus specific settler flow of dispersed phase (effect of impellor speed), HSLIX64N-copper phase system, organic continuous operation, 24°C.	102
23	Dispersion band thickness versus specific settler flow of dispersed phase (effect of impellor speed), HSLIX64N-copper phase system, aqueous continuous operation, 24°C.	103
24	Dispersion band thickness versus specific settler flow of dispersed phase (effect of impellor speed), Key Lake phase system, organic continuous operation, 35°C.	104
25	Dispersion band holdup profiles, HSLIX64N-copper phase system, organic continuous operation, 24°C, 300rpm.	106
26	Holdup profiles within dispersion band, HSLIX64N-copper system, aqueous continuous operation, 24°C, 300rpm.	107
27	Holdup profiles within dispersion band, Key Lake phase system, organic continuous operation, 35°C, 300rpm.	108

28	Change in arithmetic mean drop size of dispersion sample with time after withdrawal from mixer, Key Lake phase system, organic continuous operation, 35°C, 300rpm.	113
29	Photograph of double dispersion sample withdrawn from settler inlet, Key Lake phase system, organic continuous operation, O/A=1.5, 35°C, 300rpm.	115
30	Effect of O/A ratio and dispersed phase flowrate on arithmetic mean drop diameter at mixer overflow, Key Lake phase system, organic continuous operation, 35°C, 300rpm.	119
31	Photographs showing effect of O/A ratio on drop size of dispersion withdrawn from mixer overflow, Key Lake phase system, organic continuous operation, 35°C. (a) O/A=0.67, (b) O/A=3.0.	121
32	Effect of impellor speed on arithmetic mean drop diameter at mixer overflow, Key Lake phase system, organic continuous operation, 35°C.	123
33	Drop size profile within dispersion band for O/A=0.67, Key Lake phase system, organic continuous operation, 35°C, 300rpm.	125
34	Drop size profile within dispersion band for O/A=1.5, Key Lake phase system, organic continuous operation, 35°C, 300rpm.	126
35	Drop size profile within dispersion band for O/A=3.0, Key Lake phase system, organic continuous operation, 35°C.	127
36	Theoretical terminal drop velocity versus drop diameter for different dispersion concentrations, HSLIX64N-copper phase system, organic continuous operation, 24°C.	132
37	Theoretical terminal drop velocity versus drop diameter for different dispersion concentrations, HSLIX64N-copper phase system, aqueous continuous operation, 24°C.	133
38	Theoretical terminal drop velocity versus drop diameter for different dispersion concentrations, Key Lake phase system, organic continuous operation, 35°C.	134

ACKNOWLEDGEMENT

I would like to express my thanks to Dr. Lynton Gormely for his guidance and patience throughout the course of this work

I would also like to thank Key Lake Mining Corporation for their contribution of liquid samples for my experiments.

Financial support from the Natural Sciences and Engineering Research council is gratefully acknowledged.

CHAPTER 1 - INTRODUCTION

1.1 GENERAL

Solvent extraction is a process which has achieved widespread application in the recovery of metals from leached ores and concentrates. The process consists of an extraction section and a stripping section, with additional operations being required in specific circumstances.

The purpose of the extraction section is to purify and concentrate the metal of interest by selective extraction. The aqueous solution containing the metal of interest is intimately contacted with an immiscible organic phase containing an organic extraction reagent. The extraction reagent reacts with the metal of interest, selectively transferring it across the aqueous/organic interface into the organic phase. Undesirable constituents are left behind.

An effective organic extraction reagent is now known for virtually every metal.

The purpose of the stripping section is to transfer the extracted metal into a second aqueous phase at a concentration where further processing is economical. The desired metal is now in an aqueous phase at a higher purity and at a higher concentration than it was in the original aqueous solution. The metal can then be recovered from solution by methods such as electrolysis or precipitation.

A full description of two typical solvent extraction processes is provided in Chapter 3.

In the hydrometallurgical industries, mixer-settlers are generally used for contacting and separating the immiscible liquid phases. Mixer-settlers consist of a mixing chamber and a settling chamber. The function of the mixer is to disperse the two entering phases by means of an agitator, thus promoting mass transfer by creation of a large interfacial area (typically $500\text{--}1000\text{ m}^2/\text{m}^3$ of mixer (Hanson, 1983)), and to provide the residence time required for the desired approach to equilibrium. The dispersion generated in the mixer then enters the settling chamber and disengages by means of a gravitational settling/coalescence mechanism. The settler typically constitutes 80-90% of the total mixer-settler volume.

Due to the reversibility of the organo-metallic reactions, a cascade of several mixer-settlers providing countercurrent contacting of the phases is generally required in order to achieve the desired extraction.

In the hydrometallurgical industries, mixer-settlers are generally chosen over other contacting devices (such as column extractors) due to the following characteristics:

1. Mixer-settlers have the capacity for handling large liquid throughputs, such as those found in hydrometallurgical processes. Mixer settlers can typically handle flows up to $800\text{ m}^3/\text{hr}$ compared to a maximum of $100\text{ m}^3/\text{hr}$ for columns.

2. A close approach to equilibrium between phases can be expected in mixer-settlers, reducing the number of stages required.
3. Mixer-settlers are rugged and are relatively easy to construct and operate. Column fabrication involves more complex mechanical engineering techniques.
4. Liquid systems containing some suspended solids, such as those commonly processed in the hydrometallurgical industries, can be treated in mixer-settlers, since shut down for solids removal is relatively simple or even unnecessary (At Key Lake solids are removed during operation by 'vacuuming' them off). Solids are difficult to handle with columns.
5. Phases can be easily recirculated from the settler to attain the desired phase ratio in the mixer.
6. Process changes are possible at any time by adding or removing sidestreams.
7. Equilibria in these systems are such that relatively few stages are required, with significant mass transfer in each stage. Each stage can therefore afford to be more capital intensive.

There is considerable incentive for reducing the settler size required to achieve phase separation. Increased size represents higher capital cost for equipment, increased plant area, and higher organic inventory (reagents are expensive so that the cost of increased organic inventory can be high). Nevertheless, settler design procedures have frequently proven

to be unreliable, resulting in the use of large safety factors, and consequent settler overdesign.

The performance of a settler is influenced by a variety of parameters including throughput, temperature, phase flow ratios and continuity, and mixing conditions. Furthermore chemical composition influences the settler performance and thus different systems may behave differently.

A host of sophistications such as flow distributors and baffles have been introduced into some designs to enhance performance.

In order to improve the reliability of settler design procedures so that equipment can be confidently and conservatively designed, without the use of excessive safety factors, the effects of these parameters should be understood. Also, inherent in accurate design is an understanding of the basic mechanism of phase separation in the settler. It is the aim of this thesis to develop an understanding of these factors affecting settler performance and to investigate the separation mechanism.

1.2 RESEARCH OBJECTIVES

This project involved the experimental study of phase separation in a laboratory scale mixer-settler. The following areas were investigated:

1. The effect of settler throughput on dispersion band

thickness. The data obtained was compared with previously established scale-up criteria to confirm or question their validity. A comparison was made between the laboratory settler performance and the reportedly enhanced performance obtained with the KREBS designed mixer-settlers used at the Key Lake, Saskatchewan, uranium extraction plant. Experimentation with liquid phases obtained from Key Lake facilitated this direct comparison.

2. The effect of dispersion type (organic or aqueous continuous) and the organic to aqueous ratio on settler performance.
3. The effect of temperature.
4. The effect of mixing intensity on phase separation.
5. The effect of settler inlet configuration; i.e., method of introduction of dispersion into the settler.
6. The mechanism of phase separation. This was studied through a detailed examination of the dispersion band structure, as follows:
 - visual and photographic examination of the dispersion band including an investigation of the dispersion drop size distribution.
 - sampling to determine the organic to aqueous ratio at different points in the dispersion band.
 - observation of the flow pattern in the dispersion band.

Based on this examination, the applicability of the separation mechanism proposed by Barnea and Mizrahi (1975) to the two industrially relevant systems investigated in this study could be assessed.

7. A comparison of the phase separation behavior of the 2 experimental phase systems.

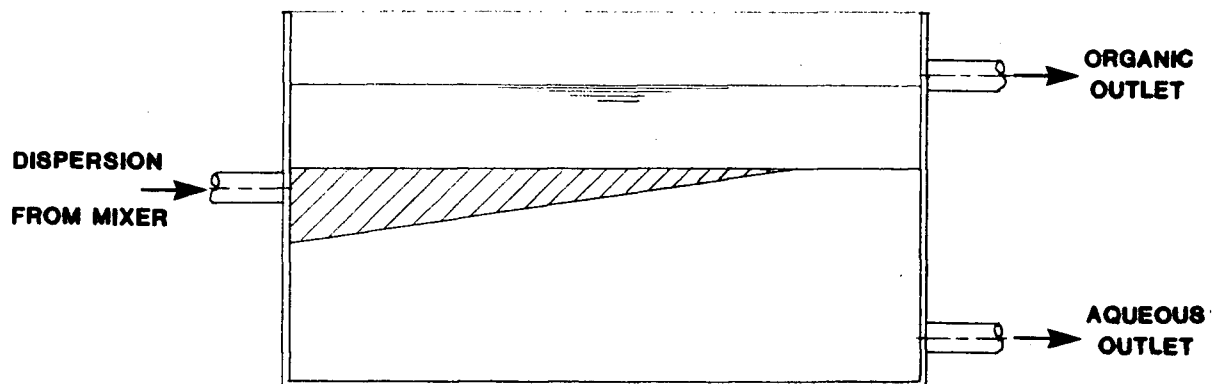
CHAPTER 2 - BACKGROUND

2.1 GENERAL SETTLER OPERATION

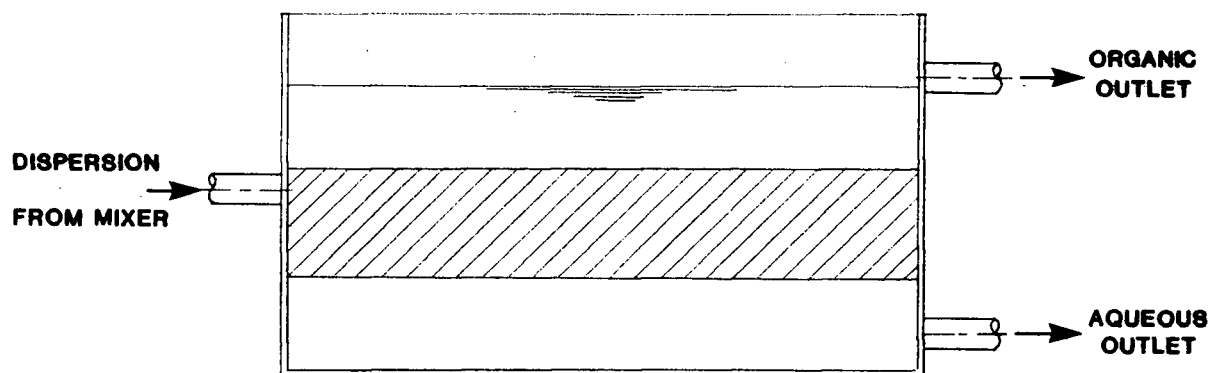
The product of the mixer consists of droplets of one liquid phase dispersed in a continuum of the other. Upon entering the settler, this dispersion behaves as a third liquid phase of a density intermediate to the two separated bulk phases. Consequently it spreads out horizontally in the settler, between the two bulk phases, producing a "dispersion band". Depending on the flowrate of dispersion to the settler, the dispersion band may take either of two forms.

When the flow rate of dispersion to the settler is relatively low, the time required for phase separation is less than the time required for horizontal spreading and the dispersion band does not extend over the entire length of the settler. The dispersion band adopts the form of a wedge (Fig. 1(a)). As the settler throughput is increased, the length of this wedge increases until the dispersion reaches the end of the settler. Beyond this point, the settler is said to be operating with a "deep-layer" dispersion band of near uniform thickness (Fig. 1(b)). Further increases in settler throughput result in an increasing thickness of this layer.

With increasing settler loading the thickness of the dispersion band eventually increases to the point where it exits through either or both the organic overflow weir and the



a) Wedge-shaped band



b) Deep-layer band

Figure 1. Wedge and deep-layer dispersion bands.

aqueous discharge port. This undesirable situation is known as flooding. Flooding conditions in a deep-layer liquid/liquid settler were studied by Barnea (1978).

The interface between the dispersion band and the separated dispersed phase is known as the "coalescence front" or active interface, since the droplets must coalesce in order to join the bulk homophase. The interface separating the dispersion band from the bulk continuous phase is referred to as the "settling front". Since drainage of the continuous phase from the dispersion band rather than coalescence occurs here, this boundary may also be called the "passive interface".

Dilute dispersions (those with a dispersed phase volume fraction less than approximately 15%), generally do not form dispersion bands. Here, settling of liquid drops constitutes the separation mechanism, whereas in the case of a dispersion band, phase separation is limited by interdroplet coalescence.

Until recently, operation of settlers in the wedge-shaped dispersion band mode was favored by some investigators (Jeffreys, Davies, Pitt, 1970). It was reasoned that sudden changes in operating conditions (a sharp increase in throughput, for example) would not be as likely to result in flooding because of the greater excess settler capacity available. It is generally accepted today, however, that operation in this mode represents a case of severe settler overdesign. This involves a penalty due to increased construction costs and due to increased organic inventory

requirements. Provided the dispersion band depth is not too great, it is possible to operate deep-layer settlers and still provide a sufficient safety margin to ensure that flooding can not occur under usual operating circumstances.

Despite the advantages of operating with a deep-layer dispersion band, some industrial settlers do operate in the wedge-shaped mode. For example, the settlers used in the extraction circuit of the world's largest copper extraction plant, at Chingola, Zambia, operate with a wedge-shaped band occupying only one half to two thirds of the settler length (Orjans et al., 1977). The overdesign of these settlers is a result of uncertainty regarding the reliability of scale-up methods and illustrates the need for scale-up criteria which can be used with confidence.

2.2 SETTLER SCALE-UP

To maintain reasonable capital cost, practical settler design should be based on use of a deep-layer dispersion band. Therefore this discussion will be restricted to scale-up procedures applicable to this mode of operation.

For a deep-layer settler, the thickness of the dispersion band is a measure of the approach to flooding and can therefore be used to characterize the flow capacity of the settler.

Ryon, Daley and Lowrie (1959) working with the Dapex process for uranium extraction from sulfuric acid leach

solution¹, observed that a straight line was produced if this thickness was plotted against the dispersed phase throughput per unit horizontal cross-sectional area on log-log coordinates. Therefore, the following relationship was proposed:

$$\Delta H = k(Q_d/A)^y \quad (1)$$

The authors' data gave the value of y as 2.5 and the correlation was found to apply over a scale-up ratio of 1000:1. The dispersion band thickness was found to be dependent only on the flow of dispersed phase per unit area, and not on that of the continuous phase. Furthermore, the thickness was observed to be independent of the power input per unit mixer volume.

Some investigators dispute Ryon's contention that the O/A ratio is not important in determining ΔH (Mizrahi and Barnea, 1973). Gondo and Kusonoki (1969) obtained a correlation of the following form:

$$\Delta H = \phi^{4.9} N^{2.8} (Q/A)^{3.1} \quad (2)$$

This correlation indicates that the phase ratio and mixer power do affect settler capacity and is therefore in disagreement with Ryon. Other experimental data confirms the importance of the phase ratio (Mizrahi and Barnea, 1975, Part IV). However, recent pilot plant studies for the copper tailings leach plant at Chingola, Zambia (Orjans et al., 1977) indicate that dispersion band depth depends only on the flow of dispersed phase, thus lending some support to Ryon's contention.

¹ (using di(2-ethyl-hexyl) phosphoric acid dissolved in kerosene modified with tributyl phosphate)

The effect of power input per unit mixer volume is also unclear. For some systems, the dispersion band thickness has been shown to increase with impellor speed. For others however, including that tested by Ryon, experiments indicate that dispersion band thickness may stay relatively constant with increasing impellor speed over a wide range of operating values. For systems used in uranium extraction, phase separation is reported to be uninfluenced by the intensity or the duration of the mixing (Merritt, 1971).

Equation (1) remains the most commonly used correlation for scale-up of settlers. The value of the exponent y is typically in the range 1-7 depending on the phase system. However, it is generally acknowledged that the value of the constants k and y may change with phase ratio or mixing intensity as well as phase continuity and temperature, and that this should be investigated experimentally for each phase system.

As an estimate for sizing cylindrical horizontal settlers, with a length/diameter ratio of 4, Treybal (1963) recommends the following rule of thumb:

$$D = 8.4(Q_c + Q_d)^{0.5} \quad (3)$$

where Q_c and Q_d are given in m^3/s

and D is given in metres.

If the horizontal cross-sectional area (A) of the settler is approximated as $D(4D)$, this equation can be modified to give:

$$(Q_c + Q_d)/A = 0.0035 \text{ m}^3/\text{m}^2/\text{s} = 12.6 \text{ m}^3/\text{m}^2/\text{hr} \quad (4)$$

Thus, equation (3), in effect, specifies a specific settler flow based on total dispersion flow of $12.6 \text{ m}^3/\text{m}^2/\text{hr}$ for this settler geometry. Equation (3) is intended only for a preliminary estimate in the absence of any actual operating data for the system of interest.

A rule of thumb of $1\text{--}1.5 \text{ USGPM}/\text{ft}^2$ ($2.5\text{--}3.7 \text{ m}^3/\text{m}^2/\text{hr}$) is used in the copper industry. This lower specific flow, compared to that recommended by Treybal would be partly explained by the different settler geometries to which they pertain. In the copper industry, settlers are rectangular and large in area ($100 - 400 \text{ m}^2$, typically) and relatively shallow (less than 1.2 m). Since the horizontal, cylindrical settler geometry specified by Treybal would have a greater depth for a given area than a typical settler used in the copper industry, the higher settler loading recommended by Treybal would be expected.

Correlations between a standardized separation time obtained from batch separation tests and the dispersion throughput per unit settler area in a continuous settler have been proposed by several investigators (Barnea and Mizrahi, 1975, part IV), (Golob and Modic, 1977). However, such procedures, using batch separation results have led to large errors when applied to the design of continuous deep-layer settlers. Despite the inadequacies of such methods, they can be useful for obtaining a general impression of the settling behavior of various systems prior to conducting continuous flow

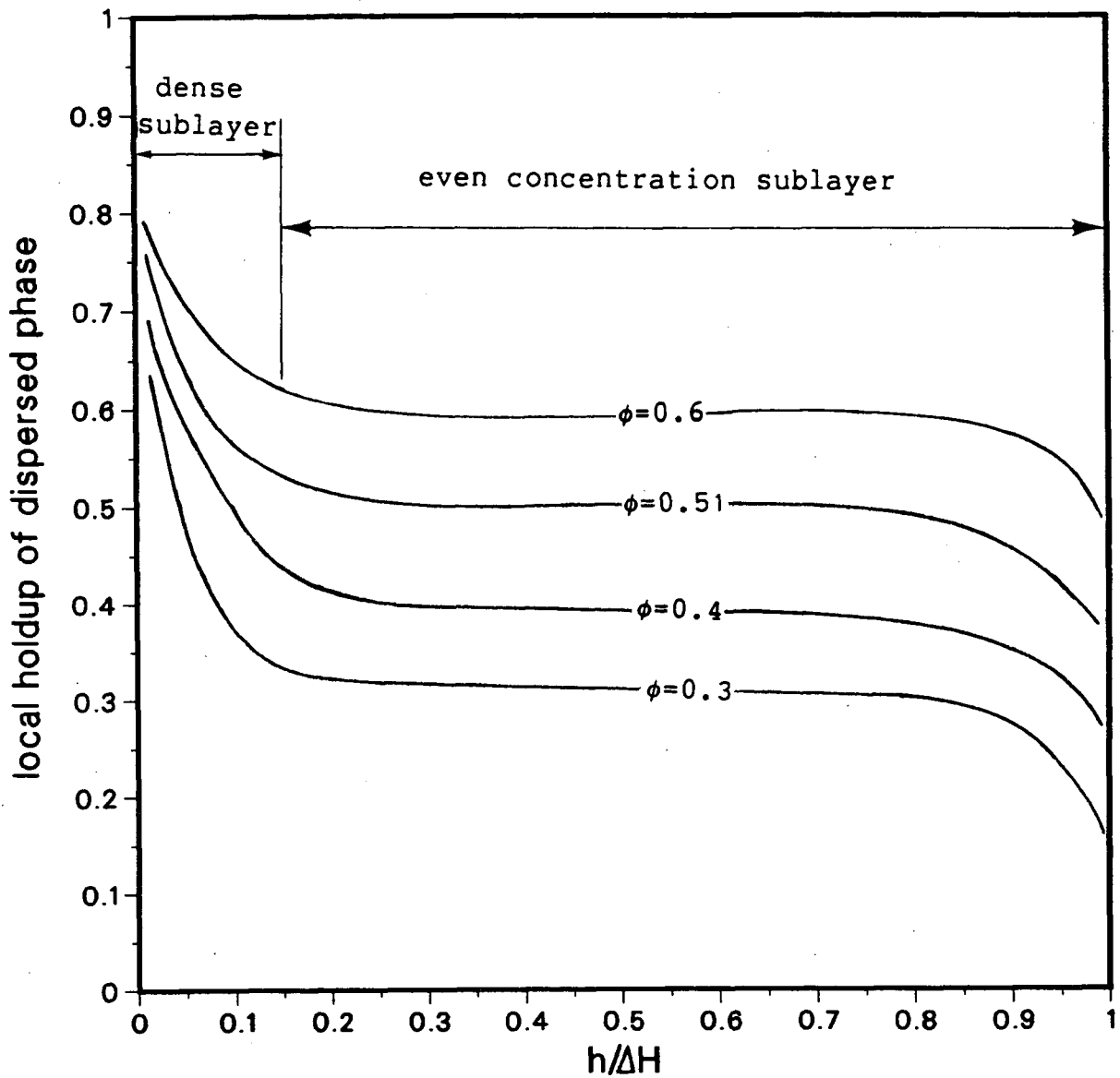
tests.

2.3 SEPARATION MECHANISM IN A DEEP LAYER SETTLER

Phase separation in a deep-layer settler involves both settling and coalescence phenomena. A general description of the separation mechanism in a deep-layer settler was presented in a series of papers by Barnea and Mizrahi (1975), based on an experimental investigation using a phase system relevant to the industrial process for the extraction of magnesium bromide and chloride from Dead Sea end brine using butanol (1975). Observations led to a proposed qualitative model for the separation process.

Barnea and Mizrahi sampled the dispersion band at various distances from the coalescence front to determine the local volume fraction of dispersed phase (holdup). It was found that, for constant settler feed composition, plotting holdup against the dimensionless vertical location in the dispersion band (obtained by dividing the actual distance from the coalescence front by the dispersion band thickness) gave a constant curve for any dispersion thickness (Fig. 2). Based on this observation, two main sublayers were identified within the dispersion band.

The "dense sublayer", in the vicinity of the coalescence front typically occupied 10 to 20% of the total volume of the dispersion band. It was structured like foam and was characterized by a hold-up level much higher than that of the



* from Barnea and Mizrahi, 1975, Part I.

Figure 2. Theoretical dispersion band holdup profiles.

settler feed. The holdup was unity at the coalescence front and decreased sharply with increasing distance from the coalescence front.

The "even concentration sublayer" comprised the remainder of the dispersion band. The holdup in this sublayer was nearly constant at a level slightly below that of the feed, decreasing slightly and nearly linearly towards the settling front where it dropped sharply to zero.

Investigation of both continuous and batch separations and observation of the flow pattern of the continuous and dispersed phases within the dispersion band led to the development of a simplified picture of phase separation in mixer-settlers and of the roles played by the two sublayers in the process.

The dense sublayer is characterized by a high rate of interdroplet coalescence and consequently increasing average drop diameters as the coalescence front is approached. Near the coalescence front, significant drop deformation is noted. It was demonstrated in batch tests that the rate of coalescence at the coalescence front itself is proportional to the effective weight of droplets in the dense sublayer. Pressure transmission between layers of drops increases the force available for "squeezing out" the thin film of continuous phase separating the layer of drops at the coalescence front from the separated bulk phase. Any change in settler feed rate results in an adjustment of dense sublayer thickness and holdup gradient and the establishment of a new equilibrium, so that the effective

dense sublayer weight is changed in direct proportion to the feed rate and subsequently changing the rate of coalescence at the interface. Thus, the progression of droplets in the sublayer is dependent on the occurrence of a coalescence event and the flow is essentially unidirectional (plug flow).

In contrast to the dense sublayer, it was observed that the droplets within the even concentration layer moved in different directions. Drops whose hindered settling velocity was less than that of the draining continuous phase were entrained towards the settling front. After a period of time these droplets were observed to reverse their direction. This observation was ascribed to a collision/coalescence occurrence with another droplet, producing a drop whose diameter is greater than the critical diameter necessary for flow in the direction of the coalescence front. From these observations it was postulated that the even concentration sublayer adjusts to the thickness which will provide the residence time which allows the smallest droplets to grow to the critical size by this collision/coalescence mechanism.

Since the even concentration sublayer occupies most of the dispersion band, Barnea and Mizrahi considered it to be the rate determining sublayer. It was therefore concluded that the capacity of a deep layer settler is limited by hindered settling and coalescence in the even concentration layer rather than coalescence at the coalescence front.

This model suggests that the capacity of a settler could be increased by production of a dispersion having a relatively narrow size distribution curve, thus eliminating the "tail" commonly exhibited by drop size distributions.

2.4 ENTRAINMENT AND PHASE CONTINUITY

If agitation is stopped during batch operation, it is often found that disengagement of the immiscible phases occurs in two stages. In the first stage (primary break), the vast majority of the dispersion coalesces and separates very rapidly. However, the continuous phase generally remains clouded to some degree by very fine droplets of the dispersed phase. There may be a much lesser quantity of continuous phase droplets in the separated dispersed phase as well. Separation of these fine droplets (secondary break) occurs very slowly.

An analogous situation exists for a continuously operated mixer-settler. The "primary break" is achieved in the dispersion band, leaving fine droplets suspended in the separated continuous phase.

As indicated by the scale-up correlations of section 2.2, settlers are designed to facilitate the occurrence of only the primary break since it is impractical to utilize settlers large enough to enable the secondary break to occur completely. Consequently, suspended droplets exit the settler and are referred to as entrainment. In designing mixer-settlers, it is important to consider the implications a design may have with

regards to entrainment. Entrainment can constitute a significant source of solvent loss or can result in contamination of process streams. If excessive, it can become a critical factor in the economic feasibility of a process. As such, measures must be taken to minimize it.

It is generally accepted that entrainment is primarily generated as a result of the formation of fine droplets in the mixer. It can typically be minimized by the avoidance of impellers which produce high shear rates (small diameters and high speeds). A second factor, of much lesser importance, is the reported formation of very fine droplets of either phase during drop-drop coalescence and coalescences at the phase boundary or at solid surfaces (Davies et al, 1970). This mechanism could partially account for the fact that there is a small amount of entrainment of continuous phase in the separated dispersed phase leaving most commercial settlers.

Air ingestion into the mixer has also been observed to increase entrainment (Orjans et al., 1977).

Through a suitable mixer start-up procedure, it is generally possible to disperse either of the two contacting phases within a certain range of flow ratios. This range is referred to as the ambivalence region and typically lies in the O/A range of $1/3$ to $3/1$ (McClary and Mansoori, 1978). Although aqueous continuous operation will generally result in narrower dispersion bands (Orjans et al., 1977), (Henkel, Lott et al., 1972), industrial mixer-settlers are generally operated organic

continuous. This is done since organic continuous operation gives the lowest organic entrainment and loss of organic is the dominant consideration. Entrainment of aqueous phase is usually not as serious.

Fluctuations in flow rates or changes in the physical properties of the phases (viscosity, density, interfacial tension) can result in phase inversion. The increase in organic entrainment which may result makes this an undesirable phenomenon.

Although it may be difficult to visually determine which phase is continuous, phase continuity can be established by a conductivity probe since an aqueous continuous dispersion is conductive while an organic continuous one is not.

Orjans et al. (1977) utilizing N'Changa pilot plant studies, found that for organic continuous operation, entrainment of aqueous phase may increase dramatically if a certain critical linear velocity of the organic phase above the dispersion band is exceeded. Therefore, in order to minimize this velocity, for a given settler area and depth, long and narrow settlers should be avoided in favor of wider, shorter ones. The width of the settler would, however, be limited by problems associated with non-uniform distribution of dispersion into a wide settler and uneven flow within it.

Although entrainment is an important factor affecting mixer-settler performance, attempts to predict the level of

entrainment encountered in plant-size equipment from laboratory experiments have proven largely unsuccessful due to the small scale of the lab equipment (DeMent, 1979).

Entrainment was not explicitly examined in this study. However, the possible effects of various designs and operating conditions on entrainment should be kept in mind.

2.5 EFFECT OF MIXER OPERATION ON SETTLER PERFORMANCE

The function of the mixer is to provide the residence time and the degree of agitation necessary for the desired extraction efficiency.

Although extraction efficiencies can be improved by increasing the mixing intensity, consideration must also be given to the possible effects this may have on the phase separation process. Increased mixing intensity can produce a dispersion which is more difficult to separate, resulting in greater settler size requirements and higher entrainment levels. Consequently, the mixer-settler operation must be optimized as a whole.

One would expect, based on the phase separation mechanism proposed by Barnea and Mizrahi, that the performance of the settler would be influenced by the dispersion drop size distribution produced in the mixer. The drop size produced by the mixer can be considered to be the result of an equilibrium between droplet break-up and interdroplet coalescence (Glasser

et al., 1976). Depending on the relative effect of agitation intensity on these opposing mechanisms, phase systems can be classified into either of two general and somewhat subjective categories; "sensitive" or "insensitive" (Mizrahi and Barnea, 1974).

With sensitive systems, increases in agitation energy result in decreased phase separation rates (thicker dispersion bands). However, an asymptotic value is eventually approached where further increases in mixing intensity do not affect separation rates appreciably. This asymptotic behavior can be explained as follows: Increasing mixing intensity simultaneously affects both the droplet break-up mechanism (as a result of higher shearing forces) and the re-coalescence mechanism (due to increased collision rates between droplets). Near the asymptotic value, increases in mixing intensity affect these two opposing mechanisms such that the drop size distribution produced by the mixer changes only minimally.

With insensitive systems, it is suggested that this asymptotic value is reached at a relatively mild mixing intensity. Phase separation rates do not change appreciably with energy input in the normal range of mixer operation.

Experimentation with relatively insensitive systems is considerably simplified since the operation of the settler can be investigated independently of the mixer. In contrast, for sensitive systems it is difficult to analyze the mixing and settling operations separately. Even if the mixing regime is

kept constant, changes in flow rates would result in a varying residence time within the mixer, and therefore a variation in the energy input per unit of dispersion volume. This could affect the drop size distribution and consequently, the settler performance.

2.6 TEMPERATURE

Temperature is an important parameter in settler design. A rule of thumb states that a 20°C temperature increase can typically result in a doubling of settler capacity.

The increase in settler capacity with temperature can be attributed to a decrease in liquid viscosities. Decreased viscosities result in higher coalescence rates due to easier drainage of the continuous phase film trapped between the droplets. Also, with respect to the separation mechanism proposed by Barnea and Mizrahi, the decrease in continuous phase viscosity would result in a smaller critical droplet size. The equilibrium between mechanical shearing and re-coalescence in the mixer could also be affected so as to produce a dispersion of a greater or lesser average drop size.

Because of the appreciable effect of temperature, a mixer-settler test unit should include a temperature control system.

2.7 SURFACE EFFECTS

Surface effects can have a significant effect on coalescence rates and phase continuity.

Ryon (1959) observed that coalescence was promoted if the dispersed phase wet the mixer settler surfaces. Thus, glass walls would promote coalescence of organic continuous dispersions and plastic walls would promote coalescence in aqueous continuous dispersions.

Although installation of packing material wet by the dispersed phase could improve settler capacity, such coalescence elements are rarely incorporated into large industrial mixer-settlers. This is due to the high cost posed by such sophistications and due to possible plugging of the elements by suspended solids (present to some extent in any industrial plant) and the corresponding requirement for periodic removal and cleaning.

Urban (1972) found that it was considerably easier to maintain a particular phase dispersed if it did not preferentially wet the mixer walls (ie: the ambivalence region was shifted). This applied for a vessel diameter of approximately 100 drop diameters.

For small test equipment where the surface area is large relative to the volume, surface effects could become significant and might invalidate the extrapolation of small

scale results to large scale equipment. Therefore, experimental test units should be as large as possible.

2.8 EFFECT OF MASS TRANSFER ON COALESCENCE

Observations of single drops suspended in a continuous liquid phase (Groothuis and Zuideweg, 1960) or rising to a flat interface (MacKay and Mason, 1961) indicate that mass transfer may promote or hinder coalescence depending on the direction of mass transfer.

If mass transfer is from the liquid drops to the continuous phase, coalescence increases. Transfer from the continuous to the dispersed phase decreases coalescence.

This behavior is attributed to gradients in interfacial tension caused by non-uniform mass transfer along the interface. It has been pointed out that higher solute concentration reduces interfacial tension (Treybal, 1963). Mass transfer from the droplet to the continuous phase produces a region of low interfacial tension in the film separating the droplets, resulting in enhanced drainage and coalescence. Transfer in the opposite direction produces a high regional interfacial tension which tends to draw in the continuous phase thus opposing film drainage.

These observations are based on studies involving single drops. It is not clear whether the effect is equally significant for the case of mixer-settlers, where there are

swarms of droplets under the influence of mass transfer, as there is no data available. For swarms of droplets, the interfacial gradients along the surface may be reduced, thus lessening the effect.

In the experimental equipment of this study, the phases were recirculated and therefore mass transfer did not occur. This raises the question of whether comparison with industrial mixer-settlers (such as those at Key Lake), where mass transfer is, of course occurring is valid even if the same phase system is used. In this study, it is assumed that since mass transfer is essentially completed in the mixer with little occurring in the settler, coalescence rates in the settler should not be affected. It is possible, however, that settler performance could be affected if the drop size distribution resulting from the dispersion/coalescence mechanism is changed appreciably by mass transfer. This possibility, however, was ignored in this work.

2.9 INSTALLATION OF HORIZONTAL PLATES

In order to more efficiently utilize a settler's volume, units have been designed containing horizontal plates which, in effect, partition a simple box-type mixer-settler into a set of thin settlers superimposed one on top of another. Improvements in settler capacity of several-fold have been claimed for such designs (Mizrahi and Barnea, 1973).

Such designs are based on the principle that the *volumetric* separation capacity of thick dispersion bands is less than that for thinner bands. If the scale-up criterion of Ryon (equation 1) is assumed to be applicable, this can be shown mathematically:

$$\Delta H = k(Q/A)^Y \quad y \gg 1 \quad (5)$$

$$Q/(A\Delta H) = Q/V = 1/(k^{1/Y} \Delta H^{1-1/Y}) \quad (6)$$

Equation (6) indicates that the settler capacity per unit volume of dispersion band (Q/V) decreases with increasing dispersion band thickness and therefore supports the utilization of superimposed, thin settlers.

Due to the higher capital cost and to problems which would be encountered as a result of crud, such designs have not, however, achieved widespread application in metallurgical extraction industries.

CHAPTER 3- DESCRIPTION OF TYPICAL SOLVENT EXTRACTION PROCESSES

3.1 INTRODUCTION

Solvent extraction is a unit operation used for purification and concentration of metals. In order to illustrate the scope of the process and the role played by mixer-settlers in it, two commercial processes will be described in some detail. These processes are those corresponding to the two systems used in the experiments of this study, namely;

- (1) The solvent extraction process of Key Lake Mining Corporation (KLMC) utilizing Alamine 336 as the reagent for extraction of anionic uranium complexes.
- (2) The process of N'Changa Consolidated Copper Mines (NCCM) at Chingola, Zambia, using LIX-64N for extraction of copper(II) from sulphate solution.

3.2 DESCRIPTION OF KLMC SOLVENT EXTRACTION PROCESS

Initial steps in the production of yellow cake from ore involve crushing and grinding of the ore to expose the uranium minerals, followed by sulphuric acid leaching of this ground ore slurry to extract over 97% of the uranium from the ore (Neven, Steane, Becker, 1985) (Neven, Gormely, 1982).

The solution from acid leaching (known as the pregnant solution) contains suspended solids (50-150 ppm of colloidal

silica) which would constitute a crud problem in the settlers, accumulating at the interface and resulting in poor phase disengagement (Ritcey, 1980). Addition of Polyox (water soluble high molecular weight nonionic polymers of ethylene oxide) to flocculate the silica, followed by solid-liquid separation in a thickener and filtration on a precoat pressure filter, reduces the silica content to <10 ppm.

This pretreated pregnant solution contains in addition to uranium, a number of impurities such as arsenic, nickel, iron, magnesium and aluminum. The composition of the pregnant solution is given in Table 1. Direct precipitation would result in a low grade and unmarketable uranium product. Therefore, impurities are eliminated by the solvent extraction process before precipitation of uranium.

A simplified flow diagram of the solvent extraction process is given in Figure 3.

The extraction section consists of four mixer-settlers operated countercurrently. The pregnant solution (flow=120 m³/hr) is contacted with an organic phase consisting of 3-6% Alamine 336 diluted in a high grade kerosene and also containing 3% isodecanol.

Alamine 336 is a tertiary amine manufactured by Henkel (formerly General Mills). This reagent extracts the anionic uranium complexes from the aqueous acid leach solution in accordance with the following reactions where R₃N represents

Table 1. Key Lake pregnant solution composition

COMPONENT	CONCENTRATION (g/l)
U ₃ O ₈	6 - 10
As	2.2 - 4.4
Ni	2.0 - 4.0
Fe	2.5 - 3.5
Mg	0.8 - 1.5
Al	0.5 - 1.5
Ra ²²⁶	800 - 1300 Bq/l
H ₂ SO ₄	15 - 20
TSS	<10 ppm

* from Neven, Steane, Becker, 1985.

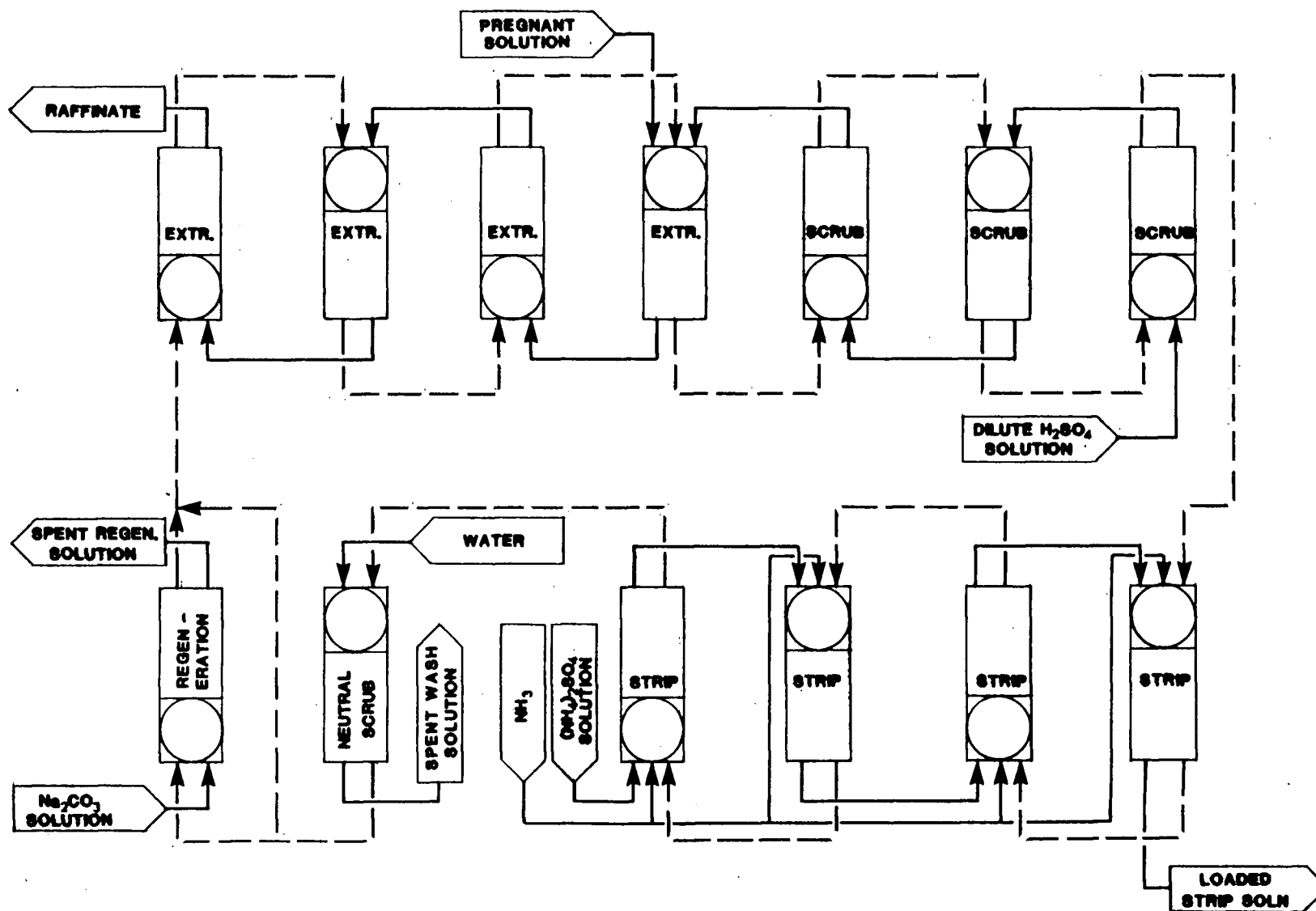
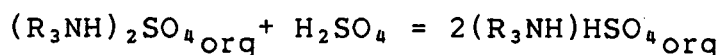
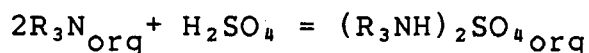


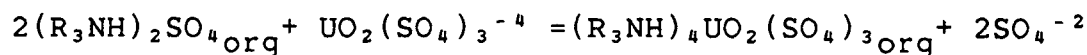
Figure 3. Flow diagram of KLMC solvent extraction process.

Alamine 336 (Merritt, 1971):

Formation of amine sulphate and bisulphate salts:



extraction:



Alamine 336 is highly selective for uranium in preference to other constituents.

Over 90% of the organic phase is a high quality kerosene (either Napoleum 470B or suitable replacement is used, manufactured by Kerr-McGee Corporation) which acts as a carrier or diluting medium for the very viscous extractant. Besides giving the desired flow properties to the organic phase it has a relatively high flash point to avoid potential fire hazards (Murray and Bouboulis, 1973), (Ritcey and Lucas, 1974).

Addition of isodecanol as a modifier improves the solubility of amine salts in kerosene, thus preventing the formation of a third phase and inhibiting the formation of stable emulsions (Ritcey and Lucas, 1974).

The organic flow rate is set to achieve maximum uranium loading on the organic, typically 7.5 gpl U_3O_8 , while maintaining the raffinate U_3O_8 at <0.001 gpl. Recycle of organic from the settler to the mixer keeps this phase in the majority in the mixer to facilitate organic phase continuity.

Despite the fact that settler capacity would be greater for aqueous continuous operation (Merritt, 1971), the extraction section, as well as all other sections are run organic continuous. This is done to minimize organic entrainment and because the tendency for forming stable emulsions is increased with aqueous continuity (Merritt, 1971).

Following the four extraction stages, the uranium bearing organic phase (loaded organic) is scrubbed with a dilute sulphuric acid solution (10-20 gpl H_2SO_4) in three countercurrent mixer-settler stages. This is done to remove quantities of impurities, especially arsenic, which may have been co-extracted with the uranium. Some loading of arsenic onto organic will occur, particularly if it is not fully loaded with uranium. The spent scrub aqueous phase is then fed back to the extraction circuit to recover any uranium that may also have been stripped off during scrubbing.

Uranium is stripped from the scrubbed, loaded organic phase into an ammonium sulphate strip solution. The pH is carefully regulated between 4.0 and 4.2 by adding vaporized anhydrous ammonia to the strip mixers. At pH values below this range, stripping is poor while at values above this range phase separation may be poor or emulsion formation could result due to precipitation of uranium yellowcake.

In the neutral scrub, barren organic from the stripping section is scrubbed with clean water in a mixer-settler to remove entrained ammonium sulphate prior to recycle of the

organic phase back to the extraction circuit. This prevents ammonia from entering the raffinate and subsequently being released to the final effluent.

Molybdenum is strongly extracted by Alamine 336, yet is not effectively removed in the stripping circuit (Merritt, 1971). Therefore, a bleed of the barren organic may be contacted with a 5% sodium carbonate solution to remove molybdenum, preventing its accumulation in the organic.

Final recovery of uranium from the uranium solution is achieved conventionally by chemical precipitation (Merritt, 1971). The strip solution pH is raised to 7.2 using ammonia gas to precipitate the uranium. The yellowcake precipitate is dewatered and roasted at 800 °C to produce the calcine product.

A typical analysis of the final yellowcake product is shown in Table 2. Comparison of this analysis with that of the pregnant solution (Table 1) shows the effectiveness of the solvent extraction circuit in removing contaminants.

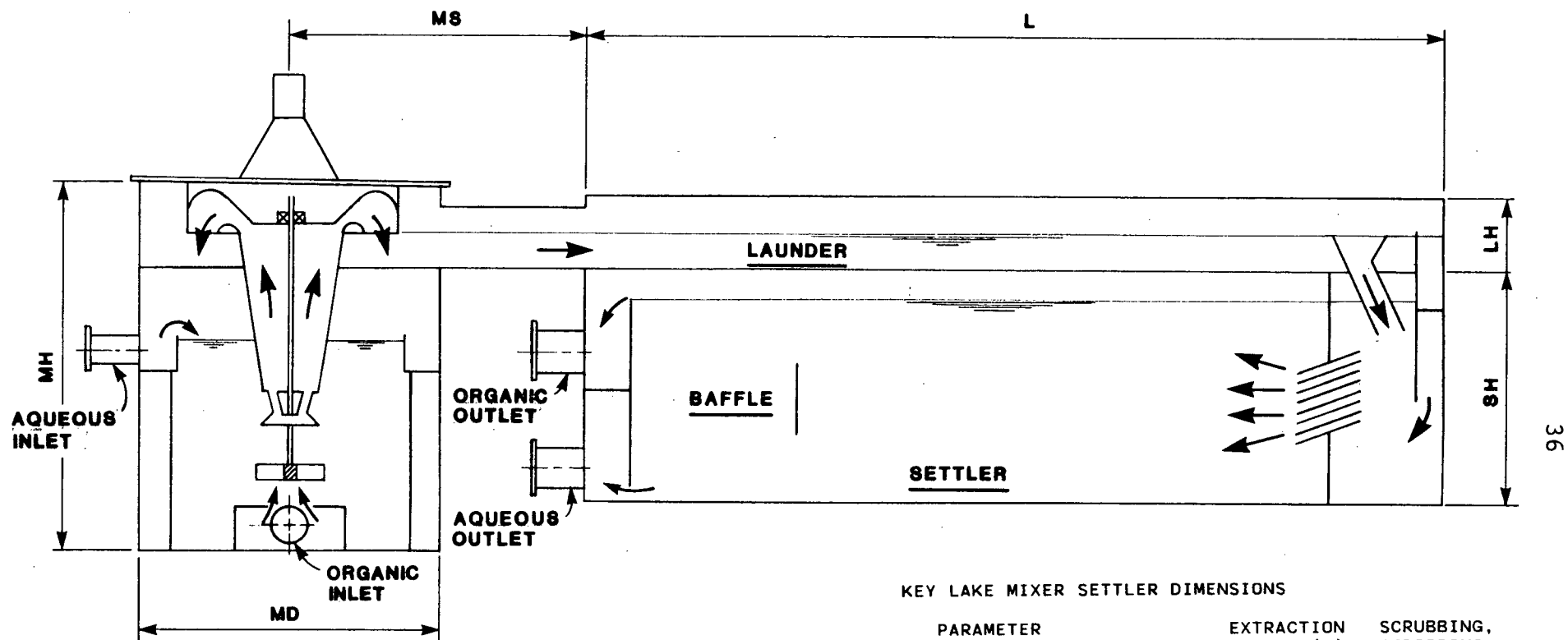
The KLMC solvent extraction plant mixer-settlers are of the KREBS design and dimensions shown in Figure 4. The KREBS design is purported to allow for a 50-75% reduction in settler size over that normally required. This improvement is attributed primarily to two features which result in partial separation of the dispersion prior its entrance into the main settling chamber; a conical pump and a superimposed launder.

Table 2. Key Lake typical product analysis

COMPONENT	CONCENTRATION (%)
U ₃ O ₈	91 - 99
S	0.1 - 4.00
As	0.01 - 0.04
Fe	0.01 - 0.03
Mo	0.02 - 0.07
Na	0.01 - 0.05
K	<0.01
V	<0.01
Ca	<0.01
Mg	<0.01
B	<0.01
Si	0.03 - 0.30
Ni	<0.01
Ti	<0.01
Zr	<0.01

* Impurities expressed on a percent U basis.

* from Neven, Steane, Becker, 1985.



36

KEY LAKE MIXER SETTLER DIMENSIONS

PARAMETER	EXTRACTION STAGES (m)	SCRUBBING, STRIPPING, REGENERATION STAGES (m)
MH (mixer height)	2.90	2.90
MD (mixer diameter)	2.44	2.44
MS	2.30	2.30
L (launder/settler length)	9.45	6.12
LH (launder height)	0.50	0.50
SH (settler height)	1.15	1.15
settler width	3.96	2.20
launder width	2.44	1.40

Figure 4. KLMC mixer-settler design and dimensions.

The conical pump transfers the dispersion from the mixer to the settler and induces initial coalescence as a result of the centrifugal forces developed. The launder feeds the dispersion to the opposite end of the settler and facilitates further phase separation.

At the end of the launder, the light and heavy partially separated phases are fed, respectively, to the upper and lower parts of the settling chamber by means of adjustable overflow and underflow weirs. A series of parallel plates extending across the full width of the settler serves to evenly distribute the partially separated dispersion in the settler. In the settler, a dispersion band forms and final separation is achieved.

3.3 DESCRIPTION OF N'CHANGA CONSOLIDATED COPPER MINE SOLVENT EXTRACTION PLANT, CHINGOLA, ZAMBIA

The NCCM solvent extraction plant is the world's largest, yet is typical of copper solvent extraction processes. It treats a total pregnant liquor flow of 3200 m³/hr in four parallel liquid streams (Hanson, 1983). A simplified flow diagram is shown in Figure 5 for one stream.

The pregnant liquor from sulphuric acid leaching of the ore contains 3-4 g/l Cu at pH 1.9-2.0. Iron salts constitute the major contaminant.

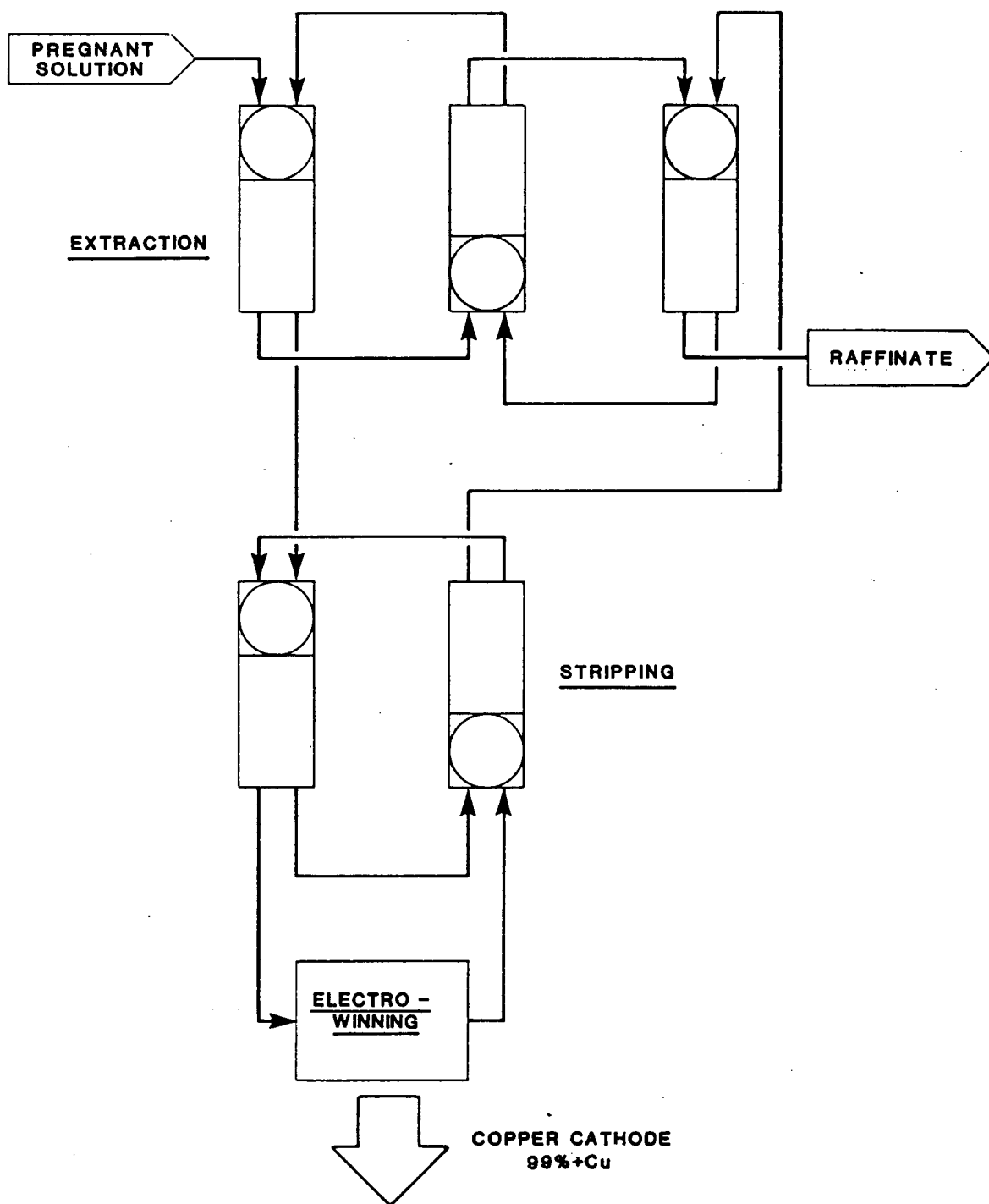
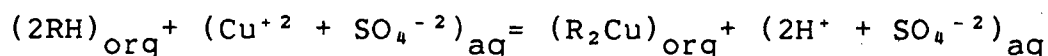


Figure 5. Flow diagram of NCCM solvent extraction process.

Each pregnant liquor stream is fed to an extraction circuit consisting of a battery of 3 countercurrently operated mixer-settlers and is contacted with an organic phase containing 22 vol% extractant in kerosene. No modifier is required as third phase formation is not a problem with this system.

LIX64N (manufactured by Henkel) serves as the extractant. (Note: LIX64N has recently been replaced by HSLIX64N which is concentrated by a factor of 1.51).

Copper extraction is achieved by shifting to the right the equilibrium existing between copper ions, the extractant (RH) and the acid solution:



Copper is thus selectively transferred from the aqueous to the organic phase, leaving iron and other impurities behind.

The loaded organic is then passed to a series of 2 countercurrently operated mixer-settler stages (constituting the stripping section) and contacted with high acid strength spent electrolyte from the electrowinning circuit. The high acidity (≈ 150 g/l H_2SO_4) shifts the equilibrium to the left, thereby stripping the copper values from the organic. The extractant is thus regenerated and is recycled to the extraction circuit.

Stripping results in a concentrated copper solution (25-60 g/l) which is suitable for electrowinning. At the cathode of the electrowinning cell, copper ions are reduced to copper metal of >99% purity. Oxygen is evolved at the lead anode.

The mixer-settlers are constructed of stainless steel lined concrete. Mixers are square in cross section and are fitted with a full width horizontal baffle to prevent vortex formation. Dispersion is discharged from the mixer by way of a flared launder leading to a full width entry slot into the settler at the level of the dispersion band. Each settler is provided with two picket fence type baffles. The function of these devices is to ensure even distribution and to reduce settler turbulence. A fence baffle consists of two rows of vertical bars, spaced such that the bars of the second row cover the gaps between the bars of the first row.

Dimensions of the N'Changa mixer settler units are provided in Table 3.

Table 3. Dimensions of NCCM solvent extraction process
mixer-settlers

APPARATUS	PARAMETER	EXTRACTION	STRIP
mixers	width	5.9 m	4.0 m
	depth	3.7 m	3.2 m
impellor settlers	diameter	2.7 m	2.3 m
	width	12.2 m	12.2 m
	length	36.5 m	26.2 m
	depth	0.76 m	0.76 m
first picket fence	distance from inlet	13.1 m	9.1 m
second picket fence	distance from inlet	30.5 m	21.9 m

* from Hanson, 1983.

CHAPTER 4 - EXPERIMENTAL PHASE SYSTEMS

Two phase systems were used in experiments.

Key Lake Mining Corporation provided samples of raffinate and loaded organic from the extraction section of the solvent extraction plant. The composition of these samples thus approximated that of the liquids in the extraction section mixer settlers, the plant's largest, and could be expected to possess similar physical properties. Comparison of experimental results and plant operating data was thus valid except for mass transfer effects, if any.

A second phase system was prepared by dissolving 8 parts by volume of HSLIX64N (Henkel, lot 4G14212W) in 92 parts diluent (90% Nap470B and 10% Kermac500T, manufactured by Kerr-McGee) to produce the organic phase. The aqueous phase was prepared by dissolving 3 g/l of copper, as copper(II)-sulphate, in water and adjusting the pH to 1.9 with H_2SO_4 . The general behavior of this phase system could be compared with that of the Key Lake phase system, providing some indication of the extent to which different systems' behavior could be predicted. However, the validity of quantitative comparisons between the experimental HSLIX64N-copper system data and copper solvent extraction plant data would be limited due to the absence of contaminants in the experimental system.

CHAPTER 5 - EXPERIMENTAL APPARATUS

5.1 INTRODUCTION

Equipment was constructed to facilitate experiments to be conducted allowing for the development of settler scale-up criteria, for determining the effects of operating parameters (temperature, phase ratio, phase continuity, mixing intensity and conditions) on settler performance, and for studying the effect of settler configuration (specifically dispersion introduction geometry) on phase separation.

Since the study was not concerned with mass transfer, the experimental phases were recirculated. The equipment was designed to be as large as possible while still being practical and could handle a maximum flow of 24 l/min of either phase.

The schematic arrangement of the entire apparatus is shown in Figure 6 and its ranges in capability are tabulated in Table 4. Its chief components are described below.

5.2 MIXER-SETTLER

The mixer-settler was constructed with 1/8 inch, 316 stainless steel with two full, wire reinforced glass walls to facilitate visual and photographic observation of the mixing and settling operations.

A continuous 1/4 inch wide strip of Gore-tex joint sealant (W.L Gore and Assoc., Inc) followed the edges of the stainless

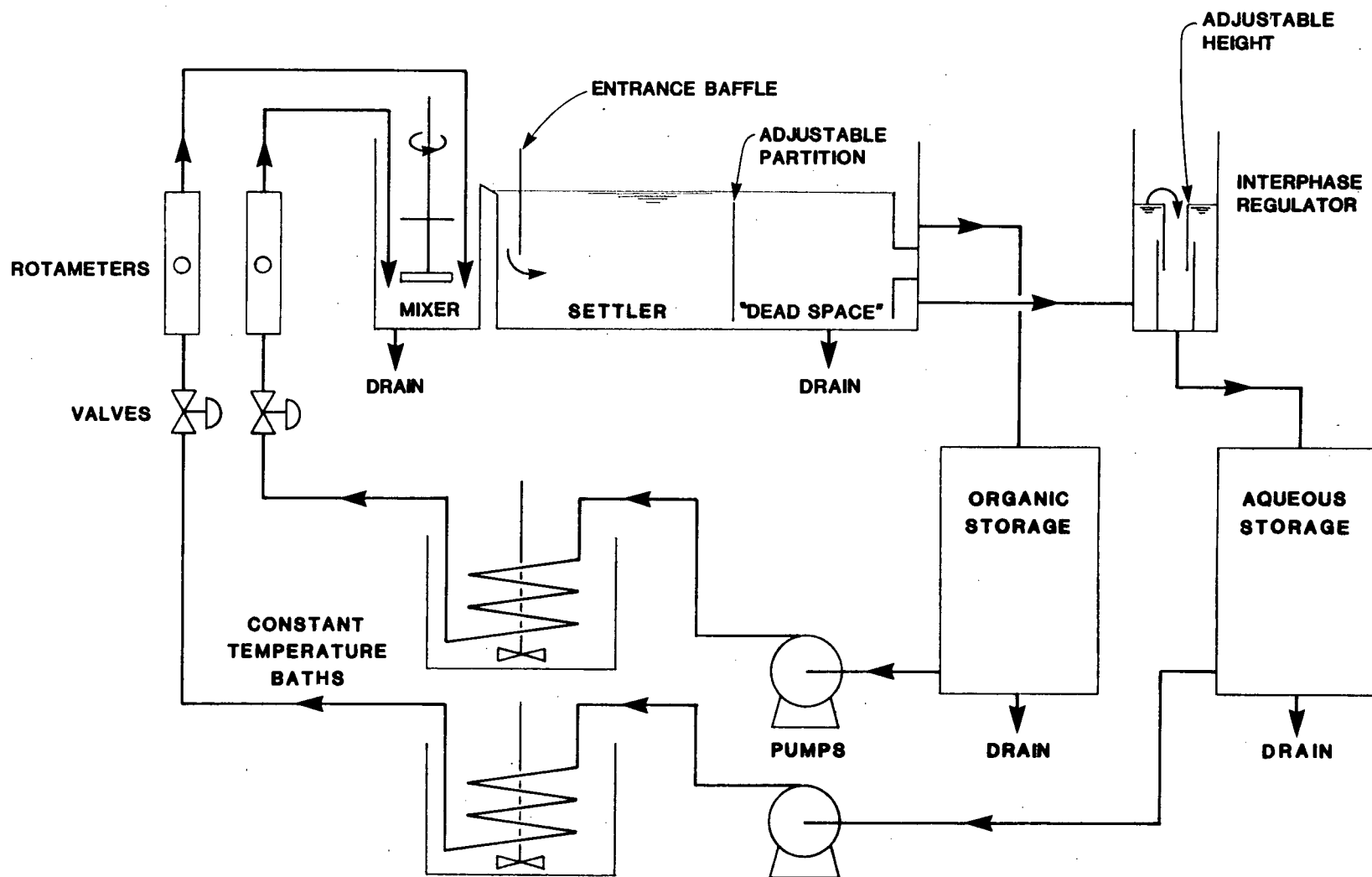


Figure 6. Schematic of experimental apparatus.

Table 4. Summary of equipment specifications and ranges in capability.

PARAMETER	RANGE	
impellor speed	0-360 rpm	
aqueous flow	4-24 litres/min	
organic flow	4-24 litres/min	
dispersion band thickness	0-30 cm	
temperature	20-45°C	
O/A ratio	6/1-1/6	
mixer dimensions	length=30.5cm	width=30.5cm
	depth=41cm	
mixer volume	38 litres	
settler dimensions	length=120cm	width=30.5cm
	depth=38cm	
	(length can be reduced with adjustable partition)	
settler cross-sectional area	0-0.36 m ²	

steel and acted as a gasket between the steel and the glass walls. Gore-tex joint sealant is a soft, foamed form of pure PTFE. It is chemically inert and therefore will not deteriorate or be extracted by the aromatic organic or the acidic aqueous phases. This eliminates the possibility of contaminating the systems with plasticizers, thus altering the physical behavior of the phases such that it would not be representative of that found under plant conditions. For this reason, plasticized flexible tubing was avoided as well, despite its convenience.

A leakproof seal was effected by applying pressure to the glass walls with 40 screws tapped into a steel "clamping frame". A relatively light clamping force was sufficient to compress the Gore-tex to a thin ribbon, thereby ensuring a reliable seal.

Sections of steel square tubing with rubber pads on one face served to distribute the force evenly along the joints and prevented chipping of the glass by the clamping screws.

An end view of the settler showing the Gore-tex seal and the method of assembly of the mixer-settler is shown in Figure 7.

Dimensions of the mixer-settler are given in Figure 8.

The mixing chamber was 30.5 cm square and 41.2 cm deep to the overflow. The square cross-section eliminated the need for vertical baffles.



Figure 7. Photograph of mixer-settler Gore-tex seal.

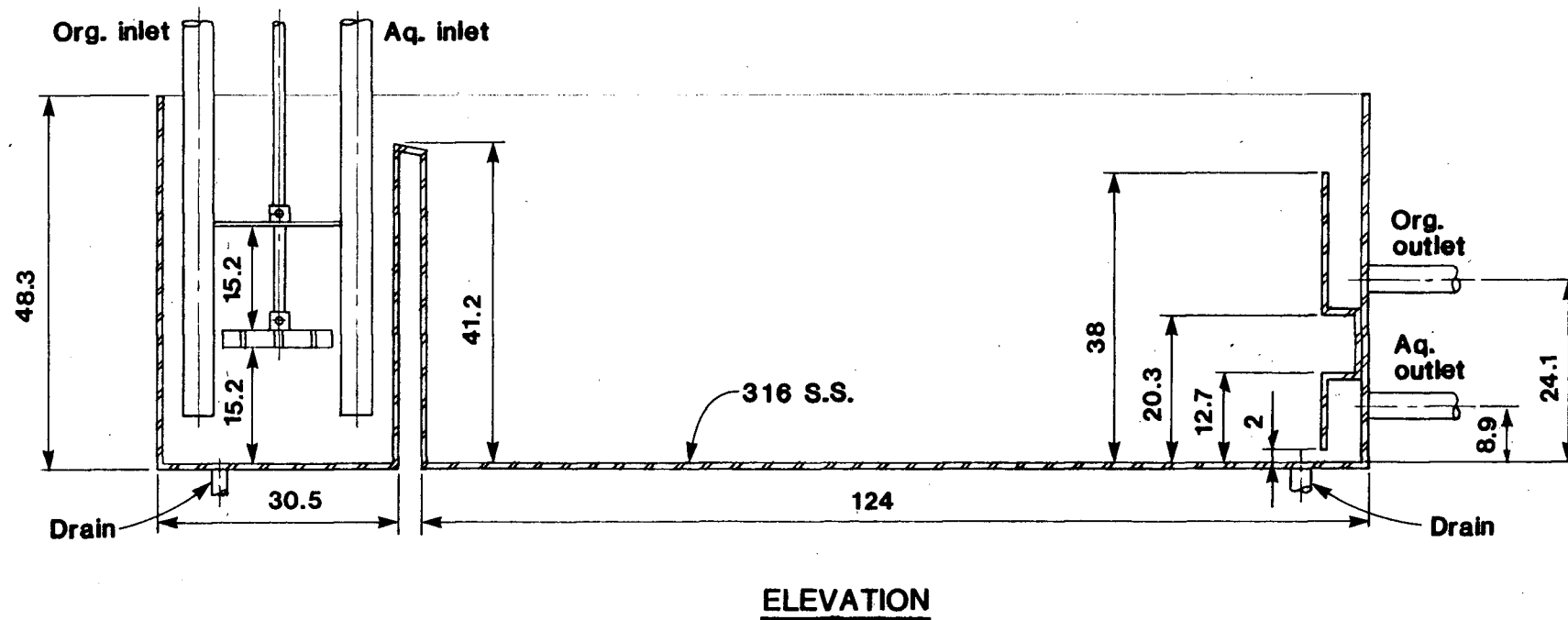
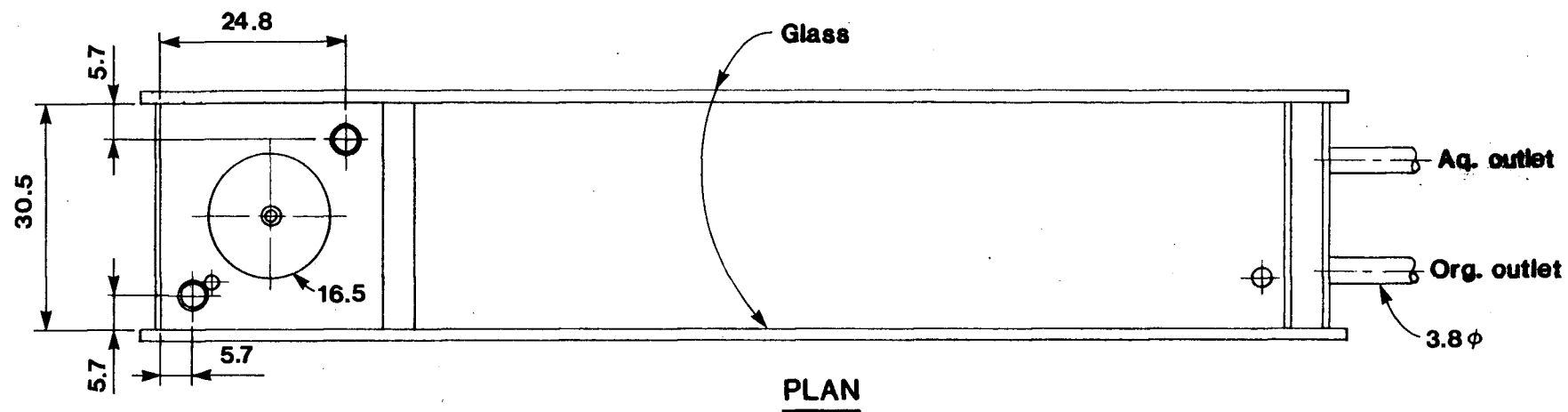


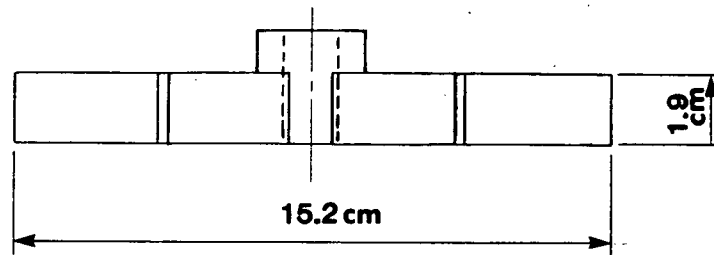
Figure 8. Dimensions of experimental mixer-settler (cm).

Agitation was provided by a 15.2 cm diameter open-style flat blade impellor having the proportions shown in Figure 9. The impellor axis was centrally located in the mixer-settler 15 cm from the mixer bottom. The vertical position of the impellor could be altered, if desired, by changing impellor shafts. The shaft was driven by a 190 W electric motor (GK Heller, model 25P4225). The speed could be varied between 0 and 360 rpm to an accuracy of $\pm 1\%$ by means of a motor controller equipped with a digital rpm display (GK Heller, model HS30-MD3). A 16.5 cm diameter disc was fitted onto the impellor shaft 16.5 cm above the impellor to prevent vortex formation.

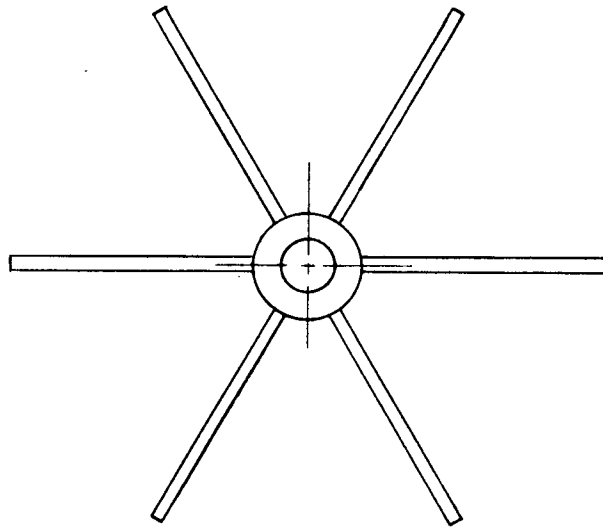
The aqueous and organic mixer inlet ports were constructed of 2.54 cm stainless steel pipe and arranged diagonally opposite each other in the mixer at equal distances from the impellor shaft. The dispersion exited the mixer via a full width overflow weir to facilitate even distribution into the settler.

A photograph of the mixing chamber is shown in Figure 10.

The relatively large settler size was chosen to minimize wall effects yet still be practical for laboratory work. The length and therefore the effective cross-sectional area of the settler could be changed by moving an adjustable partition. The volume downstream of this partition was a "dead space" containing the two separated phases. This space could serve to allow entrainment to separate. The partition was sized so as to minimize the liquid depths at the partition underflow and



ELEVATION



PLAN

Figure 9. Impellor geometry.

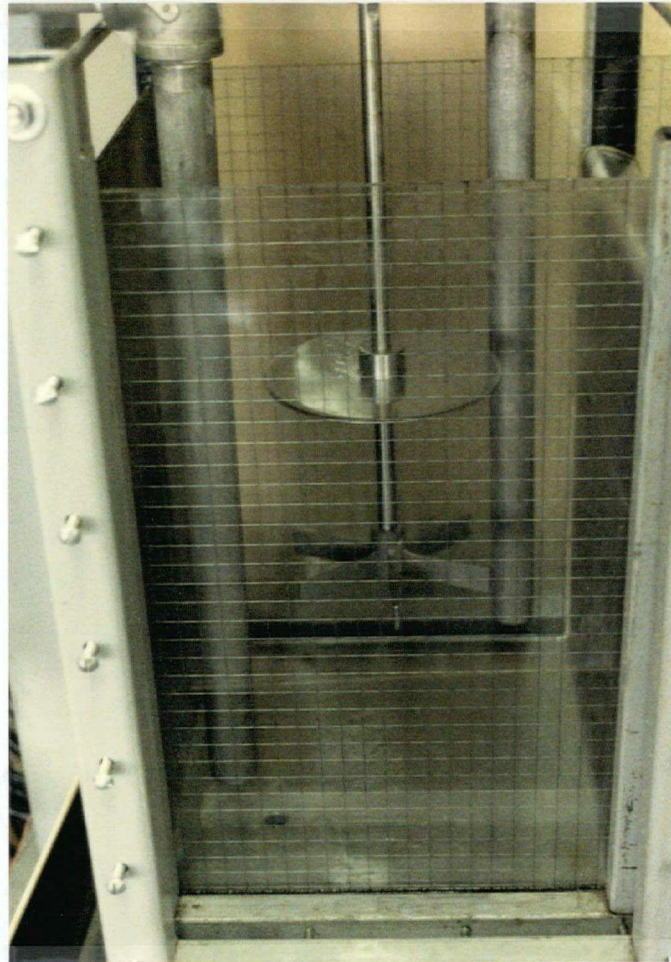


Figure 10. Photograph of mixing chamber.

overflow to eliminate backflow from the dead space to the test section.

Experiments testing the effect of settler inlet location relative to the dispersion band could be conducted by adjusting a removable entrance baffle just below the mixer overflow. Installation of this baffle created a passageway for the flow of the dispersion to the desired introduction level.

The phases exited the settler through 1 1/4 inch outlet ports. This diameter ensured that all flows up to the maximum could be easily accepted. Full width overflow and underflow weirs at the exit ports ensured that any flow disturbances resulting from the relatively high flow velocities in the withdrawal region were not conducted through the settler.

The settler outlet nipples were connected by short lengths of flexible teflon tubing to the remainder of the apparatus. This tubing section served 2 purposes:

(1) Tubing eliminates the need for a fitting requiring wrench tightening, the action of which might result in the creation of stresses in the mixer-settler assembly. This could lead to settler leakage or glass fracture. A clamp was used to secure the teflon tubing to the outlet nipples.

(2) The tubing minimizes the transmission of vibrations (which could affect coalescence) from the pumps to the mixer-settler via the rigid piping network.

Both the mixing and the settling compartments contained drains so that the mixer-settler contents could be emptied into the storage vessels.

5.3 INTERPHASE REGULATOR

The level of the nominal organic/aqueous interface in the settler (that which would be present if there were no dispersion band) could be precisely controlled by an interphase regulator (Figure 11).

This device consisted of an inner tube of 316 stainless steel sheathed by a larger outside tube. A teflon cylinder fitted between the two tubes prevented leakage between them yet permitted the inside tube to be easily raised or lowered in a telescopic fashion by means of a rod which extended out of the top of the interphase regulator.

Aqueous phase from the mixer-settler entered the outer casing of the interphase regulator and flowed over the lip of the telescopic section which acted as an adjustable weir. Closing or extending this telescopic section altered the hydraulic balance in the settler and resulted in raising or lowering of the nominal settler interface.

5.4 STORAGE VESSELS

Two 200 litre stainless steel vessels were used, one for storage of each of the phases. These vessels were large enough

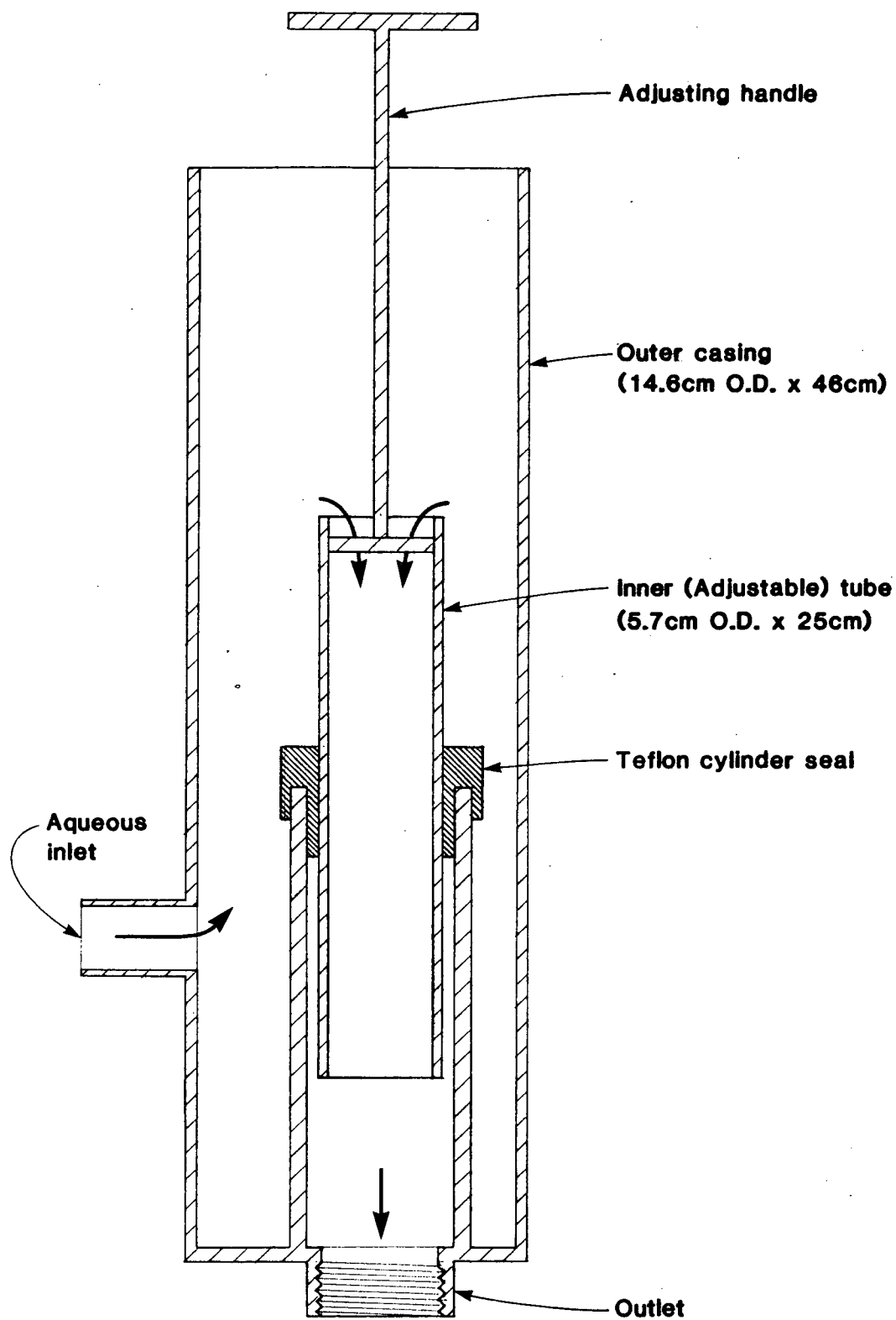


Figure 11. Interphase regulator.

to hold the entire contents of the mixer-settler and to ensure that a sufficient liquid level was maintained above the pump suction during mixer-settler operation. When the equipment was not in use, the mixer-settler contents were drained into these vessels for reasons of safety.

5.5 PUMPS

The phases were recirculated by means of 2 - 760 W centrifugal pumps (Hayward Gordon model 62RSIC-3.5) capable of providing 15 m of head (water, 20°C) at a flow capacity of 38 l/min. Construction materials were 316 stainless steel (casing and shaft) with teflon gaskets.

5.6 TEMPERATURE REGULATION

The temperature of the circulating liquids could be controlled at any desired temperature in the range 20-45°C by passing each phase through a 1.9 cm stainless steel coil immersed in a 75 litre capacity constant temperature water bath. Separate baths were provided for each stream to allow for changes in the O/A flow ratio.

Each bath was fitted with a 4.5 kW, copper sheathed, screw plug type immersion heater (Chromalox, model MT-345).

The heaters could be independently cycled on and off by a temperature controller (Barber-Coleman, model 121M) thereby maintaining the bath water and hence the phases at the desired

setpoint. The inputs for the controllers were chromel/constantin thermocouples, chosen because of their high millivolt output in the 20-45°C operating range. These were located in the aqueous and organic recycle lines upstream of the mixer inlets. A flow of cold tap water could be fed to the baths if cooling rather than heating was required.

The baths were provided with a 95 W, 1800 rpm constant speed stirrer (Prestolite-Leland, model 913507-01) for improvement of heat transfer to the coils. The immersed area of each coil was 0.25 m².

Thermometers located in the mixer-settler itself could be used to see if significant temperature differences existed between the mixer inlet and settler outlet.

5.7 FLOW METERING AND REGULATION

The flowrates of the individual phases could be measured in the approximate range 4-24 l/min by means of 2 glass tube rotameters (Brooks, model 1307). The rotameters were experimentally calibrated for each phase at several temperatures in the range 20-45°C and had a calibrated accuracy of ±1%.

Globe valves upstream of the rotameters were employed for regulation of the O/A ratio and the respective flowrates.

5.8 PANEL BOARD

All controllers and motor switches were mounted in a steel panel enclosure situated adjacent to the apparatus. The panel board display is shown in Figure 12.

5.9 SAFETY CONSIDERATIONS

Due to the potential hazard associated with flammable organic phases, all motors were explosion proof. Fumes were exhausted through a duct positioned over the mixer-settler. The oil-tight panel enclosure containing electrical devices was maintained at positive pressure by connection to an air line.

The KLMC-supplied samples contained 7.5 g/l U_3O_8 in the organic phase and trace quantities of Ra^{226} in the aqueous phase. The extremely low level of radiation associated with this small quantity of radioactive material did not constitute a significant radiation hazard or require protective shielding. Nevertheless, the laboratory was regularly tested for radiation with a geiger counter. The equipment was decontaminated upon completion of experiments.

The mixer-settler was positioned over a spill tray, of sufficient capacity to contain the entire mixer-settler contents, in case of leakage or glass fracture.

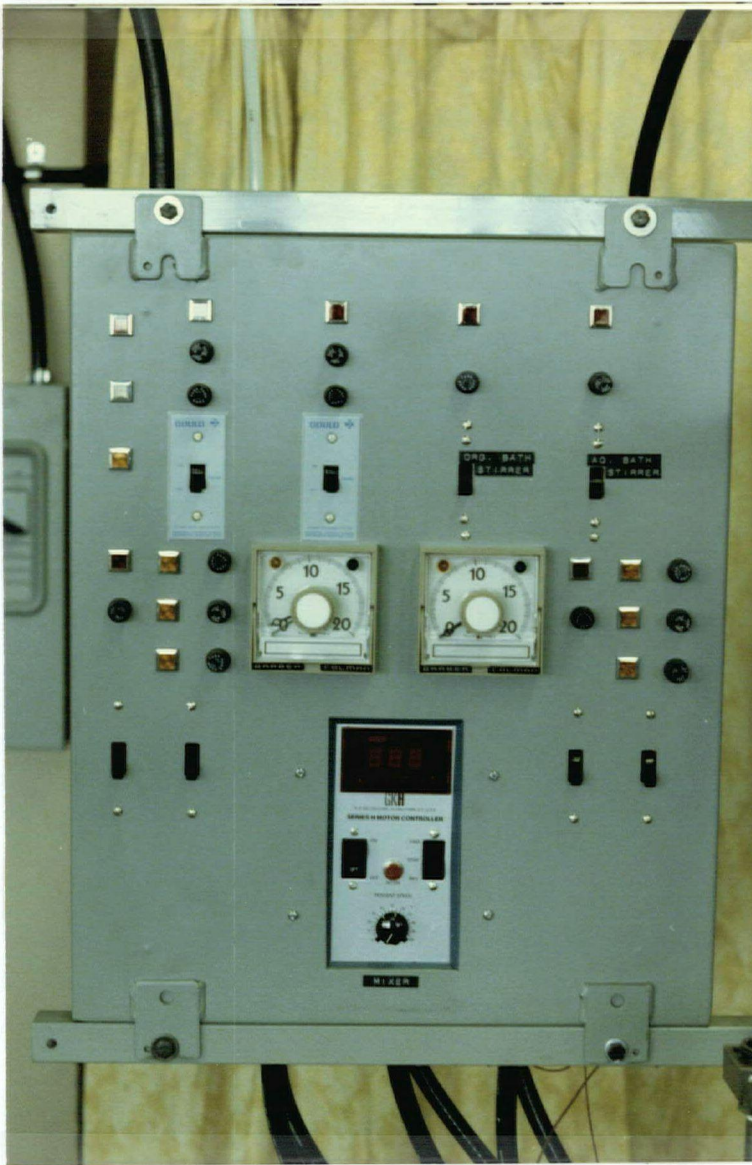


Figure 12. Photograph of panel board.

CHAPTER 6 - EXPERIMENTAL PROCEDURE

6.1 PROPERTIES OF THE PHASES

The measured physical properties of the phases are tabulated in Table 5. Viscosity was measured using the capillary tube method with a Cannon-Fenske viscometer (procedure described in ASTM D 445-79) and interfacial tension was measured using the ring method with a Du Nuoy tensiometer (procedure described in Central Scientific Company, Bulletin 101). A specific gravity bottle was used to determine the density.

6.2 MIXER-SETTLER START-UP PROCEDURE

With the HSLIX64N-copper system, the bulk liquid phase which initially covers the impellor at the time at which agitation is initiated almost invariably becomes the continuous phase. Therefore, it was necessary to adopt an appropriate mixer start-up procedure to produce a dispersion of the desired phase continuity. The procedure for mixer-settler start-up with the HSLIX64N phase system was as follows: Assume that the mixer-settler is empty and that all motors are off.

1. The settler partition was positioned as required to give the desired settler cross-sectional area and the inlet baffle was positioned as desired.
2. With the impellor turned off, the 2 phases were pumped from the storage tanks into the mixer-settler until the settler was filled to the level of the

Table 5. Physical properties of the experimental phases.

PHASE SYSTEM	PHASE	TEMP. (°C)	DENSITY (g/cm ³)	VISCOSITY (cp)	INTERFACIAL TENSION (dyne/cm ²)
HSLIX64N-copper	org.	24	0.824	2.356	-
HSLIX64N-copper	aq.	24	1.002	0.917	-
HSLIX64N-copper	org.	35	0.816	1.872	-
HSLIX64N-copper	aq.	35	0.995	0.726	-
HSLIX64N-copper	org-aq.	24	-	-	14.2
Key Lake	org.	35	0.818	2.150	-
Key Lake	aq.	35	1.034	0.836	-
Key Lake	org-aq	35	-	-	12.6

overflow weir with approximately equal volumes of organic and aqueous phases.

3. The interface level in the mixer was adjusted so that the phase to be continuous covered the impellor by a minimum of 5 cm. This was done by adding (by pumping) and removing (by draining) the necessary quantities of each phase from the mixer.
4. The impellor was turned on and set to the desired speed. A conductivity probe could then be used to confirm that the proper phase continuity had been achieved.
5. The pumps were started and the throughput of each phase, measured by means of calibrated rotameters, was adjusted to give the desired phase ratio and total throughput. The agitators in the constant temperature baths were started and the temperature controllers were set to the desired set point.
6. The two phases were now being recycled through the system. A dispersion was being formed in the mixer and separated in the settler. The liquids were circulated until the desired temperature was reached (as measured by a thermometer immersed in the mixer).
7. The interphase regulator was positioned to maintain the nominal interface in the settler at the proper level. It was necessary to monitor all flows and levels periodically and to make continued adjustments.

8. No data was recorded until it had been established that steady-state had been reached.

With the Key Lake phase system it was necessary to adopt a slightly modified start-up procedure. Since this system exhibited a tendency for forming a stable, aqueous continuous dispersion (section 7.1.3), it was necessary to start up the mixer-settler with no aqueous phase in the mixer to avoid this. The aqueous phase flow to the mixer was then slowly increased to the desired rate.

A photograph of the mixer-settler operating with the Key Lake phase system is shown in Figure 13.

6.3 TIME FOR DISPERSION BAND TO REACH STEADY STATE

The time required for the dispersion band thickness to achieve steady state is presented in Figure 14 for various operating conditions for the HSLIX64N-copper phase system. The data shows that at relatively high flow rates, when a thick dispersion band is produced, 45 minutes may be required while at low flow rates (thin dispersion bands) as little as 10 minutes would be adequate.

Based on this, when conducting experiments, at least 45 minutes were allowed after an operating condition adjustment had been made before a reading was taken. In addition, to further guarantee that steady-state had been achieved, data was only recorded after two successive dispersion band thickness readings, taken 5-10 minutes apart, agreed within 5%. The



Figure 13. Photograph of mixer-settler operation with Key Lake phase system.

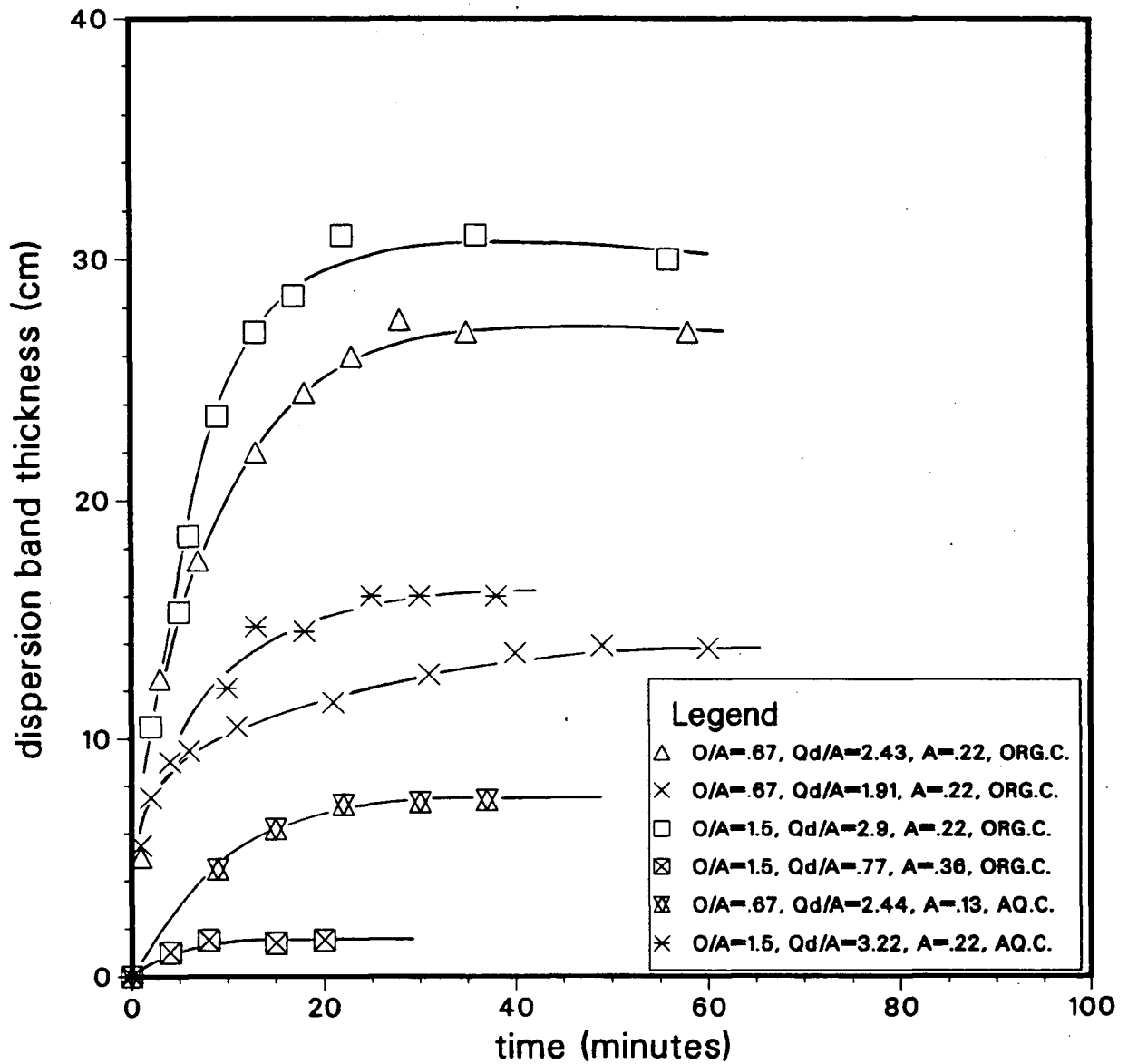


Figure 14. Time for dispersion band thickness to achieve steady-state after introduction of dispersion into settler (HSLIX64N-copper phase system).

throughput was then changed for a subsequent run.

It was realized that, although the dispersion band thickness may apparently have reached steady-state, the holdup profile and drop size distribution within the dispersion band might continue to change slightly for a period of time beyond this. Therefore, at least 90 minutes were allotted before holdup or drop size data were taken.

6.4 SAMPLING FOR DISPERSION BAND HOLDUP

Dispersion samples were withdrawn from the mixer-settler using a 100 ml pipet, connected via a stopcock and a length of tygon tubing to the suction side of an ejector. The pipet, inverted so that the larger end (0.5 mm ID) served as the tip to more readily admit the sample, could be supported in the mixer-settler by means of a clamp and stand. When the tip of the pipet was immersed at the desired level in the dispersion band and the stopcock was opened, the vacuum quickly drew a sample into the pipet. Once 100 ml had been withdrawn, the stopcock was closed and the sample was transferred to a graduated cylinder in which the phases were allowed to disengage so that their volumes could be determined.

A minimum of 90 minutes was allotted to achieve steady state before dispersion samples were withdrawn. Sampling at various vertical locations within the dispersion band was performed successively on a random basis. Data was obtained only for large dispersion band thicknesses to minimize the error associated with positioning of the pipet tip at the

desired level.

In order to test the accuracy of this technique, samples were taken from the mixer, which contained a known ratio of organic and aqueous phases. The sampled O/A ratio agreed within 2% in all cases, indicating that neither phase was preferentially withdrawn.

6.5 DETERMINATION OF DISPERSION DROP SIZE

In order to obtain quantitative information regarding the dispersion drop size distribution, an attempt was made to photograph the dispersion directly through the glass walls of the mixer-settler using a tripod mounted SLR camera equipped with a macro-zoom lens, and from the photographs to determine the average drop size. This method failed because the magnification was insufficient and also because excessive light reflection off the glass walls rendered the photos indistinct.

In order to circumvent these problems, it was necessary to withdraw a sample of dispersion into a small, specially constructed, glass-walled cell mounted on the stage of a 40X light microscope, and to photograph the sample through the microscope's ocular system.

The cell into which the samples were charged is illustrated in Figure 15. Using 6 bolts, two circular glass windows (1/8" thick) could be clamped to a 3/8" thick brass cylinder to form a 4" diameter X 3/8" cavity. Strips of Gore-Tex joint sealant ensured that the cavity was leakproof.

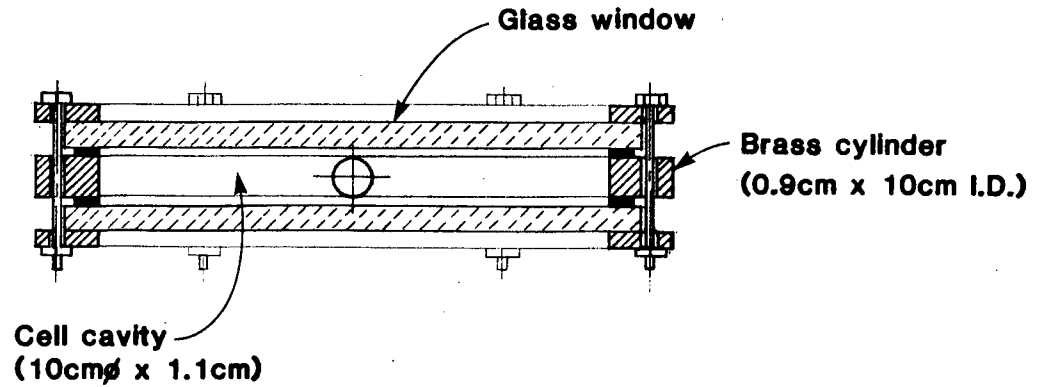
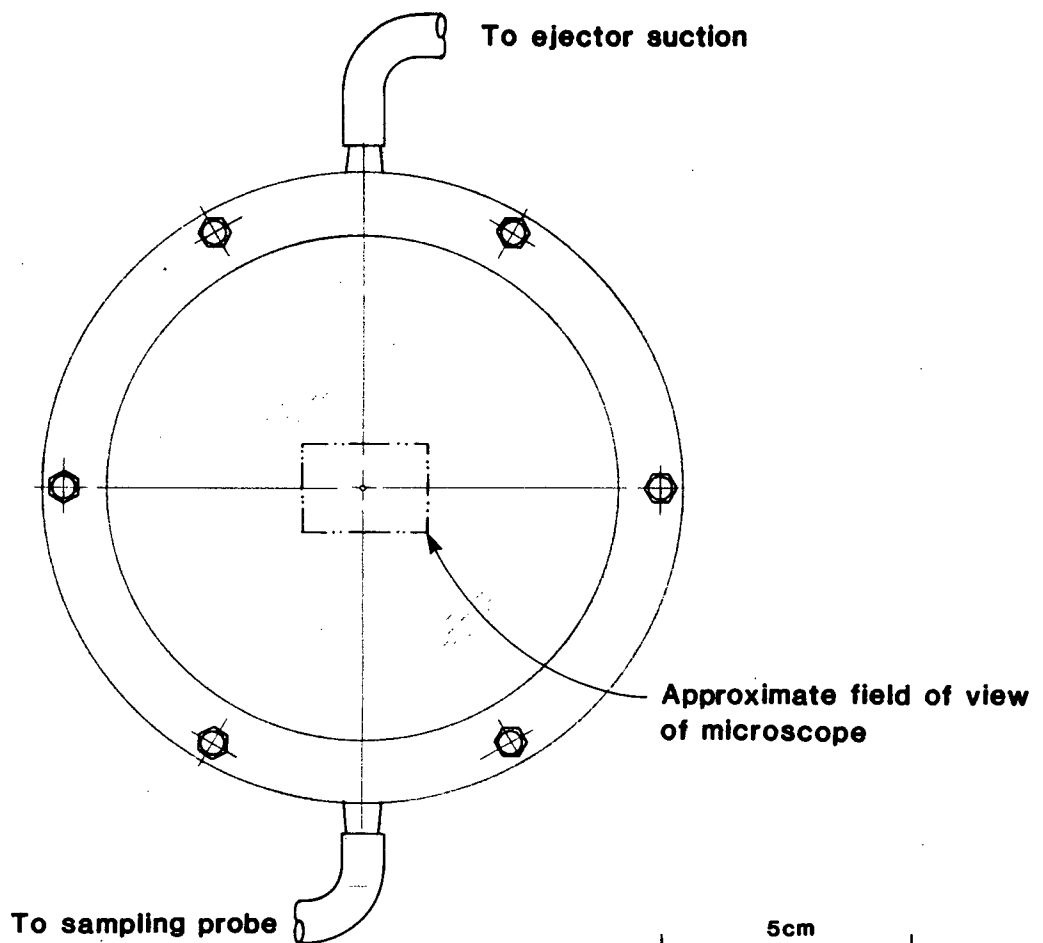
**SECTIONAL VIEW****FRONT VIEW**

Figure 15. Design of glass-walled cell used for determination of dispersion drop size.

Holes drilled through the cylindrical brass section at two diametrically opposite points were fitted with nipples which were connected to lengths of tygon tubing. One length of tubing was connected to the suction side of an ejector so that a vacuum could be applied to the cell when a stopcock on the line was opened, thereby drawing a sample of dispersion from the mixer-settler into the cell via the second length of tubing. The cell was fixed to the microscope stage such that the sample inlet connection was at the bottom and so that light from the microscope lamps could be admitted through one glass window while photographing the cell interior through the other.

The tygon sampling line was connected to a smooth-tipped glass sampling tube which could be immersed to withdraw dispersion samples from any desired location within the mixer-settler. This probe and the connecting tygon tubing had a relatively large inside diameter of over 0.7cm (approximately 10-30 drop diameters) to minimize redispersion of the sample in the line. No coalescence was observed in this transparent line during sampling.

The microscope's field of view at 40X magnification was approximately 2500 μm . Because of the apparently rapid movement of individual droplets in the sample when viewed at this magnification, a shutter speed of 1/1000 sec. at f 2.8 was utilized as well as a fast film (Fujichrome P1600D slide film) pushprocessed to 1600 ASA. The microscope lamp was adjusted to its maximum intensity. These conditions resulted in sharp

images being produced of Key Lake phase system dispersions. However, because of the opacity of the HSLIX64N organic phase, light penetration through samples of this phase system was insufficient to permit photography. Therefore, only the Key Lake phase system (organic continuous) was analyzed for drop size distribution using the microscope.

Slides of the dispersion samples were projected onto a digitizer board logging to a computer and 3 points on the circumference of each projected drop were touched with the digitizer probe. A computer program stored the coordinate values, calculated the diameter of each drop and statistically analyzed the data to determine the mean drop diameter (both arithmetic average and volume average) for each sample (slide).

6.6 ORIENTATION OF MICROSCOPE

When the organic continuous Key Lake sample was charged into the cell, batch separation commenced and the coalescence front developed at the bottom of the cell. With the cell positioned on the stage of the microscope and with the microscope maintained in an upright position, photographs of the sample would be of the coalescence front because of the camera's location below the cell. Observation of the sample in the cell with the unaided eye revealed that, as a result of the coalescence process, droplets at the coalescence front were considerably larger on average than those in the remainder of the sample. This indicates that photographs taken with this setup were not representative of the original sample.

In order to avoid the problem of obtaining photographs of the coalescence front, the microscope was tipped on its side (it had been modified to permit this) and the cell was carefully positioned on the microscope stage so that the coalescence front would not (initially) occupy the field of view of the microscope (Figure 16).

About 10 seconds normally elapsed between the time sample withdrawal was initiated and the time at which the cell was full and the first photograph could be taken.

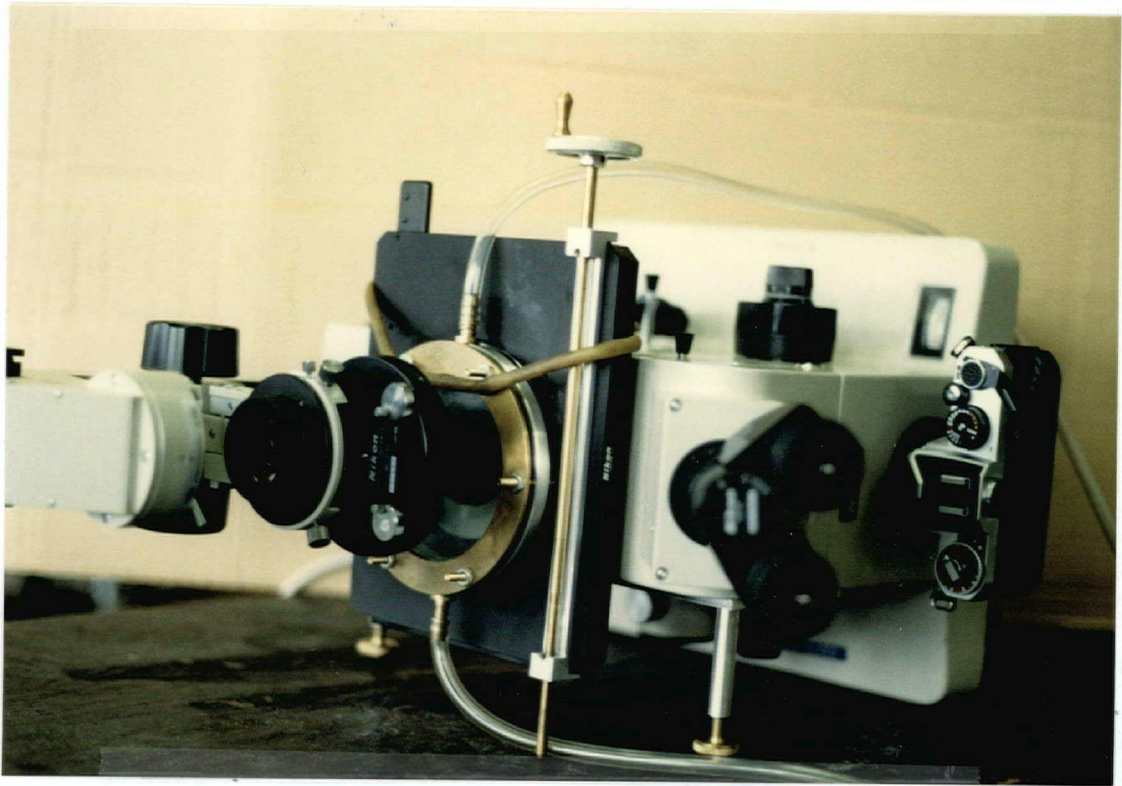


Figure 16 Photograph of arrangement of microscope and cell.

CHAPTER 7 - RESULTS AND DISCUSSION

7.1 GENERAL OBSERVATIONS OF MIXER-SETTLER OPERATION

7.1.1 DISPERSION BAND APPEARANCE

For the HSLIX64N-copper system at pH 1.9, the loaded organic phase was black in color and nearly opaque; light penetration was only a few millimeters. This contrasted with the clear gold appearance of the organic phase prior to being loaded with copper. The aqueous phase was blue-green in color and clear when free of organic entrainment. Because of the opacity of the organic phase it was necessary to utilize an intense (500 W) spotlight in order to observe the dispersion band and to identify the location of the interface between the dispersion band and the bulk organic phase.

Unlike the HSLIX64N-copper system, both phases in the Key Lake system were clear. The loaded organic phase was golden yellow in color and the aqueous phase was blue-green. The dispersion band interfaces were clearly visible to the unaided eye.

The clarity of the Key Lake phase system facilitated photographic analysis of the dispersion. The HSLIX64N - copper system, however, did not lend itself to this because of the opacity of the organic phase.

For both systems, deep layer dispersion bands existed for all experimental runs. The dispersion band thickness varied between 1 cm and 30 cm and was essentially uniform in thickness between the front and back of the settler. Only when the throughputs were reduced almost to zero was it possible to obtain a wedge-shaped band; in general the wedge was very thin and long, tapering slowly from a thickness of less than 1 cm at the settler inlet.

Although the coalescence front was sharp in all cases, the settling front sharpness depended on the O/A ratio of the dispersion and on the specific settler flow. For concentrated dispersions the settling front was easily distinguishable, while for "dilute" dispersions (i.e.: $O/A = 3$, organic continuous) the settling front became indistinct. Increased throughputs (larger ΔH 's) tended to further obscure the settling front.

It was found that, if no inlet baffle was utilized, the dispersion band would oscillate in a wavelike fashion, especially with thicker dispersion bands. Operation with the inlet baffle essentially eliminated this. The use of the baffle also reduced entrainment, as could be observed by the degree of haziness of the clear aqueous phase during runs.

Close observation of the coalescence front indicated that a significant source of entrainment was the ejection of very small continuous phase droplets, possibly produced during the coalescence of two larger droplets at the coalescence front,

into the separated phase. This had previously been observed by Davies (1970) and was thought to be a result of hydrodynamic forces.

It was generally possible, to a limited extent, to visually identify the two sublayers described by Barnea and Mizrahi. In the "dense sublayer" near the coalescence front, the droplets were closely packed regardless of the concentration of the dispersion entering the settler. The even concentration sublayer consisted of more loosely packed droplets. Although the overall movement of these drops was towards the end of the settler and towards the coalescence front, individual drops, of all sizes, appeared to move somewhat randomly.

The distinction between the two sublayers was not sharp; i.e., it appeared, visually at least, to be a somewhat gradual transition. Although there is no sharp boundary, the concept of two distinct sublayers is a useful one since readily observable structural differences do exist between the dispersion near the coalescence front and the dispersion more distant from the coalescence front.

Visual observation indicated that various flow patterns existed within the dispersion band. Besides the primary horizontal flow from settler inlet towards the end of the settler, sometimes there was also a backflow above or below the primary horizontal flow.

For other cases, it was observed that large vertical circulation patterns developed, whereby the droplets moved in one direction along the glass walls and the other direction in the interior of the settler. For example, with an organic continuous dispersion, where the coalescence front was the lower surface of the dispersion band, a relatively rapid and unexpected movement of droplets upwards along the glass walls was sometimes observed.

Such circulating flow patterns were usually, but not always, associated with high throughputs, producing thick dispersion bands. Generally, thinner dispersion bands (less than 10-15 cm) did not exhibit such circulation patterns.

Despite this generalization, it was not possible to develop any reliable criteria by which the flow pattern in the settler could be predicted. The settler frequently operated in an unpredictable manner with respect to flow patterns.

A practical conclusion which may be drawn from these observations is that the flow pattern existing in the settler may wield a considerable effect on the thickness of the dispersion band by upsetting its normal structure. Since circulation patterns usually are associated with thicker dispersion bands (the industrially significant ones) flow patterns could conceivably have a profound effect on the operation and performance of industrial settlers.

Close observation of the coalescing behaviour of the dispersion band seemed to indicate, as contended by Ryon (1959), that the majority of the coalescence did indeed occur at the coalescence front, or at least within a few centimeters of the coalescence front. Observation of the remainder of the dispersion band revealed that the droplets moved randomly and collided frequently, resulting in some coalescence, but that the amount of coalescence occurring here was small in comparison. This does not necessarily contradict the view of Barnea and Mizrahi that the coalescence in the even concentration sublayer is the limiting mechanism determining the dispersion band thickness since they contended only that its role was to coalesce droplets to the critical size permitting flow countercurrent to the draining continuous phase. This does not necessarily suggest that the number of coalescences or the volume of dispersed phase coalesced is greater in the even concentration sublayer.

7.1.2 CRUD

For both phase systems, over an extended period of time, crud would accumulate at the dispersion band interfaces, primarily at the back of the settler. Crud was silky and fibrous in appearance and possessed the color of the organic phase. It hindered coalescence and also restricted visual observation of the interior of the settler by deposition on the glass walls.

Crud was periodically removed (every 4-6 hours) from the operating mixer-settler with a strainer before accumulating to a level which appreciably hindered coalescence. This was done so that various experimental runs were not conducted with significantly differing degrees of crud buildup. The mixer-settler was also occasionally drained and cleaned to remove crud adhering to the glass walls.

Crud formation is a complex and poorly understood phenomenon, and the reader is referred to other authors for a detailed discussion of its causes (Ritcey, 1980). In general, crud can be loosely defined as the material resulting from the agitation of an organic phase, an aqueous phase and fine solid particles, commonly siliceous in nature. Living organisms existing in the aqueous phase, which die upon entering the organic phase have also been cited as a possible cause (Hill, Evans, Davies, 1967).

Crud formation appeared to be minimized by operation at higher temperatures, possibly because of greater solubility of crud-causing constituents. Also, the rate of crud accumulation with time decreased slightly as the phase liquids aged. This may simply be a result of the cumulative reduction in crud-causing constituents arising from the periodic removal of crud with the strainer.

7.1.3 OPERATION AT DESIRED PHASE CONTINUITY

With the HSLIX64N - copper system it was possible to operate either organic or aqueous continuous by adopting an appropriate start-up procedure, as described in section 6.1. For either continuity, the dispersion was stable (i.e., phase inversion did not occur) provided that the O/A ratio was maintained in the range corresponding to dispersed phase concentrations of 0% to 80% . Below 20%, however, no dispersion band was formed in the settler. Instead the dispersion entering the settler was "hazy" and limited primarily by gravitational settling rather than coalescence.

With the Key Lake system however, only organic continuous operation was possible since when aqueous continuous operation was attempted, a stable emulsion was formed in the mixer-settler which took many hours to several days to separate batchwise. Mechanical agitation reduced this time to perhaps 1/2 hour. This phenomenon occurs in industrial installations, including the Key Lake uranium extraction mill. Furthermore, when running organic continuous with the Key Lake system it was not possible to operate with a dispersed phase concentration exceeding 65% without the occurrence of phase inversion and production of a stable emulsion. In other words, the ambivalence region for the Key Lake system (organic continuous) was significantly narrower than that for the HSLIX64N-copper system.

In order to ensure that a stable emulsion did not form, it was necessary to take special precautions during startup. The impellor was started with the mixer containing only the organic phase. Thereafter, the organic and aqueous phase flowrates could be adjusted as required. It was not sufficient to simply start up the mixer with the impellor immersed in the phase to be continuous. If a significant volume of aqueous phase was present in the mixer at startup, then some stable emulsion was formed even if the dispersion eventually became organic continuous.

During organic continuous operation with both the HSLIX64N-copper phase system and the Key Lake phase system, it was sometimes observed that relatively large aqueous continuous slugs of dispersion (2-5 cm in diameter) entered the settler along with the organic continuous dispersion. It was estimated that the volumetric flowrate of the slugs constituted roughly 5-10% of the total dispersion flow to the settler. With the HSLIX64N-copper phase system, this "slug" phenomenon was also sometimes observed during aqueous continuous operation. Slugs of organic continuous dispersion would issue from the mixer along with the majority aqueous continuous phase.

The appearance of slugs was linked to two operating conditions:.

1. Inadequate mixing intensity in the mixer. Use of an impellor speed below 200-250 rpm, approximately, increased the tendency for slug formation.

2. Operation with a high dispersed phase concentration (greater than roughly 60% with the Key Lake system and 75% with the HSLIX64N-copper phase system). This may be attributed to the higher effective viscosity of a concentrated dispersion compared to a dilute dispersion. In order to adequately disperse the phases, a higher impellor speed would be required with a more concentrated dispersion.

Slug formation frequently preceded total phase inversion which could be triggered if the dispersed phase concentration was further increased or the impellor speed was decreased.

The range of O/A ratios and impellor speeds used during experiments was such that slug formation was avoided. No data was taken under conditions for which the phenomenon was observed.

7.1.4 DRIFT IN PHYSICAL BEHAVIOR OF PHASES

It was observed for the HSLIX64N-copper phase system that the dispersion band thickness obtained for identical organic continuous runs, performed roughly 2 weeks and 3 months after the newly-prepared phases had been introduced into the mixer-settler, differed substantially. Invariably, the value of ΔH obtained at the later date was greater (roughly 10-20%). A shift for aqueous continuous operation was much harder to detect (ΔH increased perhaps 5-10% for a given run). The shift may be attributed to a change in the physical properties of the phases as they aged, possibly due to the evaporation of the

more volatile components of the organic phase. A resulting increase in organic phase viscosity with time would account for the increased values of ΔH obtained at later dates. Since the viscosity of the aqueous phase would not be expected to change appreciably with time, this could explain why no large shift could be distinguished for aqueous continuous operation.

To minimize the effect of this shift and to ensure that valid comparison of different experimental runs could be carried out, all data reported for the HSLIX64N-copper system was taken within an 8 week period (starting about 2-3 months after the phases had been introduced into the equipment).

With the Key Lake system no shift in phase separation characteristics with ageing was observed. However, since experimentation with this phase system was conducted after experience in operating the equipment had been obtained with the HSLIX64N-copper system, a relatively short (4-6 week) period was sufficient to complete Qd/A- ΔH experiments.

7.1.5 EFFECT OF INTRODUCTION LEVEL ON ΔH

The entrance to the settler was fitted with an entrance baffle which served to minimize turbulence and ensure even dispersion distribution into the settler. The baffle was secured to the glass walls of the settler by clamps and could be positioned to form a 5 cm X 30 cm passageway for the flow of the dispersion to the desired introduction level. By varying the vertical position of the baffle and the setting of the

interphase regulator, the effect of the level of introduction relative to the dispersion band interfaces was determined.

The results for the HSLIX64N-copper system are tabulated in Table 6 for various operating conditions (for both organic and aqueous phase continuity). Analysis of this data does not reveal an appreciable effect of introduction level on settler performance.

For the Key Lake system, however, the level of introduction was found to have a major impact on dispersion band thickness. Examination of Table 7 reveals that in general, for a given throughput, introduction of the dispersion at or near the coalescence front resulted in the poorest settler performance (largest ΔH). This is illustrated graphically in Figure 17. In some cases (cases 1,2,3,4,9) the thickness of the dispersion band was as much as 50% greater when the dispersion was introduced at the coalescence front rather than at the settling front or interior of the dispersion band. For other cases, the magnitude of the effect was much less (cases 5,11,12,13,14,15).

Close scrutiny of Table 7 and Figure 17 shows that the primary parameter influencing the magnitude of this effect appears to be the settler area. From the table, it can be seen that for the largest settler area 0.36m^2 , the introduction level did not have a major effect on dispersion band thickness since ΔH remained constant regardless of the inlet location. This contrasts sharply with the data taken for the smallest

TABLE 6. EFFECT OF DISPERSION INTRODUCTION LEVEL ON
DISPERSION BAND THICKNESS
(SYSTEM : HSLIX64N-copper; TEMPERATURE : 24°C)

CASE	SETTLER AREA (m ²)	SPECIFIC SETTLER FLOW, Qd/A (m ³ /m ² /hr)	O/A	INTRODUCTION LEVEL (cm from coalescence front)	ΔH (cm)
A) ORGANIC CONTINUOUS:					
1.	0.13	2.76	1.5	3.	27.5
				14.	27.
				23.	27.5
2.	0.13	1.17	1.5	0.	7.
				3.	6.5
				6.5	6.5
3.	0.13	2.16	3.0	2.	19.5
				5.5	19.5
				15.	20.
4.	0.22	1.97	0.67	2.	18.5
				6.5	18.
				16.	18.5
5.	0.22	1.80	1.5	0.	11.
				5.	10.5
				10.5	10.5
6.	0.36	2.15	0.67	2.	13.5
				5.5	13.3
				12.	13.5
7.	0.36	2.22	1.5	3.	22.
				11.	21.
				18.	21.5
8.	0.36	1.33	3.0	0.	6.2
				3.	6.3
				6.	6.4
B) AQUEOUS CONTINUOUS:					
1.	0.13	2.77	0.33	0.	12.
				6.5	12.
				12.	12.
2.	0.13	3.28	0.67	1.5	15.5
				7.	15.
				14.	15.
3.	0.22	1.80	0.33	0.	6.
				3.	6.
				5.	5.5
4.	0.22	3.27	1.5	2.	20.5
				5.5	19.5
				18.	19.5
5.	0.36	2.71	1.5	1.	12.5
				6.	12.6
				13.	13.
6.	0.36	2.18	1.5	0.	8.5
				5.	8.5
				8.	8.

TABLE 7. EFFECT OF DISPERSION INTRODUCTION LEVEL ON
DISPERSION BAND THICKNESS
(SYSTEM : KEY LAKE; TEMPERATURE: 35°C).

CASE	SETTLER AREA (m ²)	SPECIFIC SETTLER FLOW, Qd/A (m ³ /m ² /hr)	O/A	INTRODUCTION LEVEL (cm from coalescence front)	Δ H (cm)
1.	0.13	2.95	1.5	3. 17.5 24.	34. 27. 27.
2.	0.13	2.67	1.5	6. 19.5	24. 19.5
3.	0.13	2.53	1.5	2. 7. 15.	22. 14.5 15.
4.	0.13	2.34	1.5	0. 4.5 11.5	16.5 12.5 11.5
5.	0.13	2.11	1.5	0. 5. 10.	10.5 9.5 10.
6.	0.13	2.15	3.0	1 6.5 15.5	18.5 16. 15.5
7.	0.22	2.13	0.67	0. 8.	8.5 8.
8.	0.22	2.25	1.5	0. 5.5 10.5	14.5 11. 10.5
9.	0.22	2.18	1.5	0. 6. 10.5	18.5 11. 10.5
10.	0.22	2.18	3.0	0. 10.5 20.	27. 21. 20.
11.	0.36	2.83	0.67	0. 9. 18.	18. 18. 18.
12.	0.36	2.33	0.67	0. 7.5 14.5	14. 15. 14.5
13.	0.36	2.17	0.67	0. 5. 10.5	10.5 9.5 10.5
14.	0.36	1.30	0.67	0. 3.	3. 3.
15.	0.36	2.45	1.5	0. 8. 16.	20. 16. 16.

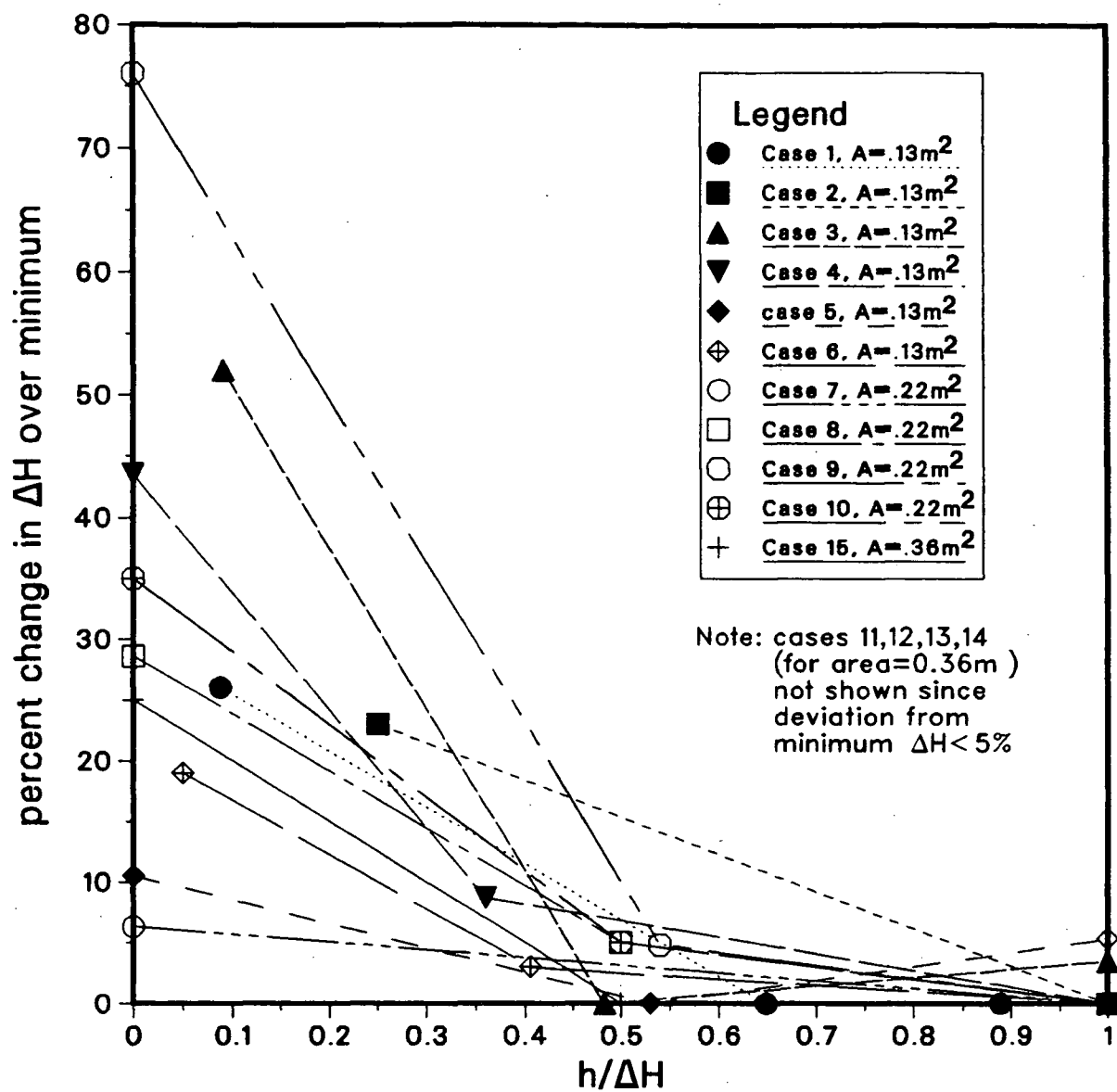


Figure 17. Effect of dispersion introduction level for Key Lake phase system for cases identified in Table 7.

settler area, 0.13m^2 , where the effect is very considerable. For these cases, (cases 1-6) the dispersion band thickness may vary by as much as 50% from the optimum depending on the introduction level.

Although the data indicates that locating the introduction level at the coalescence front should be avoided, there does not appear to be any significant advantage in locating the introduction level at the other extreme, the settling front rather than the dispersion band interior. For example, in case 3, locating the introduction level at the settling front results in a 15cm thickness as opposed to 14.5cm when the dispersion introduction level is 7cm from the coalescence front. (The thickness when introduced at the coalescence front is 22cm.) The same observation can be made for cases 1, 6, 10 and 11.

A relatively simple explanation exists for the observed trends if one considers the structure of the dispersion band in terms of the dense and even concentration sublayer concept. The dense concentration sublayer, it may be recalled, occupies the region close to the coalescence front and consists of larger and more compacted droplets than those in the even concentration sublayer. Final coalescence occurs here. The even concentration sublayer, occupying the majority of the dispersion band, consists of randomly moving, loosely packed droplets and has a density roughly equal to that of the dispersion issuing from the mixer. When the dispersion was

introduced at the level of the coalescence front, the dispersion was observed to flow towards the even concentration sublayer, as would be expected because of the density of the feed relative to the two sublayers. This flow (observed by Barnea and Mizrahi, 1976) and referred to as the "chimney flow" displaces the dense concentration sublayer near the settler inlet, effectively reducing the horizontal cross-sectional area of the settler (defined as the cross-sectional area of the coalescence front) and results in a thicker dispersion band.

If the dispersion is introduced in the even concentration sublayer, by contrast, the volume of the chimney becomes small and the dense concentration sublayer is not disturbed. The level of dispersion introduction had no observable effect on flow patterns provided that it was within the even concentration sublayer. This observation is reflected in the curves of Fig. 17; the level of introduction has no appreciable effect on dispersion band thickness provided that the dispersion is not introduced close to the coalescence front. From this, it can be concluded that the natural or optimum level of introduction is anywhere within the even concentration sublayer.

It had been noted that for large settler areas, the negative impact of introduction at the coalescence front was greatly reduced. This can be attributed to the chimney flow displacing a smaller area (on a percentage basis) of the coalescence front as settler size is increased. This suggests

that for large industrial settlers, the introduction level may not be critical.

With the HSLIX64N-copper system, introduction level had no appreciable effect on ΔH , even for small settler areas. It is suggested that this is due to differences in hydrodynamic behavior between phase systems; The chimney flow for the HSLIX64N-copper system does not disturb the dispersion band structure as seriously with this phase system.

For runs conducted to determine the ΔH - Q_d/A relationship (section 7.2) for both the Key Lake phase system and the HSLIX64N-copper system, it was ensured that the dispersion introduction level was maintained in the interior of the dispersion band, well away from the coalescence front. In this way it was ensured that the recorded values of ΔH were the optimum values. Furthermore, this practice ensured that data was taken consistently. Consistency errors which would be introduced by locating the introduction level at the coalescence front in one case and in the settler interior for another case were thereby avoided.

7.2 Q_d/A - ΔH RELATIONSHIP

By measuring the dispersion band thickness as a function of the specific settler flow it was possible to determine the validity of the settler scale-up criteria proposed by Ryon et al.(1959). This is expressed mathematically in equation (1), rewritten below:

$$\Delta H = k(Q_d/A)^y \quad (1)$$

Equation (1) implies that if ΔH is plotted against Q_d on log-log coordinates, a straight line (referred to as the characteristic curve for the phase system) should be produced. The experimental data has been presented in this conventional graphical fashion for three main cases;

1. Organic continuous operation with the HSLIX64N-copper system (Figure 18).
2. Aqueous continuous operation with the HSLIX64N-copper system (Figure 19).
3. Organic continuous operation with the Key Lake system (Figure 20).

Furthermore, for each of the above cases, data was obtained in three different sized settlers (with horizontal cross-sectional areas of 0.13m^2 , 0.22m^2 and 0.36m^2) at three different O/A ratios (corresponding to dispersion concentrations of 25%, 40%, and 60%). The mixer impellor speed was held constant at 300 rpm throughout.

7.2.1 CASE 1- HSLIX64N-COPPER SYSTEM (ORGANIC CONTINUOUS OPERATION)

The data for this case is plotted in figure 18 showing the best fit line, for all data points, obtained by least squares analysis to determine the constants k and y . The individual k and y values for each particular operating condition (i.e.: operating at one particular phase ratio for one settler size) are tabulated in Appendix 2 for Figure 18 and all subsequent

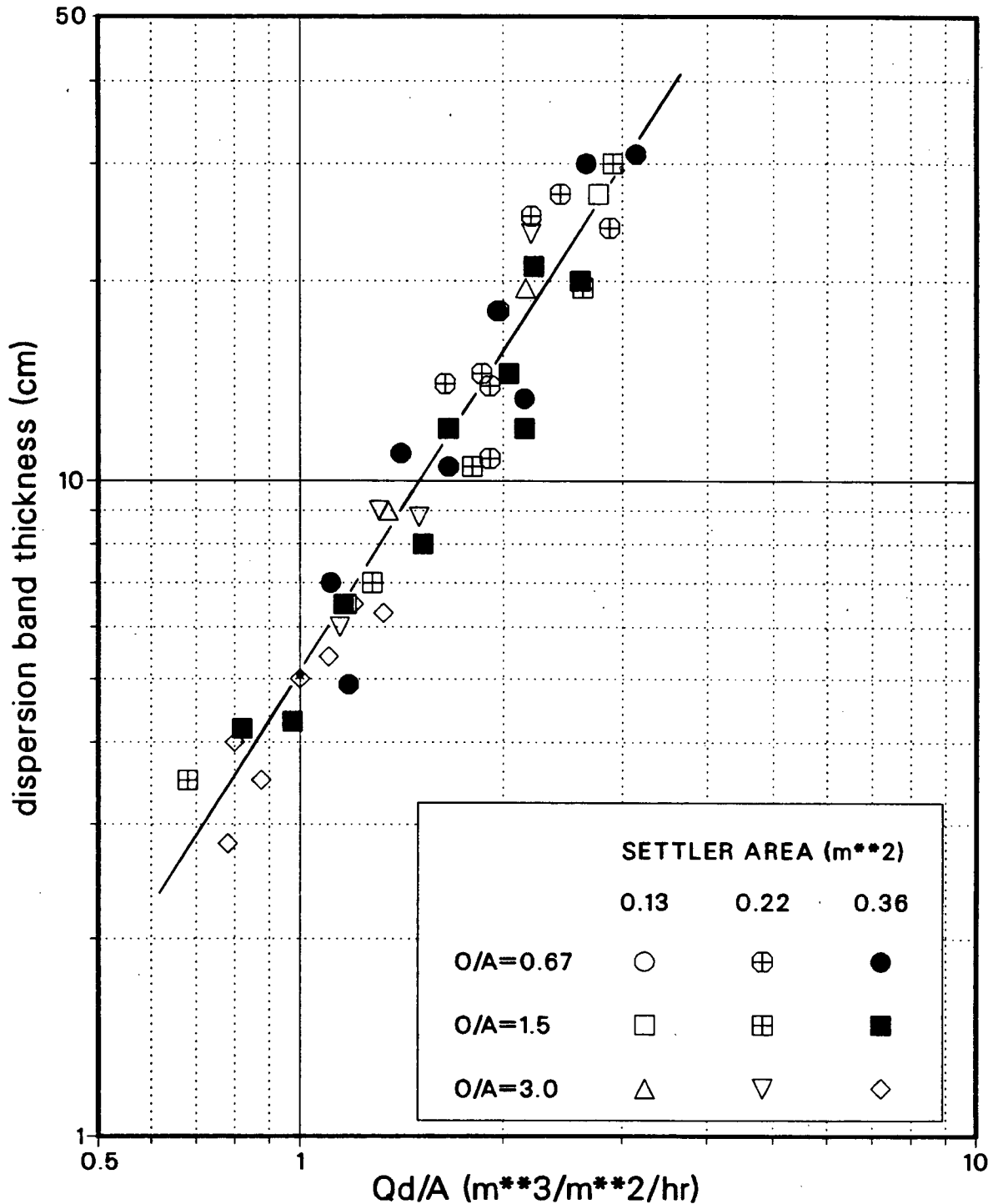


Figure 18. Dispersion band thickness versus specific settler flow of dispersed phase (effect of O/A ratio and settler area), HSLIX64N-copper system, organic continuous operation, 24°C, 300rpm.

$Q_d/A-\Delta H$ graphs.

Close scrutiny of Figure 18 shows that although there is some scatter of the points around the best fit line, the data obtained for this phase system fits the basic concept of Ryon et al. For any value of Q_d/A , regardless of the O/A ratio, the experimentally determined dispersion band thickness is within 30-40% of that predicted by equation (1). This indicates that, with the HSLIX64N-copper phase system (organic continuous), the dispersion band thickness depends only on the flow of dispersed phase and not on that of the continuous phase. A single characteristic curve can be used to adequately fit the data for all three phase ratios. This is shown statistically in Appendix 2.

This conclusion is supported by pilot plant data for the tailings leach plant at Chingola, Zambia, for a similar phase system. This system employed 23 V/V LIX64N (an earlier and less concentrated form of HSLIX64N) in Escaid 100 as the organic phase. The aqueous phase consisted of 1 g/l H_2SO_4 and had an original copper concentration of 3 g/l. This testwork had also concluded that the dispersion band depth is dependent only on the flow of dispersed phase and thus independent of the phase ratio. Phase ratios of O/A=1.0 and O/A=1.5 were employed in this study. The Chingola pilot plant data characteristic curve, however, differed substantially from the author's data. It could only be described by either a linear relationship or by an exponential relationship of lower exponent (y less than 2).

The effect of the O/A ratio is very important in industrial operation since the phase ratio can be adjusted by internal recycling between the mixer and the settler.

The data of Figure 18 exhibits considerable, apparently random scatter around the best-fit characteristic curve. Several sources of experimental error may have contributed to this:

1. After the dispersion band thickness had reached steady state, there was still some minor oscillation of the value of ΔH with time (contributing a maximum estimated error of roughly 5% to the recorded value of ΔH).
2. There was some inaccuracy involved in precisely locating the level of the settling front, especially for low dispersion concentrations.
3. The rotameter readings fluctuated slightly necessitating constant monitoring.
4. Unpredictable and varying flow patterns developed for different runs. This may alter the structure of the dispersion band somewhat and affect the dispersion band thickness produced.
5. There was a significant drift of physical behavior with time as the phase system aged, as discussed in section 7.1.4

7.2.2 CASE 2- HSLIX64N-COPPER SYSTEM (ORGANIC CONTINUOUS OPERATION)

As was the case for organic continuous operation, with aqueous continuous operation a single characteristic curve adequately predicts the settling behaviour for different phase ratios. (See Appendix 2 for a statistical analysis verifying this) This further supports the contention of Ryon that dispersion thickness is independent of continuous phase flow. Figure 19 plots all the experimental data points and shows the best fit line, obtained by considering all data points.

Comparison of Figure 18 and Figure 19, shows that, although the curves are nearly parallel, for a given value of Q_d/A , aqueous continuous operation produces a dispersion band which is roughly 50% narrower than that produced with organic continuous operation. Considered alone, this would seem to suggest that, to maximize settler capacity, aqueous continuous operation should be employed. However, visual observation revealed that a high level of haze in the aqueous phase was associated with aqueous continuous operation. This haze, resulting from organic entrainment, would constitute excessive and economically unacceptable loss of organic in a commercial plant, and explains why industrial installations operate organic continuous.

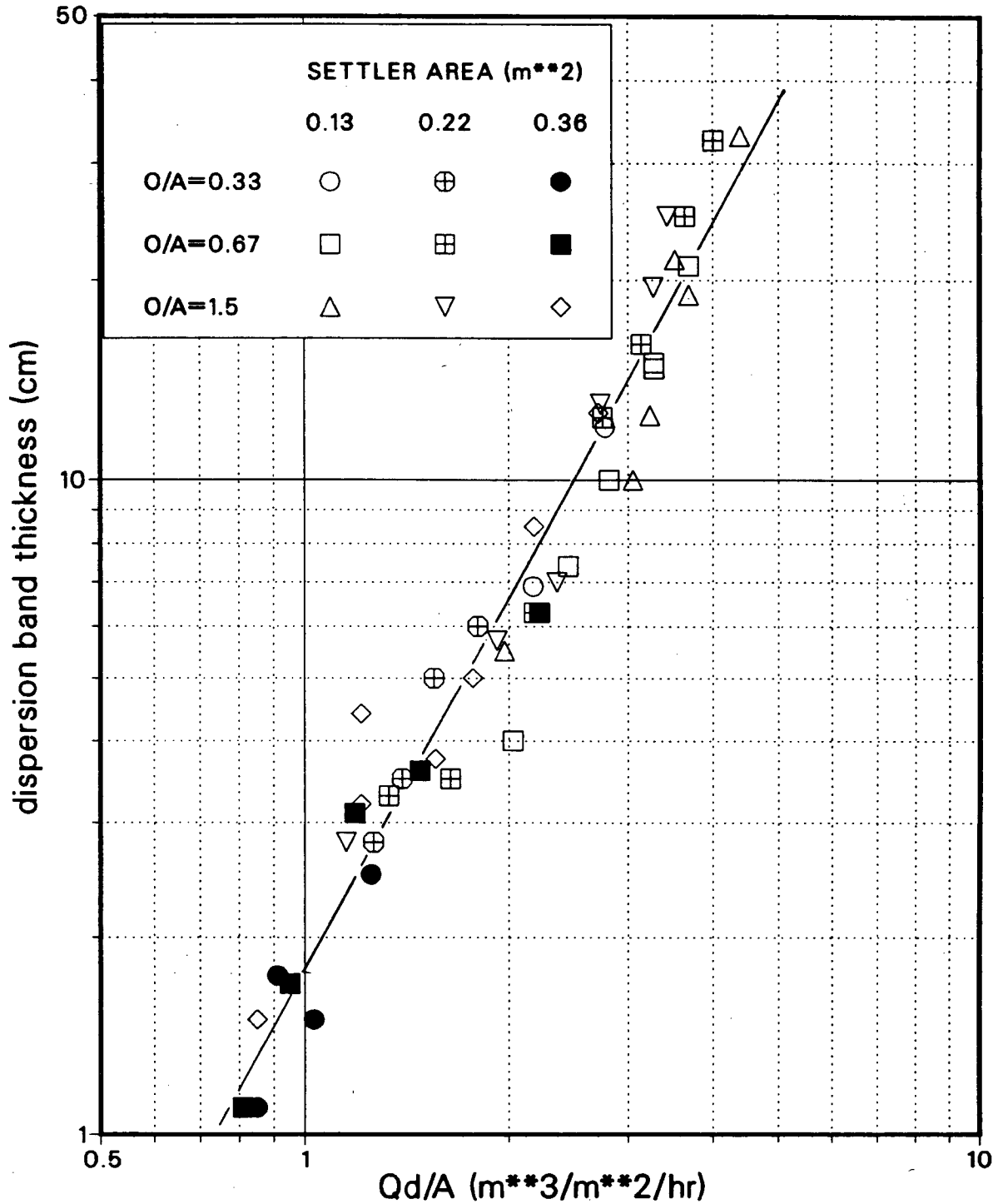


Figure 19. Dispersion band thickness versus specific settler flow of dispersed phase (effect of O/A ratio and settler area), HSLIX64N-copper system, aqueous continuous operation, 24°C, 300rpm.

7.2.3 CASE 3- KEY LAKE SYSTEM (ORGANIC CONTINUOUS OPERATION)

Because of the stability of the emulsion formed during aqueous continuous operation with this phase system, only organic continuous operation could be studied. The results, plotted in Figure 20, differ from those obtained for the HSLIX64N-copper system in one very important respect; the dispersion band thickness is here a function of both organic and aqueous flowrate (ie: it is dependent on the O/A ratio). It can be seen that a family of parallel curves are produced for different phase ratios. This has been confirmed by the statistical analysis of Appendix 2.

Although the difference in the location of the characteristic curves for $O/A=0.67$ and $O/A=1.5$ is barely perceptible, a considerable shift exists for the $O/A=3.0$ curve, representing a less concentrated dispersion. For $O/A = 3.0$, the dispersion band thickness for a given value of Qd/A is roughly 50% greater than that for $O/A = 0.67$ and $O/A = 1.5$.

In the uranium industry an O/A ratio of roughly 1.0 to 1.5 is generally employed in the extraction circuit. This, according to Figure 20, closely corresponds to the optimum with respect to phase separation. Recycling of the organic phase to raise the O/A phase ratio would result in poorer phase separation for this phase system, whereas for the HSLIX64N-copper system, settler performance would not be changed significantly.

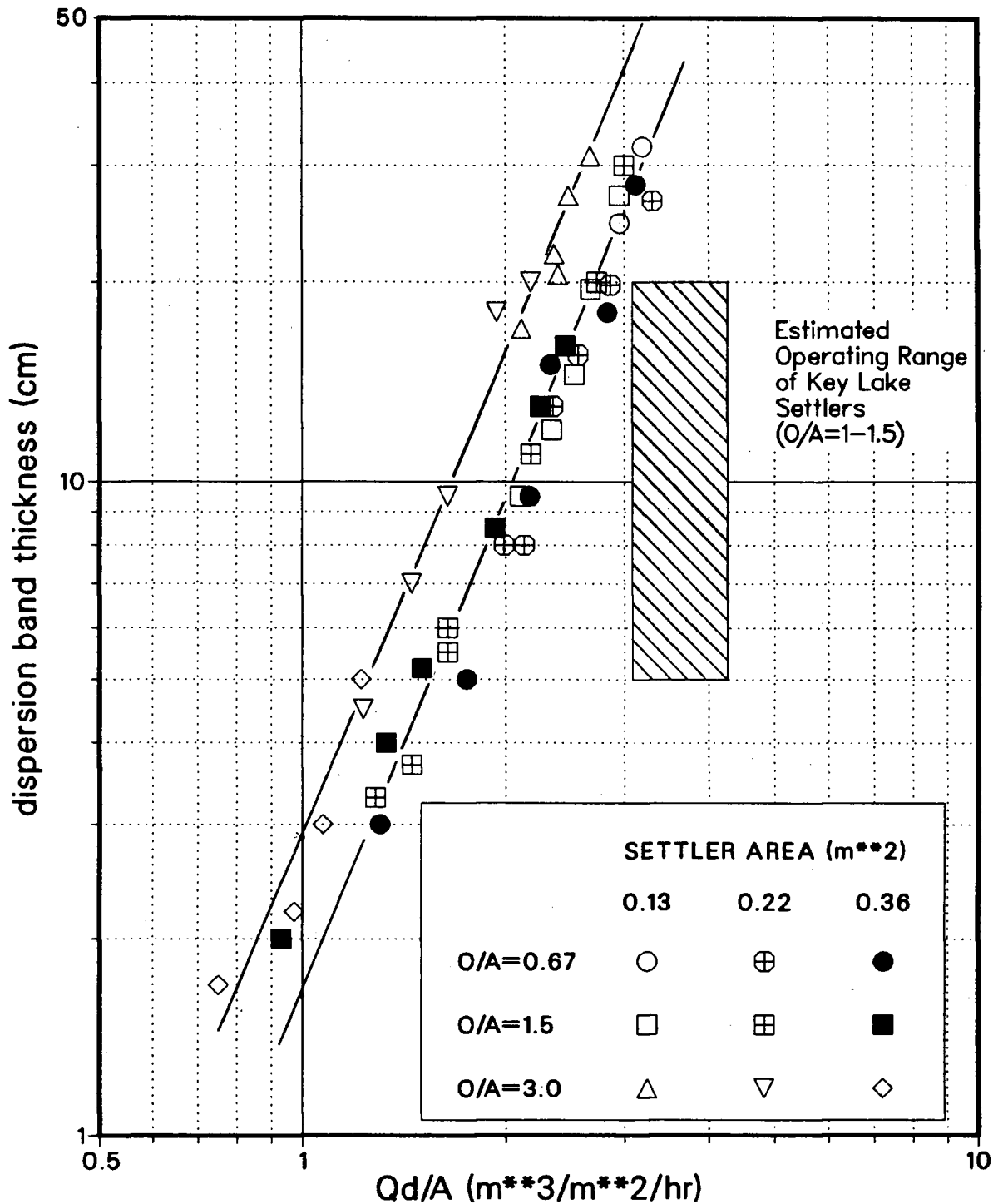


Figure 20. Dispersion band thickness versus specific settler flow of dispersed phase (effect of O/A ratio and settler area), Key Lake phase system, organic continuous operation, 35°C, 300rpm.

Another characteristic of this phase system is the low degree of scatter of the points around the best fit curve, relative to the HSLIX64N-copper system. No obvious satisfactory explanation can be forwarded for this difference in behavior, although it is possible that the behavior of this system did not drift with time to the same extent as that of the HSLIX64N-copper system, thereby minimizing this error source. The shorter duration over which the relevant data for the Key Lake system was obtained may have been a factor in this.

7.2.4 Qd/A-ΔH DATA AT KEY LAKE, SASK.

The specific settler flow, Qd/A, in the KLMC extraction stage settlers can be calculated to range from 3.08 m³/m²/hr to 4.27 m³/m²/hr. This is based on the following data:

aqueous phase flowrate:	90-125 m ³ /hr
settler width:	3.96 m
settler length [distance between inlet distributor and baffle (fig. 4)]:	7.4m

Although accurate measurements of dispersion band thickness in the Key Lake settlers are not conducted by plant personnel, ΔH has been estimated to range from 5-20 cm (Neven, 1987). The dispersion band is of the "deep-layer" type and is of near uniform thickness. The O/A ratio is maintained between 1 and 1.5 and the operating temperature is approximately 35°C.

The settler operating range corresponding to these values of Qd/A and ΔH is represented by the shaded area of Figure 20.

Comparison with the data taken from the experimental settler shows that the Key Lake settlers operate with a considerably narrower dispersion band thickness than that which would be predicted from experimental data. The data supports the claims that the Krebs settler design allows a reduction in the settler area of one-quarter to one-half of that required by conventional settlers

Two primary features of the Krebs design (Fig. 4) are purported to facilitate this enhanced performance;

1. A conical pump generates centrifugal forces which result in some coalescence of dispersion prior to discharge into the launder.
2. The launder allows some phase separation to occur before the dispersion enters the settling chamber.

It was shown mathematically in section 2.9 that if the scale up criterion of Ryon applies (as was shown to be the case in section 7.2.3), thin, superimposed settlers will provide improved settler capacity over a non-partitioned settler. This may partly explain the improved performance of the Krebs settler design; the launder may, in fact act as a thin settler, superimposed over the main settling chamber.

No data was found to provide an indication of the magnitude of the improvement due to the conical pump's centrifugal action. Therefore, the relative importance of the launder and the conical pump on the settler performance is difficult to gauge.

7.3 EFFECT OF OPERATING TEMPERATURE

The effect of operating temperature on the location of the characteristic curve was investigated for the HSLIX64N-copper system. The results, graphed in Figure 21, show that a higher operating temperature results in an increased settler capacity, the characteristic curve being shifted downwards without perceptible change of slope. This can be attributed primarily to the decrease in the continuous phase viscosity with increased temperature which does the following:

1. increases the rate of drainage of the continuous phase between 2 drops, facilitating more rapid coalescence.
2. increases the terminal settling velocity of the droplets.

The Key Lake system was studied only at 35°C because of its increased tendency for stable emulsion formation at lower temperatures.

In industrial operation, the increased settler capacity facilitated by operation at higher temperatures must be weighed against any extra costs associated with heating of process solutions.

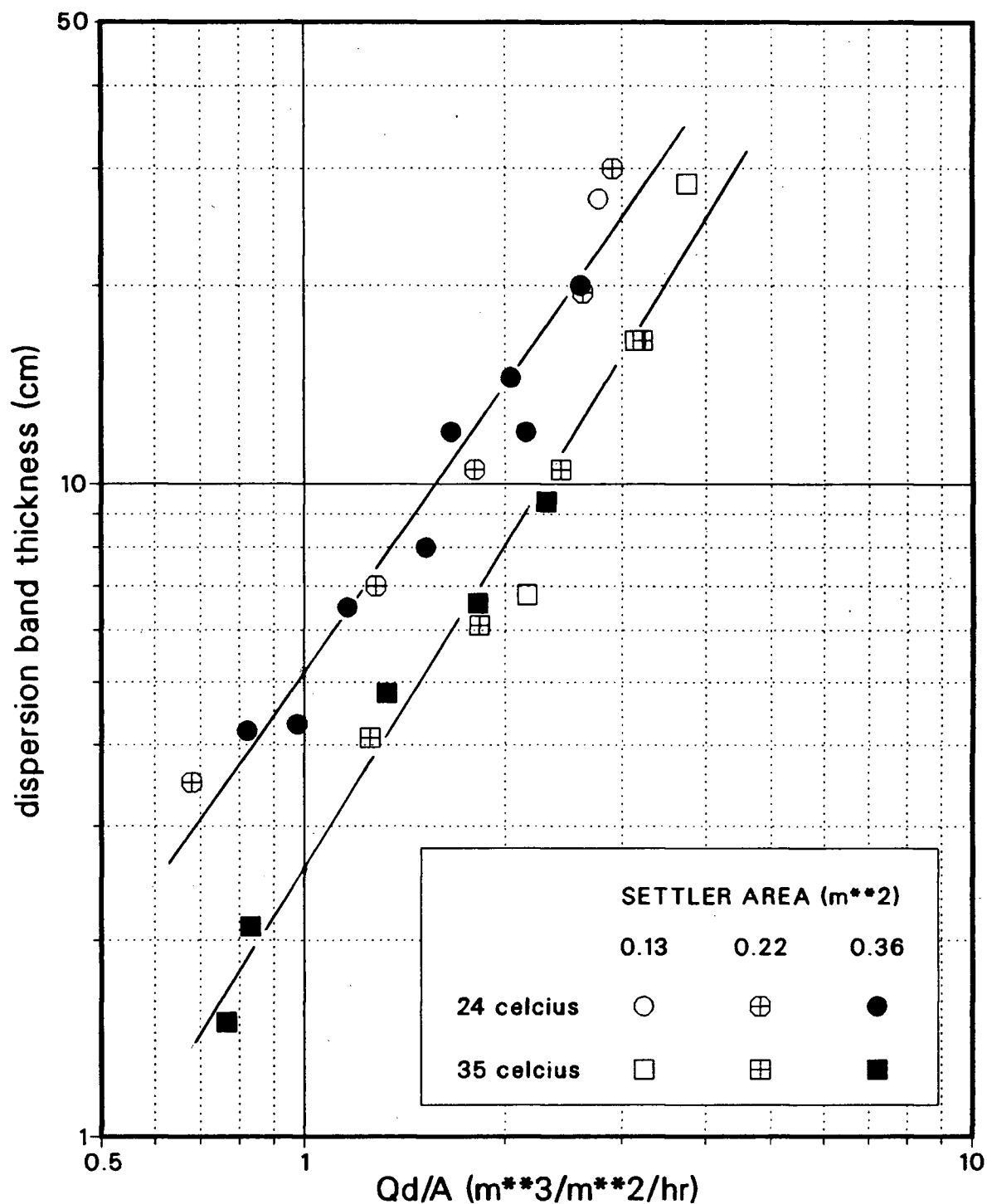


Figure 21. Dispersion band thickness versus specific settler flow of dispersed phase (effect of operating temperature), HSLIX64N-copper phase system, organic continuous operation, 300rpm, $O/A=1.5$.

7.4 EFFECT OF IMPELLOR SPEED

In order to establish the degree of "sensitivity" or "insensitivity" of the experimental phase systems to mixing intensity, runs were conducted at impellor speeds of 250, 300 and 350 rpm (the maximum speed of the mixer). No runs were conducted with impellor speeds under 200 rpm since visual observation showed that the dispersion produced was sometimes not homogeneous in the sense that relatively large slugs of a single phase would exit the mixer without a dispersion being produced (section 7.1.3). Sampling of the local holdup in the mixer confirmed the homogeneity of the dispersion above 250 rpm. Above this speed the O/A ratio was constant throughout the mixer, even at points just centimeters from the inlet ports.

Results of this study are tabulated in Figures 22, 23 and 24 for the cases of organic continuous operation (HSLIX64N-copper system), aqueous continuous operation (HSLIX64N-copper system), and organic continuous operation (Key Lake system), respectively. In all cases, the impellor speed had no discernable effect on the characteristic curve within the range studied, indicating that the systems were insensitive to agitation intensity. Had the systems instead been found to be sensitive, then comparison of runs in which the residence time of the phases in the mixer was different (i.e., different flow rates) would have become very difficult. With a sensitive system, if the flowrate were changed, the change in the power input per unit volume would also change the dispersion

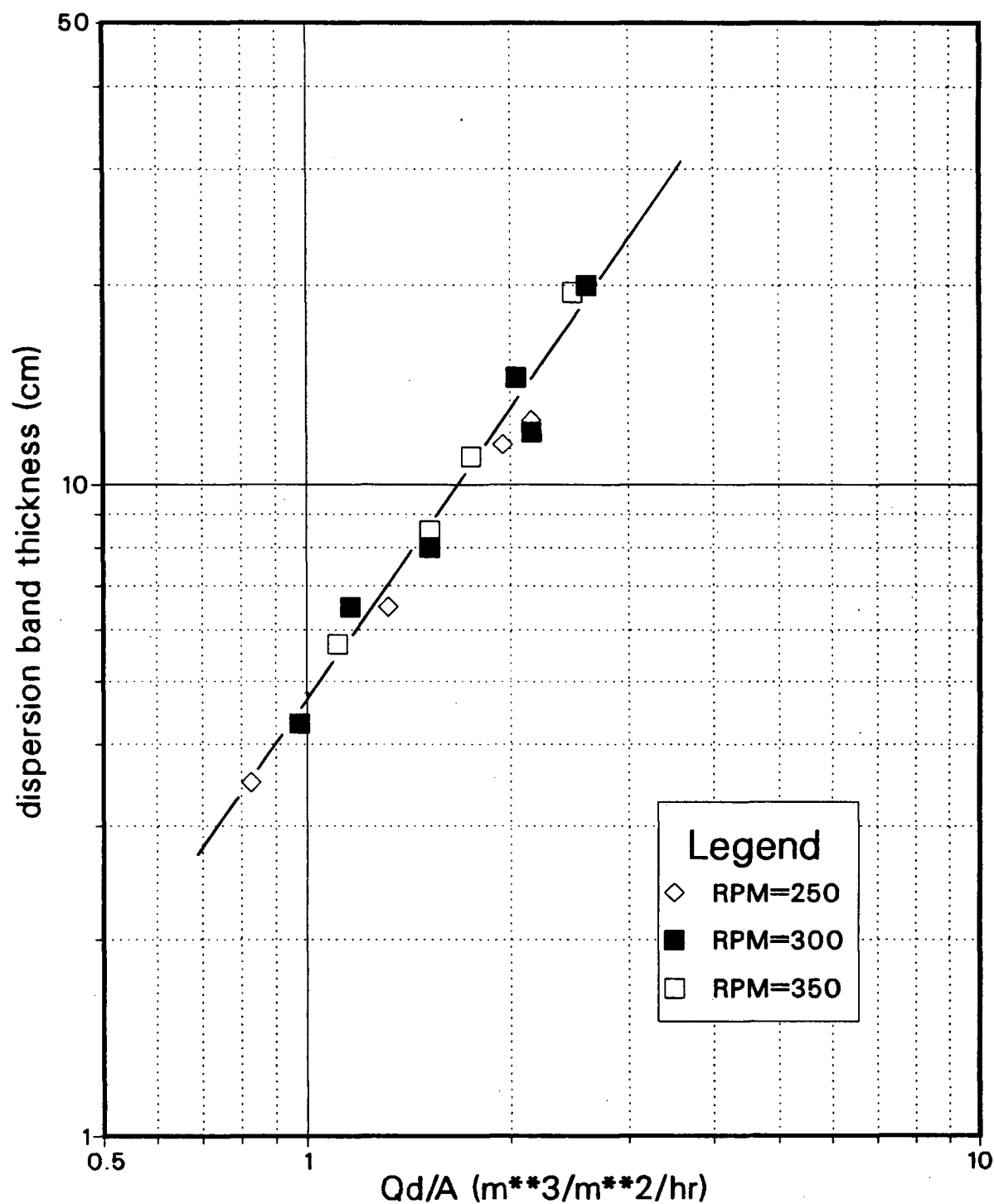


Figure 22. Dispersion band thickness versus specific settler flow of dispersed phase (effect of impeller speed), HSLIX64N-copper phase system, organic continuous operation, 24°C.

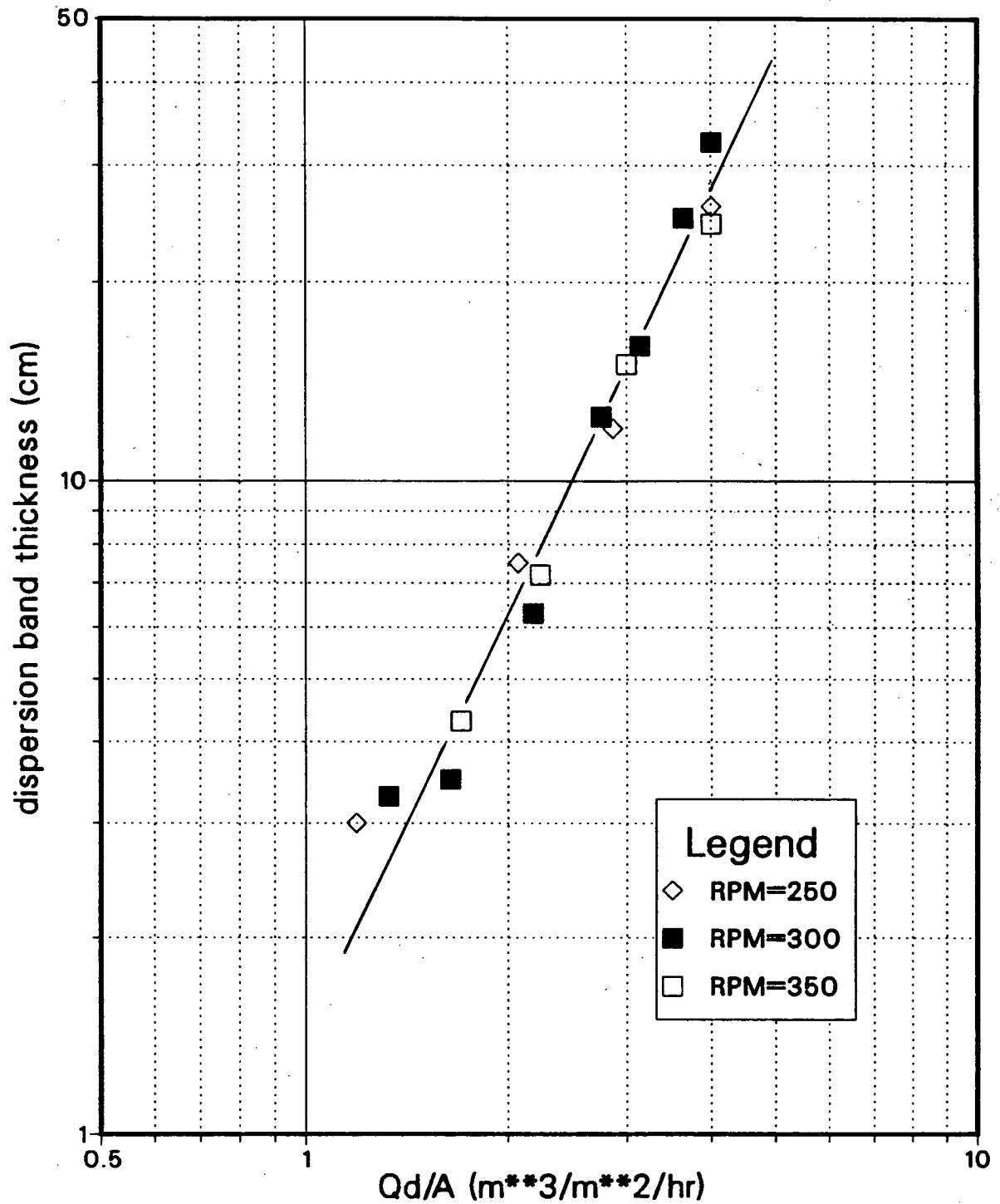


Figure 23. Dispersion band thickness versus specific settler flow of dispersed phase (effect of impellor speed), HSLIX64N-copper phase system, aqueous continuous operation, 24°C.

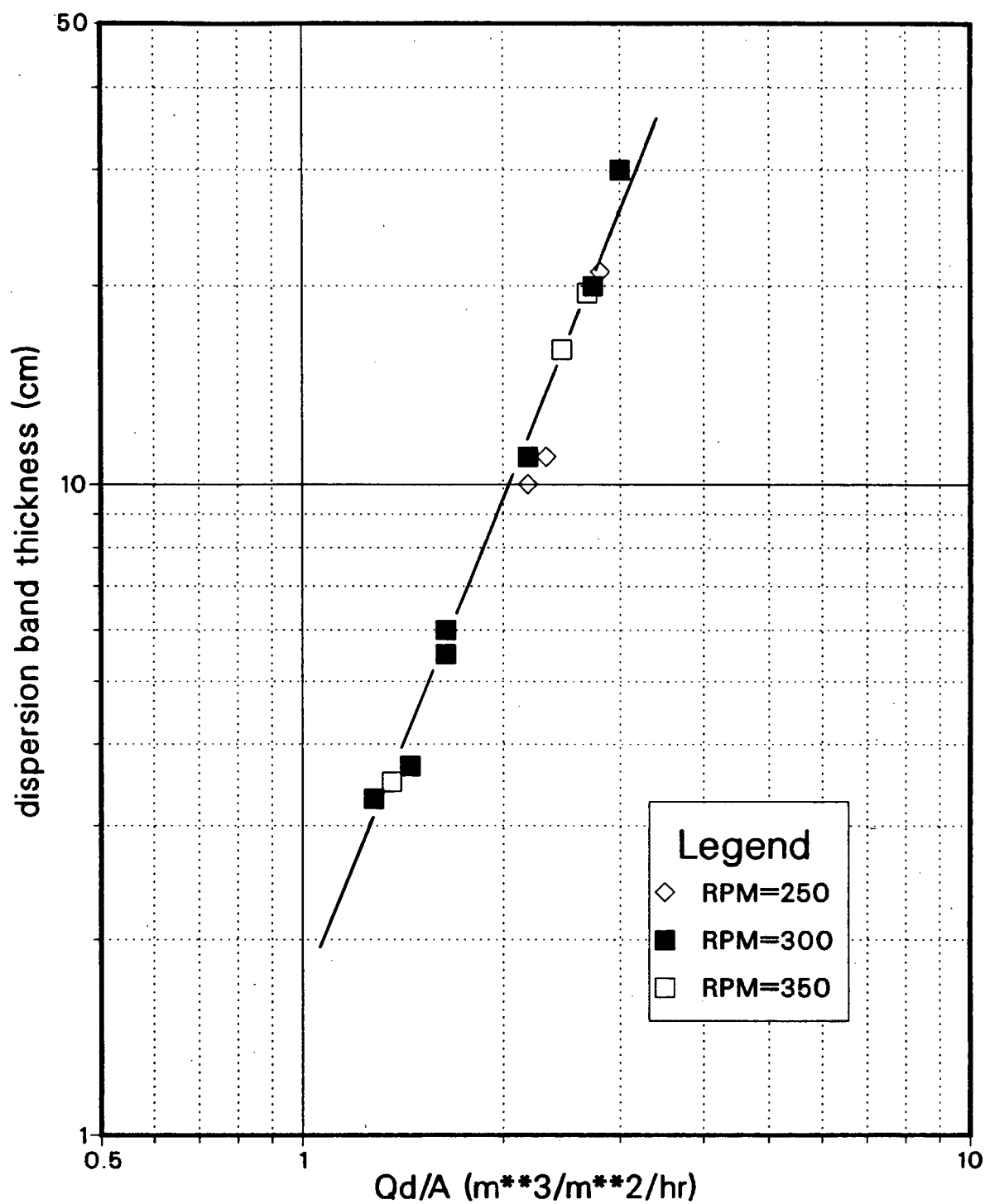


Figure 24. Dispersion band thickness versus specific settler flow of dispersed phase (effect of impellor speed), Key Lake phase system, organic continuous operation, 35°C.

characteristics. Fortunately, the systems being investigated did not exhibit strong sensitivity to mixing, thereby making exact duplication of mixing regimes for different runs less critical.

7.5 DISPERSION BAND HOLDUP PROFILES

In order to gain insights into the mechanism of phase separation, an experimental investigation of the structure of the dispersion band was undertaken by withdrawing samples from various vertical locations within the dispersion band to determine the dispersion band holdup profile. It was then possible to compare these results with those of Barnea and Mizrahi (section 2.3).

The following cases were studied:

1. organic continuous operation (HSLIX64N-Copper System), Fig. 25.
2. aqueous continuous operation (HSLIX64N-Copper System), Fig. 26.
3. organic continuous operation (Key Lake System), Fig. 27.

The results for these three cases indicate that the concept of the existence of two distinct sublayers cannot be extended equally to all phase systems.

For the case of organic continuous operation with the HSLIX64N-copper system (Figure 25), it can be seen that for low feed concentrations (0.3, 0.4, 0.5 vol. % dispersed phase) it was not possible to distinguish the two sublayers. The

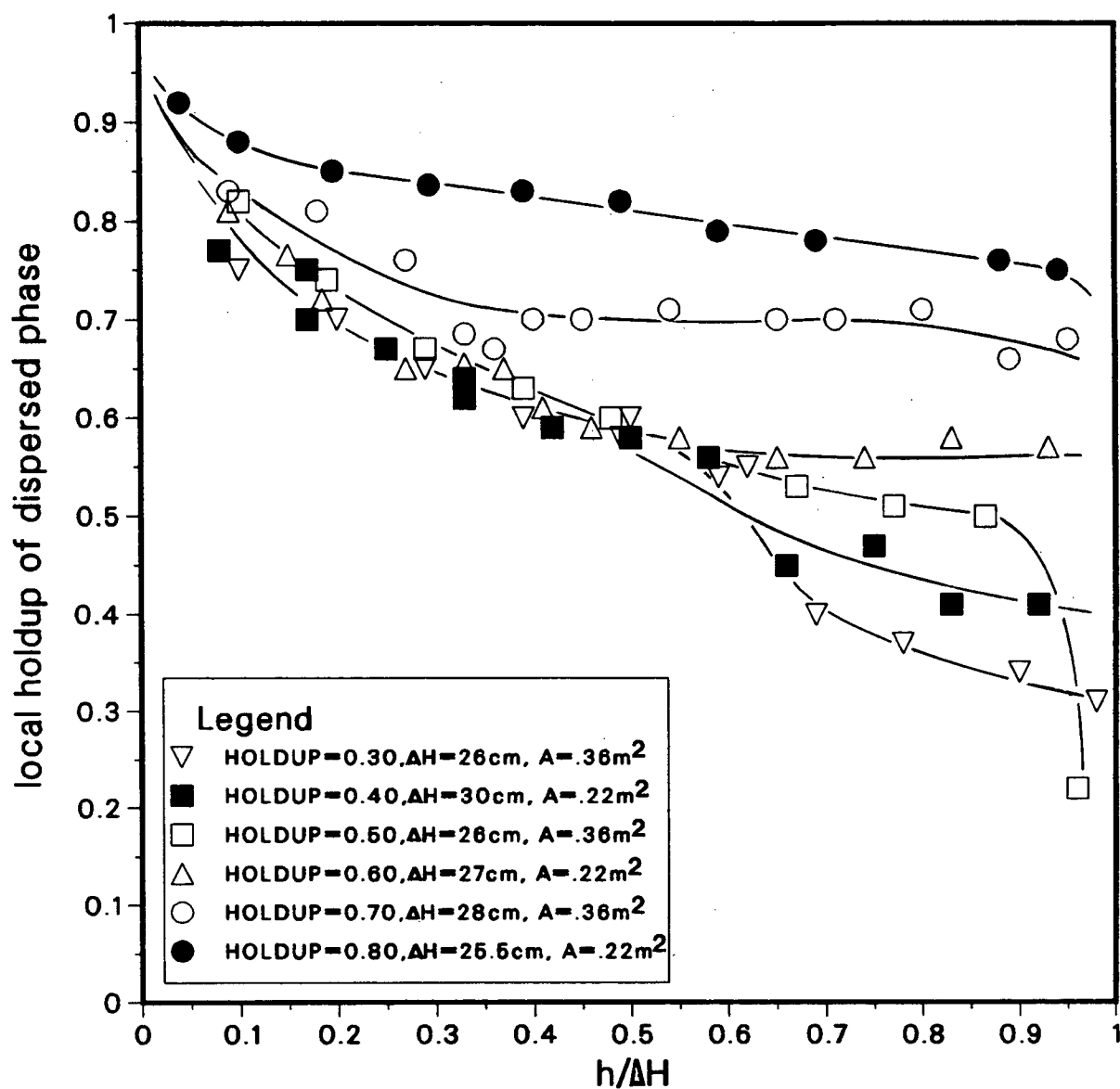


Figure 25. Holdup profiles within dispersion band, HSLIX64N-copper phase system, organic continuous operation, 24°C, 300rpm.

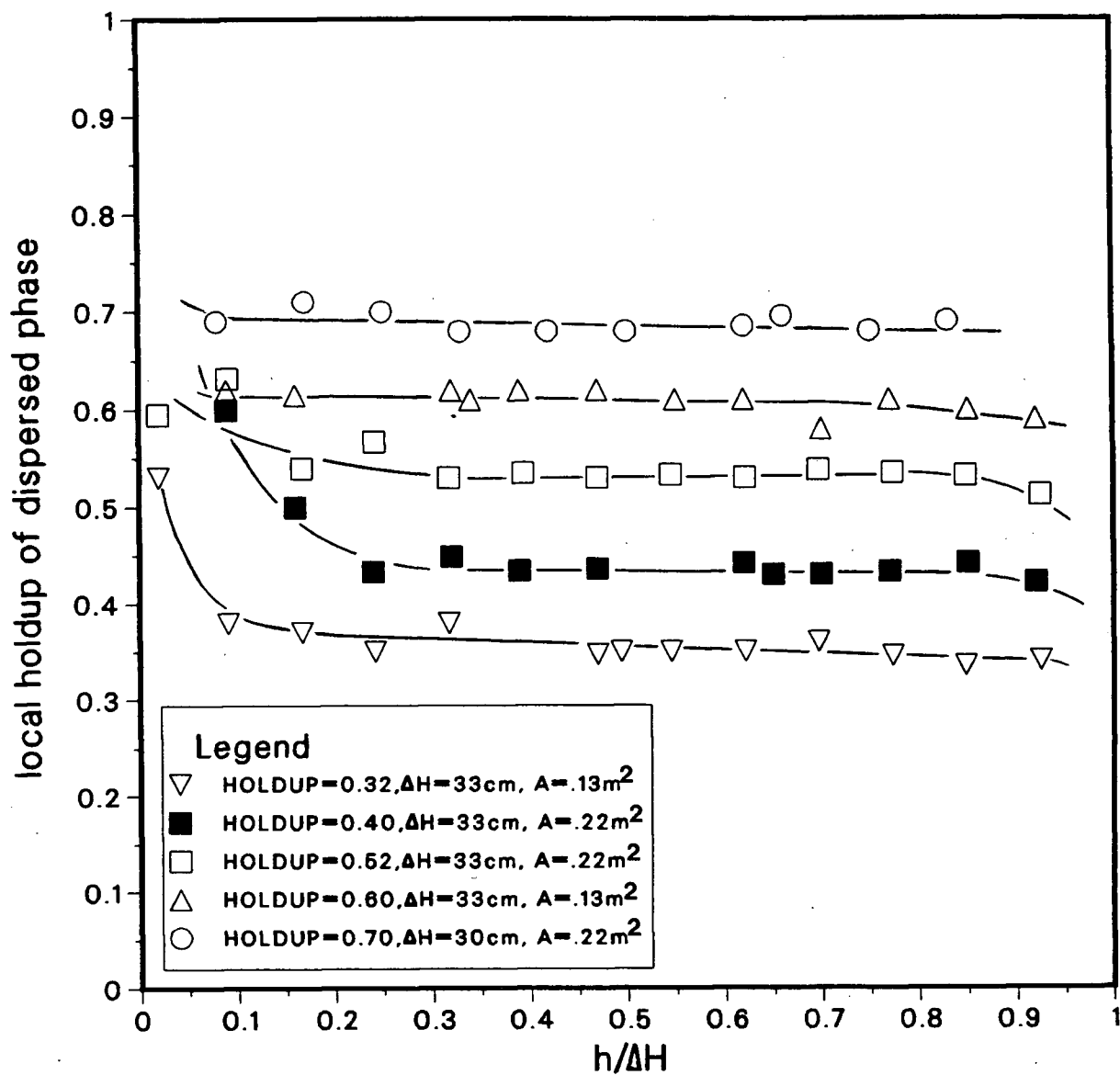


Figure 26. Holdup profiles within dispersion band, HSLIX64N-copper system, aqueous continuous operation, 24°C, 300rpm.

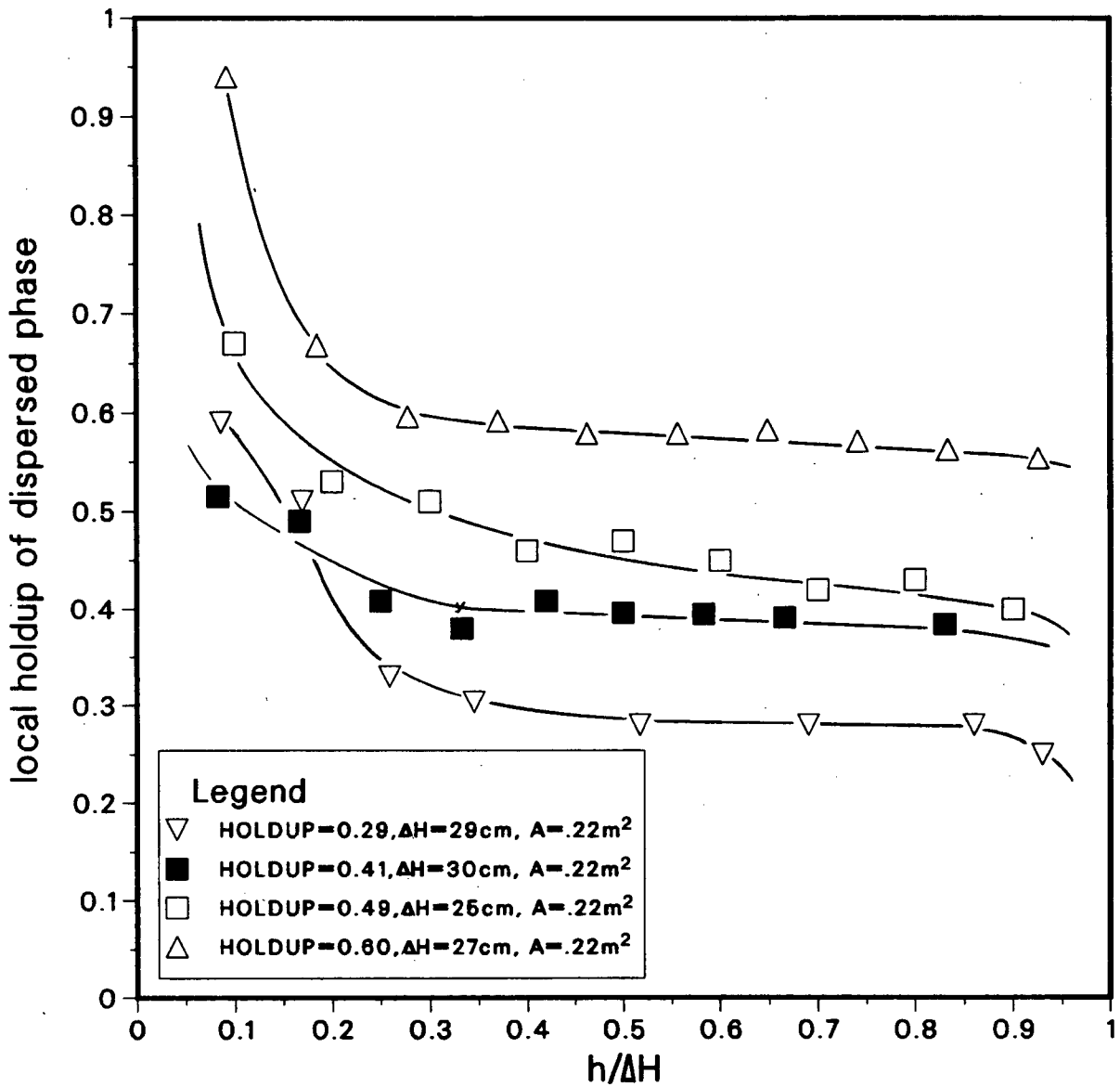


Figure 27. Holdup profiles within dispersion band, Key Lake phase system, organic continuous operation, 35°C, 300rpm.

concentration increased smoothly and evenly from the settling front to the coalescence front. For these cases, the results support the observations of Gondo and Kusonoki (1969) who found that, regardless of the concentration of the feed to the settler, the overall (average) holdup in the dispersion band was roughly 0.55.

For higher feed concentrations, however, (0.6, 0.7, 0.8 vol. % dispersed phase) the concentration was found to be relatively constant throughout the majority of the dispersion band (identifying the even concentration sublayer), with a discernable increase at the coalescence front (identifying the dense sublayer).

Figure 26, for aqueous continuous operation with the HSLIX64N-copper system, shows closer agreement with the studies of Barnea and Mizrahi. For all feed concentrations, the concentration profile showed an even concentration throughout the dispersion band extending essentially to the coalescence front. For some curves, no increase in concentration near the concentration front could be detected, suggesting that the dense concentration layer, if present, must be very narrow to avoid detection with the sampling probe, occupying less than perhaps 5% of the dispersion band.

Figure 27, for the Key Lake system (organic continuous) exhibits the best agreement with the predictions of Barnea and Mizrahi. For all holdup values studied, both the dense concentration sublayer and the even concentration sublayer are

clearly distinguishable. The dense concentration sublayer for this case occupies roughly 20-25% of the dispersion band. The concentration in the even concentration sublayer is roughly that of the incoming feed.

The variation in the relative sizes of the two sublayers and the actual lack of distinguishable sublayers in some cases illustrates the tremendous variation in the behavior of various phase systems and the difficulties encountered in developing a universally applicable concept of the phase separation mechanism.

7.6 DISPERSION DROP SIZE DISTRIBUTION

7.6.1 GENERAL OBSERVATIONS

Visual observation of dispersion drops through the glass walls of the settler showed that the droplets near the coalescence front were, in general, noticeably larger than those in the remainder of the dispersion band and grew larger as they approached the coalescence front. In addition, these droplets appeared to increase in size towards the end of the settler. With the unaided eye, however, for those droplets occupying the remainder of the dispersion band, no appreciable difference in drop size in either the horizontal or vertical direction could be detected.

Because of the small diameter of the droplets (50-500 μm), the use of the unaided eye alone was inadequate for detailed analysis of the dispersion drop size distribution and could

provide only the most general information regarding drop size. In order to obtain more quantitative information, the technique described in section 6.5 was used. Dispersion samples were charged to a glass cell, mounted on the stage of a microscope and then photographed through the microscope's ocular arrangement. The drop size distribution was then determined from the photographs.

When a sample was charged to the cell, batch separation would commence; the coalescence front and settling front would develop and would advance towards each other until, 20 to 40 seconds after the sample had been charged to the cell, disengagement of the 2 phases would be complete.

For each sample, it was visually observed through the microscope, that the average drop size remained substantially constant with time until approximately 30-50 seconds after initial sample withdrawal, the coalescence front had advanced to briefly occupy the microscope's field of view. Droplets in the vicinity of the coalescence front were considerably larger and more compacted than those in the remainder of the sample and coalescence occurrences were readily observable. In contrast, no significant coalescence was observed before the coalescence front had advanced to fill the field of view.

The visual observation that the drop size did not change substantially with time except at the coalescence front, was verified photographically. Samples, representative of the dispersion entering the settler for 5 different mixer operating

conditions, were withdrawn from the mixer overflow. Through analysis of photographs taken successively after the cell had been charged, the change in sample arithmetic mean drop size prior to the coalescence front occupying the field of view, as observed through the microscope, was determined (figure 28).

Examination of Figure 28 shows that the arithmetic mean drop diameter changed minimally (less than 20 %), between the time of the first photograph, taken 15 seconds after sample withdrawal, and the time of successive photographs. An exception is sample 1 with an O/A ratio of 0.67. In this case, the last photograph of the series, corresponding to $t=30$ seconds represents a mean drop diameter of over 600 μm , compared to 375 μm for the first point of the series ($t=10$ seconds). This large drop size can be attributed to inadvertently photographing the coalescence front as it passed through the microscope's field of view immediately before completion of phase disengagement.

The observation that the drop size changes minimally with time is an important one. It establishes the validity of the assumption that the size distribution determined from a photograph taken after the cell had been charged, about 10 seconds after initial sample withdrawal, was representative of that of the dispersion taken from the mixer-settler. Had the drop size changed significantly with time, photographic analysis for drop size distribution would have been complicated in that it would have been necessary to extrapolate drop size

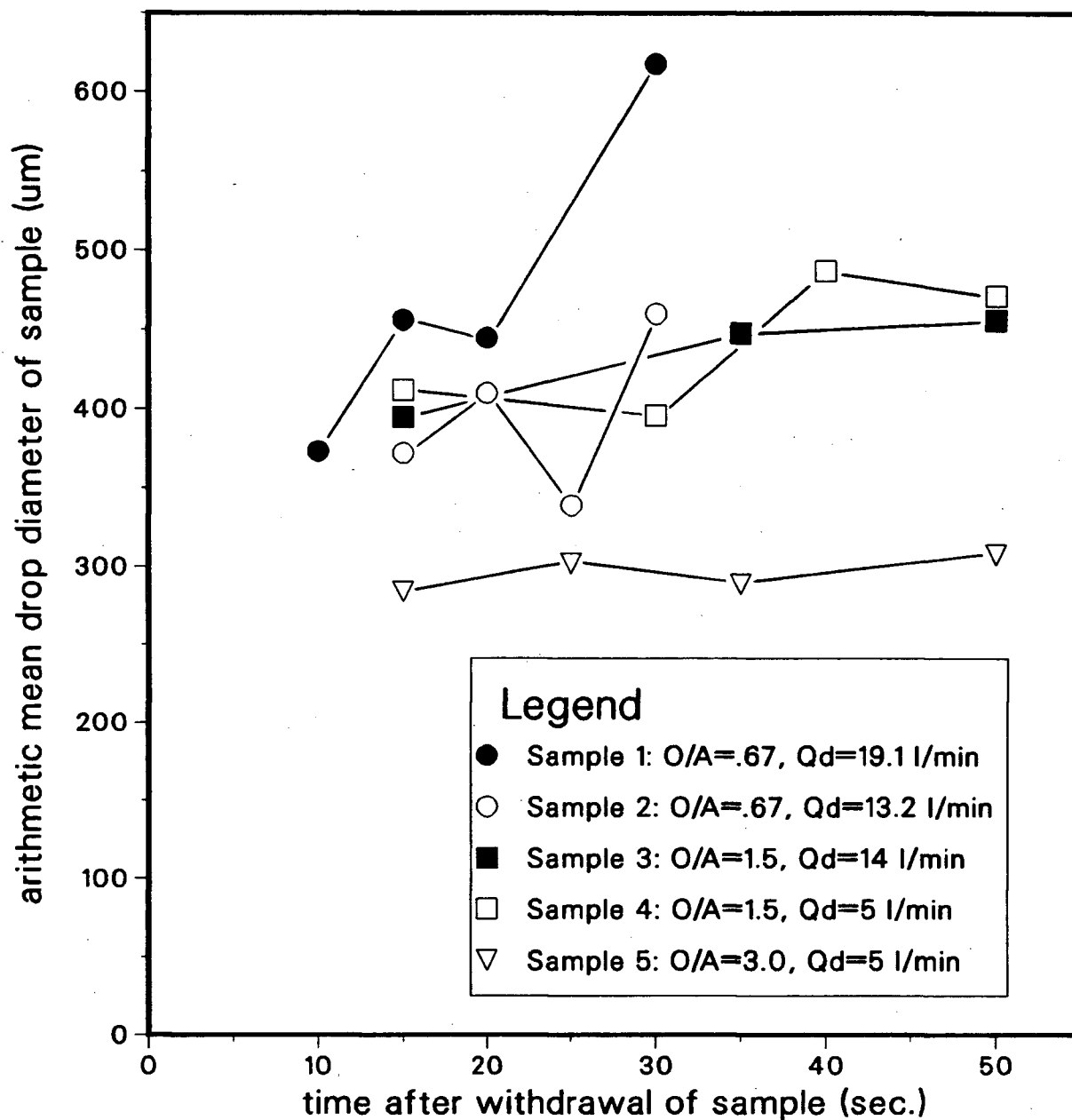


Figure 28. Change in arithmetic mean drop size of dispersion sample with time after withdrawal from mixer, Key Lake phase system, organic continuous operation, 35°C , 300rpm.

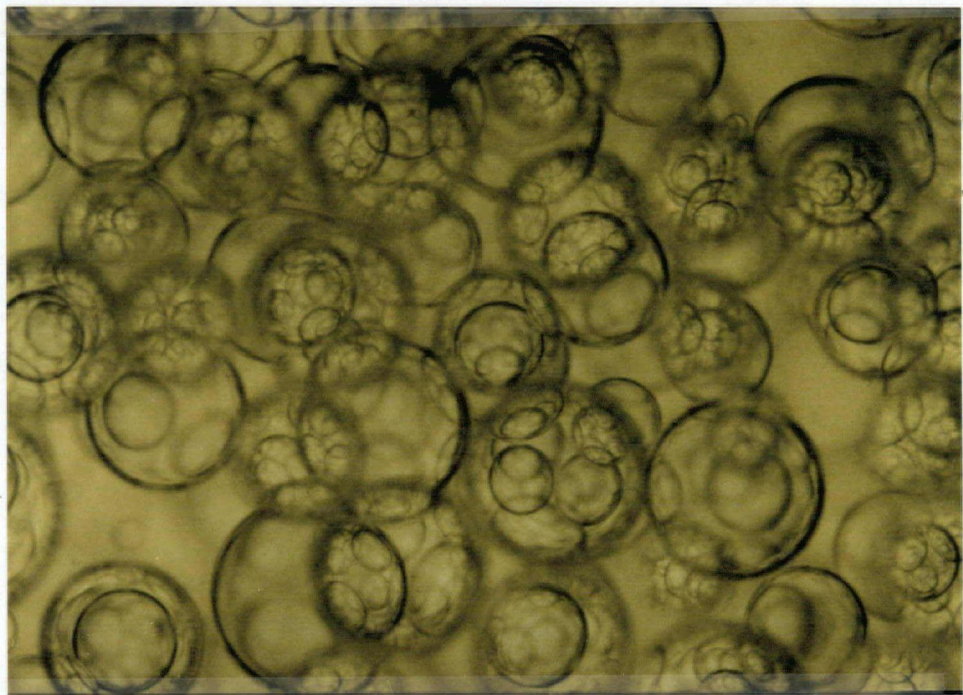
data back to zero time in some manner, in order to approximate the actual mean drop size of the original sample.

Data points were obtained in all cases from single photographic slides, typically showing about 30-60 droplets. Although this sample size is relatively small and could result in a significant statistical error in mean drop size, it was thought to be acceptable since the purpose of the drop size determinations was merely to establish general trends in dispersion mean drop size with changing parameters, not to obtain precise drop size values. In any case, determining the precise drop size would have no practical application since impellor geometries and mixer-settler arrangements and operating conditions vary between industrial installations and would result in varying drop sizes.

7.6.2 DOUBLE AND TRIPLE DISPERSIONS

An interesting revelation of the photography was the appearance of double and, to a lesser extent, triple dispersions; that is, drops within drops within drops. The outer, primary drop (aqueous phase) was spherical in all cases while the secondary drops within this drop (organic phase) were somewhat deformed (Figure 29).

The phenomenon, although significant for all samples under all operating conditions, appeared to be somewhat less prevalent for samples withdrawn close to the dispersion band coalescence front. This indicates that the encapsulated



1000 μm

Figure 29. Photograph of double dispersion sample withdrawn from settler inlet, Key Lake phase system, organic continuous operation, $O/A=1.5$, 35°C , 300rpm.

droplets were expelled to some degree as the droplets aged, possibly as a result of coalescence.

Note: In analyzing the slides, secondary and tertiary drops were not digitized and therefore they did not influence the calculated drop size distribution. These drops were omitted since each assembly moved as a single unit.

The appearance of a double and triple dispersion has several implications.

1. The secondary organic droplets could be carried close to the coalescence front by the encapsulating primary droplet and then be ejected when the primary (aqueous) droplets coalesce. This would be expected to increase organic entrainment and losses in the mixer-settler. Because of this adverse effect of multiple dispersions, it would be worthwhile to strive to design industrial mixers to minimize the occurrence.
2. Since the effective density of primary droplets varies depending on the number and size of encapsulated droplets, mathematical analysis of the settling process is complicated: individual droplets have different terminal velocities and thus exhibit different hydrodynamic behaviors.

During observation of the dispersion band in the mixer-settler, it was noted (section 7.1) that the coalescence of two droplets at the coalescence front was frequently

accompanied by the ejection of a small continuous phase droplet into the settled dispersed phase. This was attributed to hydrodynamic forces. However, it is also possible that the ejected droplets may actually have been secondary (encapsulated) droplets, released upon the coalescence of the primary droplet. Because of the small sizes and the difficulty of observing the phenomenon, the mechanism was not clearly established.

Key Lake Mining Corporation has indeed reported organic losses greater than expected; two to three times higher than guaranteed (Neven, 1987). Since no microscopic examination of the dispersion itself has been carried out at the plant to date, it cannot be confirmed whether these high organic losses could be attributed to double dispersion formation.

Observations at Key Lake have revealed large "slugs" of aqueous continuous dispersion entering the settler when the circuit is upset. This slug phenomenon was also observed in the experimental mixer-settler, principally when the concentration of the dispersed phase was high or when the mixer impellor speed was insufficient to adequately disperse the phases (section 7.1.3).

This similarity in behavior, coupled with the fact that the experimental phase system should be representative of that existing in the Key Lake circuit, allows one to conclude that it is highly likely that the double dispersion phenomenon occurs at Key Lake. It is possible that this may be

contributing to the high solvent losses.

No references to the appearance of double and triple dispersions in industrial phase systems were found. Pike and Wadhamen (1971) observed the phenomenon using a phase system consisting of water and a commercial aliphatic petroleum fraction (AMSCO 460 solvent, by the American Mineral Spirits Company, Palatine, Ill.). The small size of the secondary and tertiary droplets makes it difficult to distinguish them with the unaided eye, possibly explaining the limited reports on the subject. It would be reasonable to assume, however, that the phenomenon does occur to some degree in industrial mixer-settlers, at least with the Key Lake phase system, since it was observed experimentally under all operating conditions.

7.6.3 EFFECT OF O/A RATIO AND Q_d ON MIXER DROP SIZE

A series of samples were taken at the mixer overflow in order to determine the effect of mixer O/A ratio and dispersed phase flowrate on the arithmetic mean diameter of the droplets entering the settler.

The results, presented in Figure 30 show that, for a given O/A ratio, the dispersed phase flowrate has no appreciable effect on the drop size. This indicates that residence time in the mixer at a given phase ratio, does not critically affect the mean drop size of the dispersion produced.

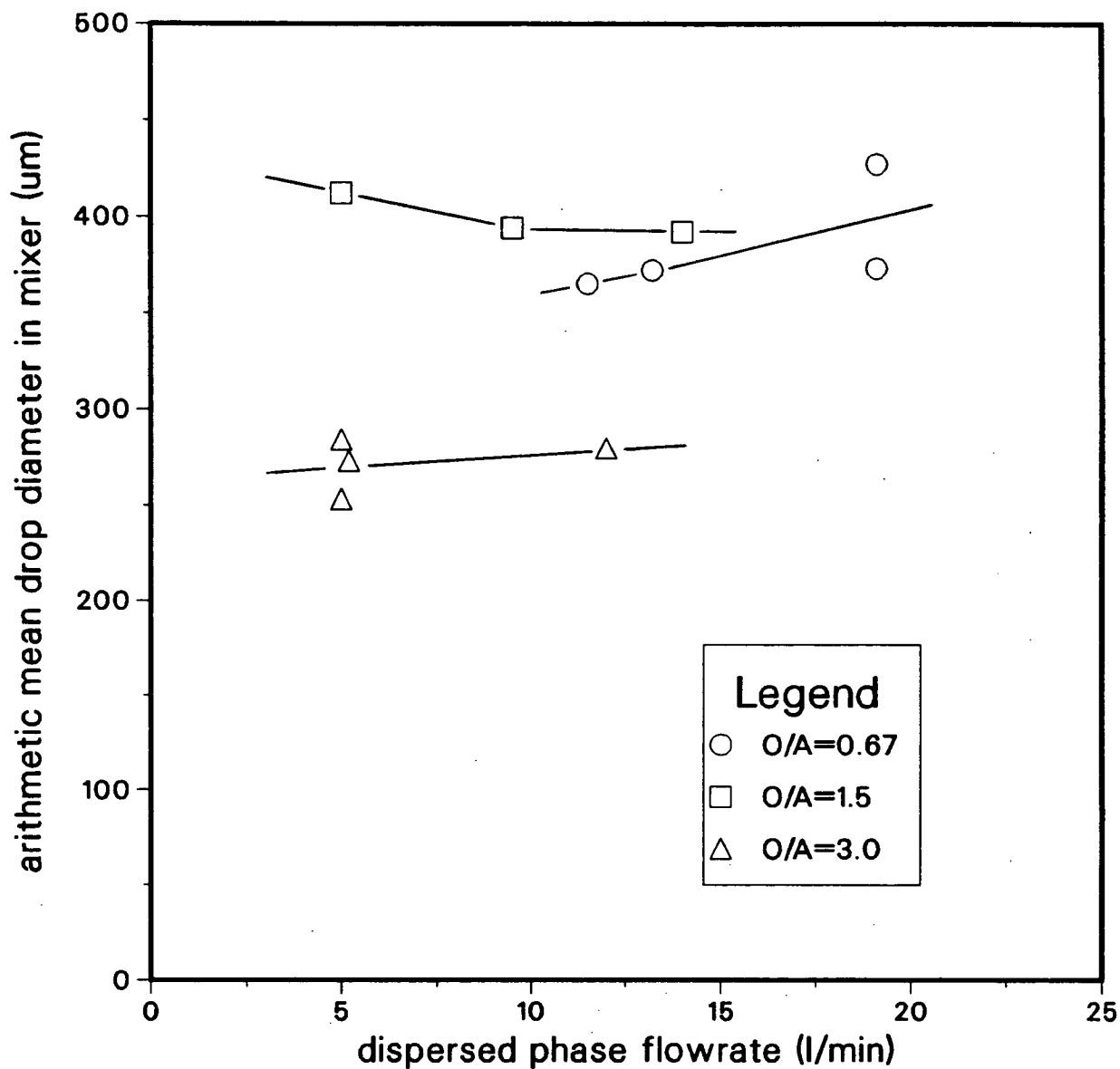
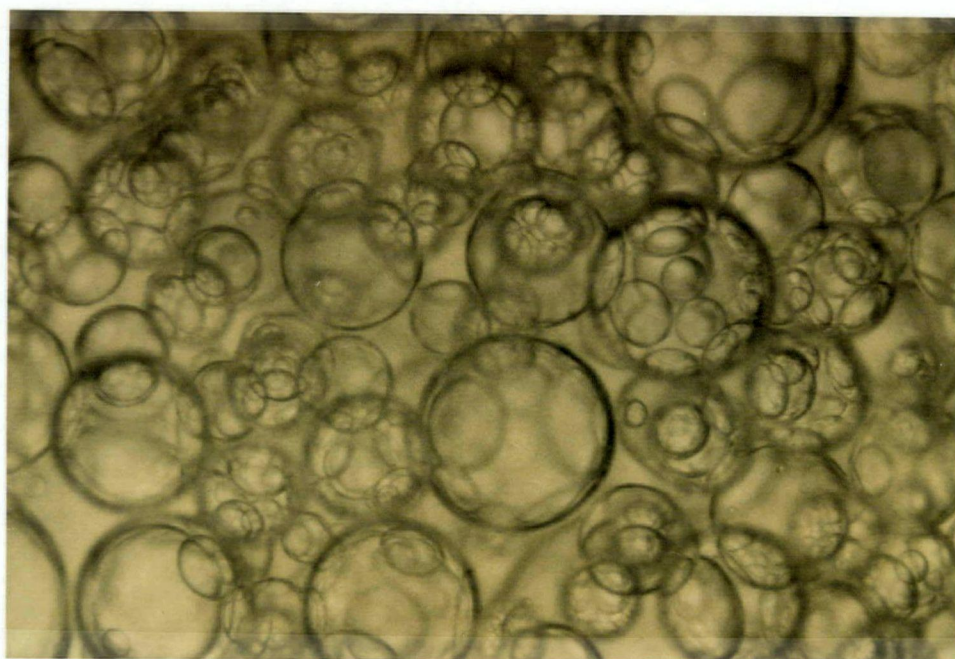


Figure 30. Effect of O/A ratio and dispersed phase flowrate on arithmetic mean drop diameter at mixer overflow, Key Lake phase system, organic continuous operation, 35°C , 300rpm.

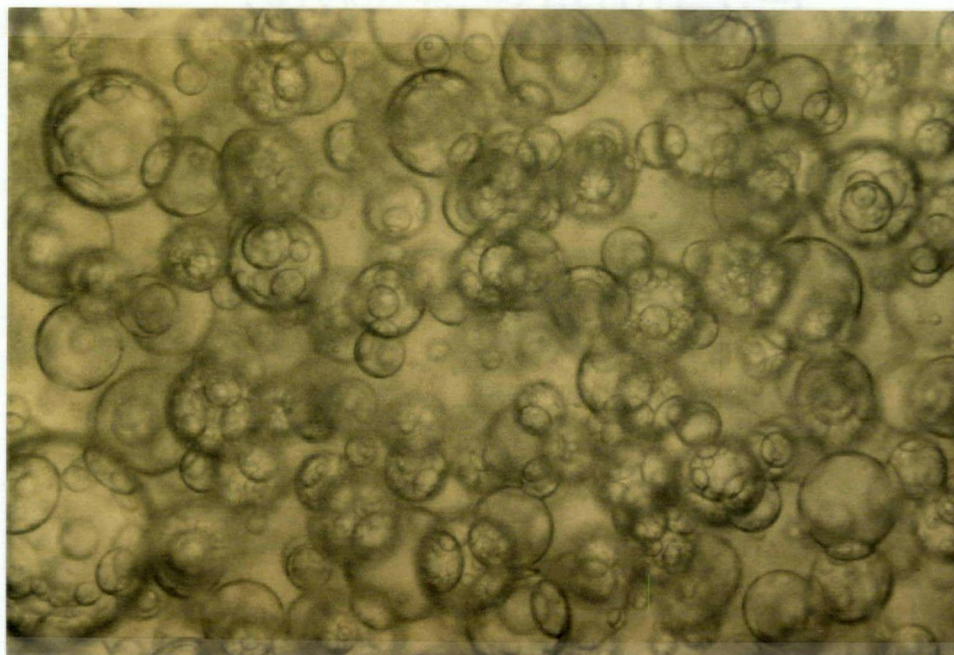
The O/A ratio itself, however, can have a crucial effect on the drop size produced. Figure 30 shows that, although there is no significant difference in the dispersion produced at $O/A=0.67$ and $O/A=1.5$, the mean drop size produced for the more dilute dispersion ($O/A=3.0$) is considerably smaller than that produced for the more concentrated dispersions. Photographs of dispersions with O/A ratios of 0.67 and 3.0, shown in Figures 31(a) and 31(b) respectively, illustrate this difference.

This result provides an explanation for the differences between the characteristic curves observed for the three different phase ratios with the Key Lake system (Figure 20). It had been determined that, although the characteristic curves for $O/A=0.67$ and $O/A=1.5$ are essentially identical, the curve for $O/A=3.0$ was shifted upwards, indicating that for a given dispersed phase throughput, a thicker dispersion band was required. This would be expected from the drop size data obtained, since a finer dispersion (such as that produced for $O/A=3.0$) would require a greater dispersion band thickness for phase disengagement to occur.

The essentially identical arithmetic mean drop diameter as well as the identical characteristic curves produced for $O/A = 0.67$ and $O/A = 1.5$ has implications for industrial operations. Since, in general, industrial mixer-settlers for uranium extraction maintain O/A ratios deviating little from 1.0, the generalization that phase separation with such phase systems does not depend on the O/A ratio (i.e.: on the continuous phase



(a)

1000 μm 

(b)

Figure 31.

Photographs showing effect of O/A ratio on drop size of dispersion withdrawn from mixer overflow, Key Lake phase system, organic continuous operation, 35°C. (a) O/A=0.67, (b) O/A=3.0.

flow) appears to be valid, practically speaking, over this normal, limited range of operation. However, as can be seen from Figures 20 and 30, the generalization is no longer correct when extended to more dilute dispersions ($O/A=3.0$); the mean drop size appears to be sufficiently smaller to shift the characteristic curve upwards.

7.6.4 EFFECT OF IMPELLOR SPEED ON MEAN DROP SIZE

The effect of impellor speed on the arithmetic mean drop size of the dispersion produced appears to depend on the O/A ratio of the dispersion (Figure 32).

For $O/A = 0.67$ and $O/A = 1.5$, increasing impellor speed tends to have a moderate effect, producing a somewhat finer dispersion. From this, one would expect that the characteristic curve at these phase ratios would be shifted upwards with increasing impellor speed. However, from Figure 22, this was not observed, suggesting that the decrease in drop diameter with impellor speed over the range tested is not sufficient to appreciably change the settling characteristics of the dispersion.

For $O/A=3.0$, the mean drop size does not appear to be sensitive to impellor speed.

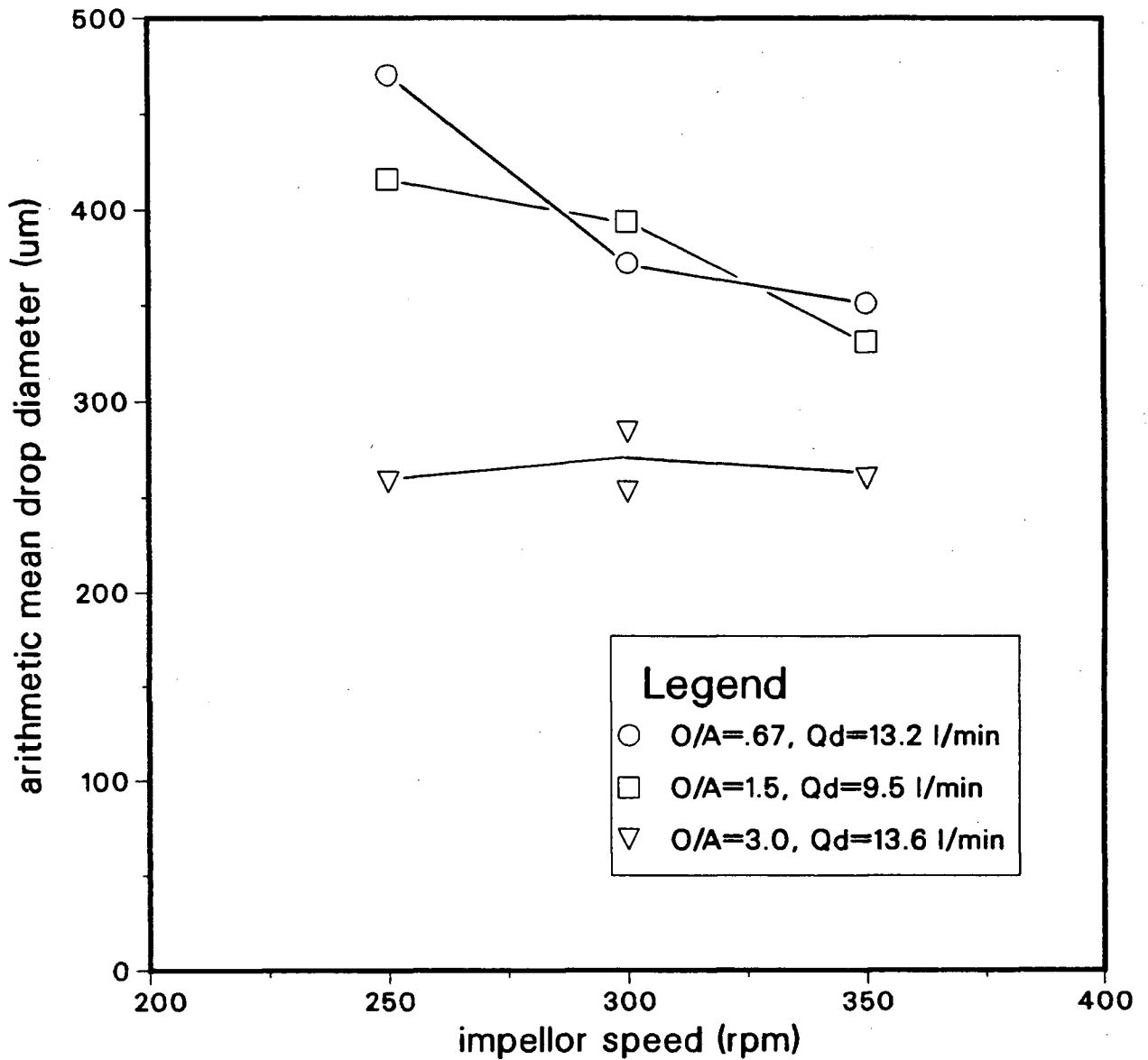


Figure 32. Effect of impeller speed on arithmetic mean drop diameter at mixer overflow, Key Lake phase system, organic continuous operation, 35°C.

7.6.5 DROP SIZE PROFILE WITHIN DISPERSION BAND

Dispersion samples were withdrawn from various points in the dispersion band to obtain the dispersion band drop size profile, relating arithmetic mean drop size to the vertical location in the dispersion band (expressed as the reduced dimensionless distance from the coalescence front; 0=coalescence front, 1=settling front). The dispersion band drop size profile was obtained for settler feed O/A ratios of 0.67, 1.5 and 3.0 (Figures 33, 34 and 35, respectively). Furthermore, for each of these three cases, the profile was determined at two horizontal locations within the dispersion band;

1. At a point one third of the distance between the settler inlet and the end of the settler.
2. Approximately 5-10 cm from the end of the settler.

Constant parameters were dispersion type (organic continuous), temperature (35°C) and settler size (0.22 m²).

Comparison of Figures 33, 34 and 35 reveals a definite similarity in the shapes of the profiles for these three cases. Furthermore, the general shape of the drop size profile corresponds closely to that for the concentration (holdup) profile of the dispersion band. In fact it is possible to arbitrarily distinguish the two sublayers, the even concentration sublayer and the dense concentration sublayer based on drop size data alone. With respect to drop size, the even concentration sublayer, comprising roughly 80 % of the

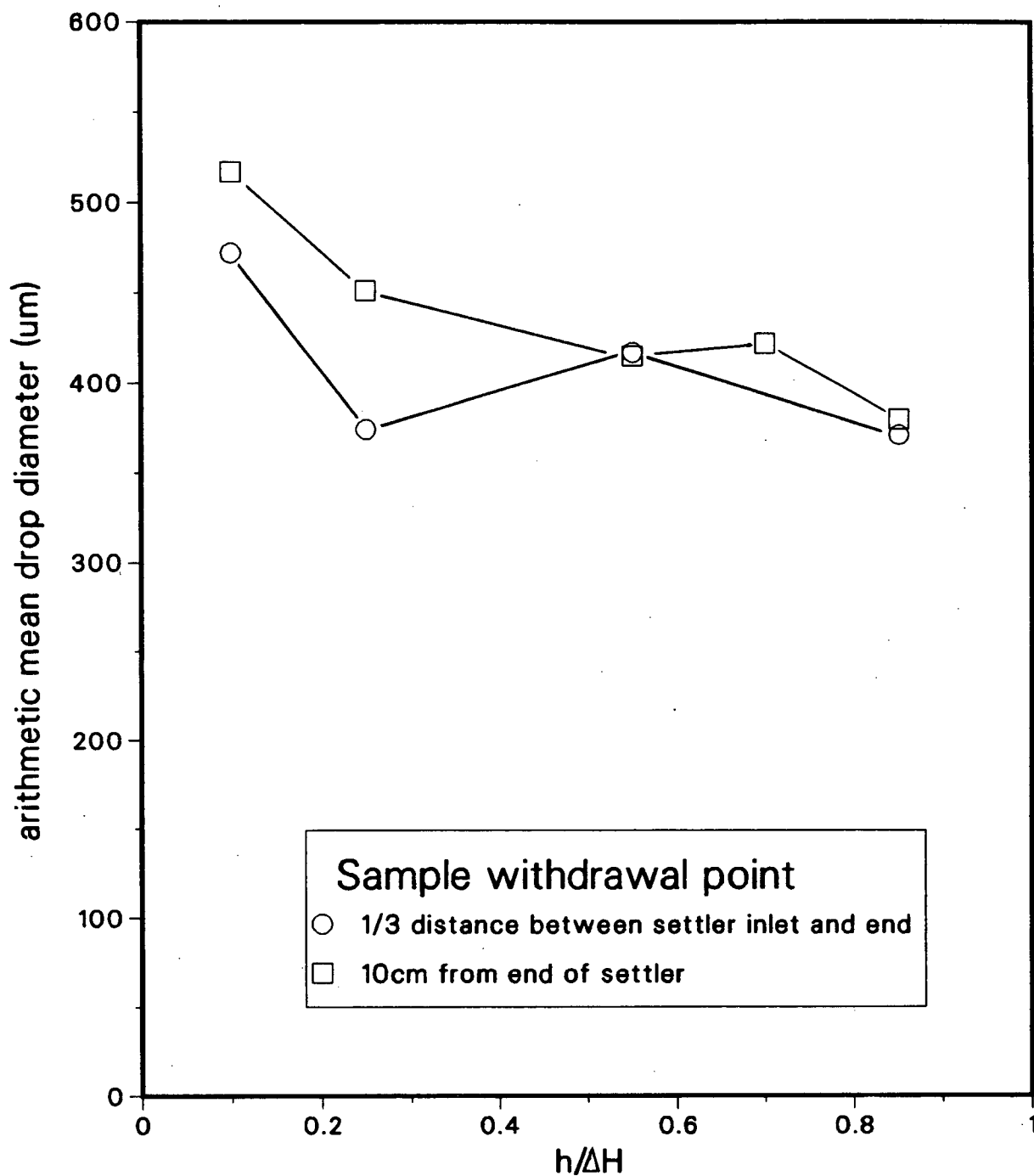


Figure 33. Drop size profile within dispersion band for $O/A=0.67$, Key Lake phase system, organic continuous operation, 35°C , 300rpm.

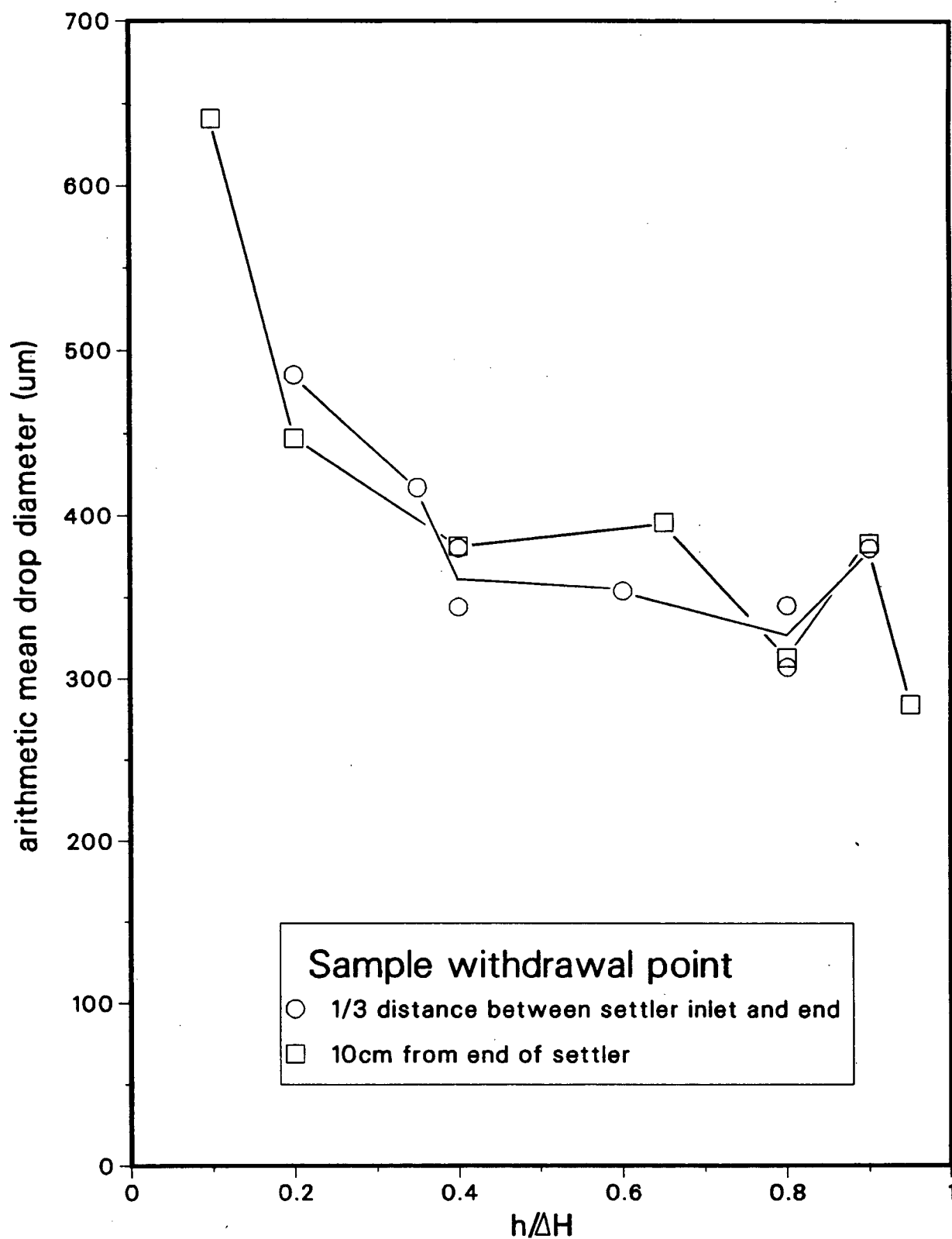


Figure 34. Drop size profile within dispersion band for $O/A=1.5$, Key Lake phase system, organic continuous operation, 35°C , 300rpm.

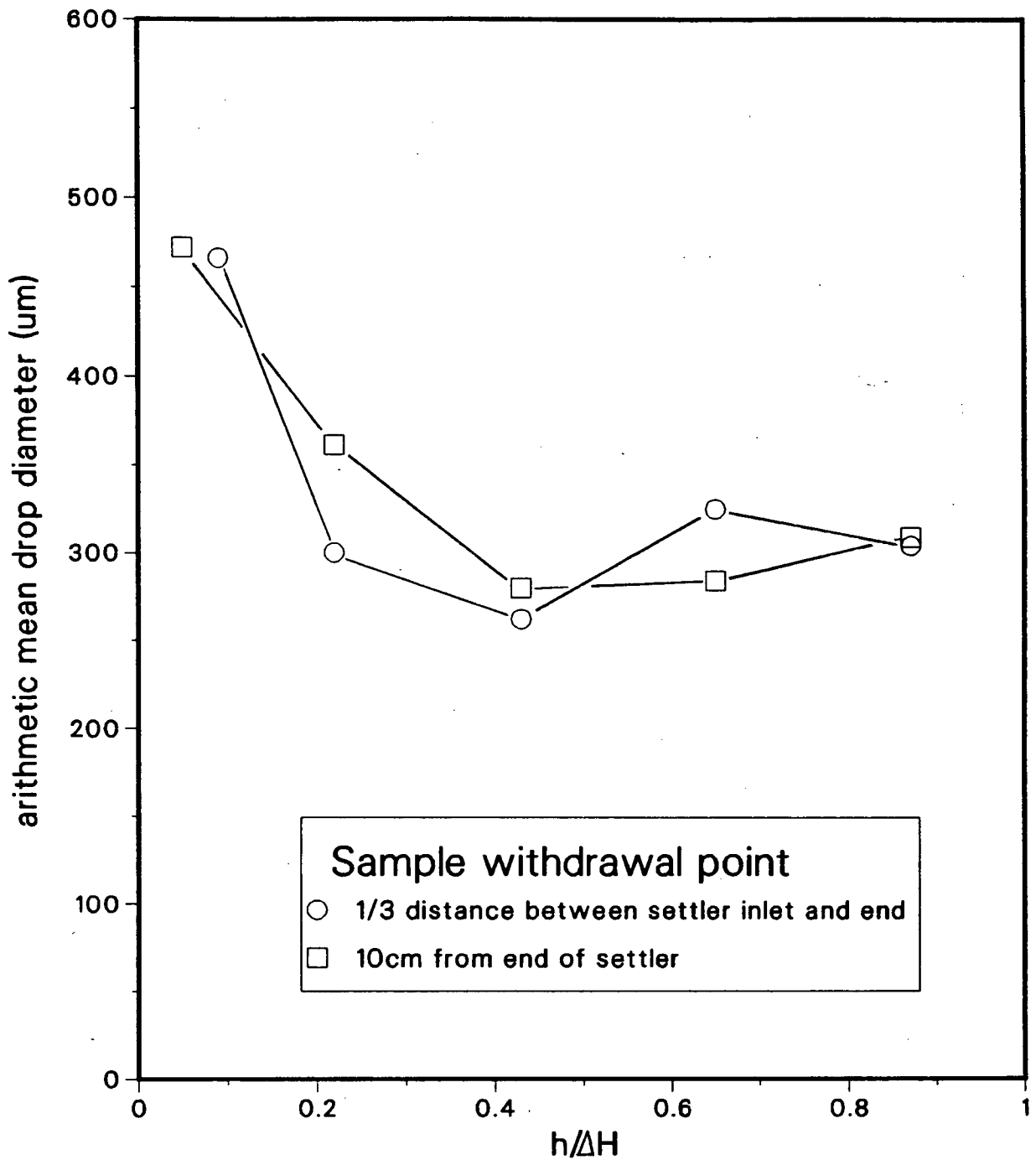


Figure 35. Drop size profile within dispersion band for $O/A=3.0$, Key Lake phase system, organic continuous operation, 35°C .

dispersion bands' volume consists of droplets of approximately constant mean diameter. Near the coalescence front, however, a definite increase in the mean diameter is detectable, identifying the dense concentration sublayer.

Comparison of the approximate mean drop size of the even concentration layer with that of samples taken at the mixer overflow reveals that the drop size is approximately equal to that issuing from the mixer. This is analogous to the situation encountered when comparing the concentration in the even concentration sublayer with that in the mixer; they too are approximately equal.

Comparison of the arithmetic mean drop size profile existing near the inlet of the settler with that near the outlet shows that no substantial difference between the two can be detected. This agrees with visual observation of the dispersion band except in one respect; although no change in drop size with horizontal position was visually detected in the even concentration sublayer, it was possible to notice an increase in drop size with distance from the settler inlet at the coalescence front. It is likely that the trend observed at the coalescence front was not detected photographically due to limitations in the sampling technique. That is, it was not possible to precisely withdraw a sample within 1-2 cm of the coalescence front.

The fact that no substantial change in drop size occurred between the front and the back of the settler appears to

confirm that most of the coalescence occurs at the coalescence front. Otherwise, in the even concentration layer, an increase in drop size would be detectable as the dispersion advanced towards the back of the settler and aged.

The two sublayers had also been distinguishable in observations of batch separation in the cell (section 7.6.1); drop size remained relatively constant with time as long as the "even concentration" sublayer was in the microscope's field of view. When the coalescence front occupied the field of view, this was marked by larger more compacted drops.

Figures 33, 34 and 35 confirm the results obtained from sampling at the mixer overflow. The mean drop size in the even concentration sublayer was about equal at 400 μm for $O/A=0.67$ and $O/A=1.5$. For $O/A=3.0$, however, the mean drop size was about 300 μm , considerably smaller.

7.7 THEORETICAL TERMINAL VELOCITY

In order to gain some insight into the role played by hindered settling in the phase separation process, it is desirable to have available information on the effect of drop size, viscosity, density, and the volumetric concentration of dispersed phase on the terminal velocity of the droplets.

Barnea and Mizrahi (1975, part III) developed a general semitheoretical correlation, supported by experimental results from fourteen independent sources, which could be used to

estimate the terminal settling velocity of liquid droplets in a concentrated dispersion. This correlation states that the relationship established for a single spherical droplet, between the drag coefficient, C_D and the Reynolds number, Re , is valid for the case of concentrated dispersions provided that C_D and Re are modified as follows:

$$C_{D\phi} = \frac{4d(\rho_d - \rho_c)g(1 - \phi)}{3\rho_c U_\phi^2 (1 + \phi^{0.33})} \quad (7)$$

$$Re_\phi = \frac{U_\phi d \rho_c}{\mu_\phi} \quad (8)$$

where μ_ϕ is the effective viscosity of the dispersion.

For the case of liquid spherical droplets with unretarded internal recirculation (which results in surface motion, increasing the terminal velocity), μ_ϕ can be expressed as follows:

$$\mu_\phi = \frac{\mu_c (2\mu_\phi' + 3\mu_d)}{(3\mu_\phi' + 3\mu_d)} \quad (9)$$

$$\text{where } \mu_\phi' = \mu_c \exp \frac{5\mu_d + 2\mu_c}{3\mu_d + 3\mu_c} \frac{\phi}{1-\phi} \quad (10)$$

The above relationships are based on the following assumptions:

- the particles are spherical
- the particles' spacial positions are completely random
- there is no wall effect
- interactions between particles are hydrodynamic only

The well known relationship between Reynolds number and the drag coefficient can be approximated by the following three equations (Perry V, p. 5.61).

$$C_{D\phi} = \frac{24}{Re_{\phi}} \quad \begin{array}{l} Re_{\phi} < 0.3 \\ \text{(Stoke's Law)} \end{array} \quad (11)$$

$$C_{D\phi} = \frac{18.5}{(Re_{\phi})^{0.6}} \quad \begin{array}{l} 0.3 < Re_{\phi} < 1000 \\ \text{(Intermediate Law)} \end{array} \quad (12)$$

$$C_{D\phi} = 0.44 \quad \begin{array}{l} 1000 < Re_{\phi} < 200000 \\ \text{(Newton's Law)} \end{array} \quad (13)$$

Using equations 7-13 and the property data of table 5, terminal velocities for drops of various diameters and in dispersions of various concentrations, have been calculated. The results are graphed in Figures 36, 37 and 38 for the following three cases:

1. HSLIX64N-copper phase system (org. cont.); Figure 36.
2. HSLIX64N-copper phase system (aq. cont.); Figure 37.
3. Key Lake phase system (org. cont.); Figure 38.

The practical information which may be gleaned from the terminal velocity data is rather limited, as it does not consider the coalescence aspect of phase separation. Furthermore, the flow patterns and eddies existing in the dispersion band are also disregarded. The theoretical data would also have limited validity for the case of double dispersions, where drop densities vary. Nevertheless, some very general observations may be made. For example:

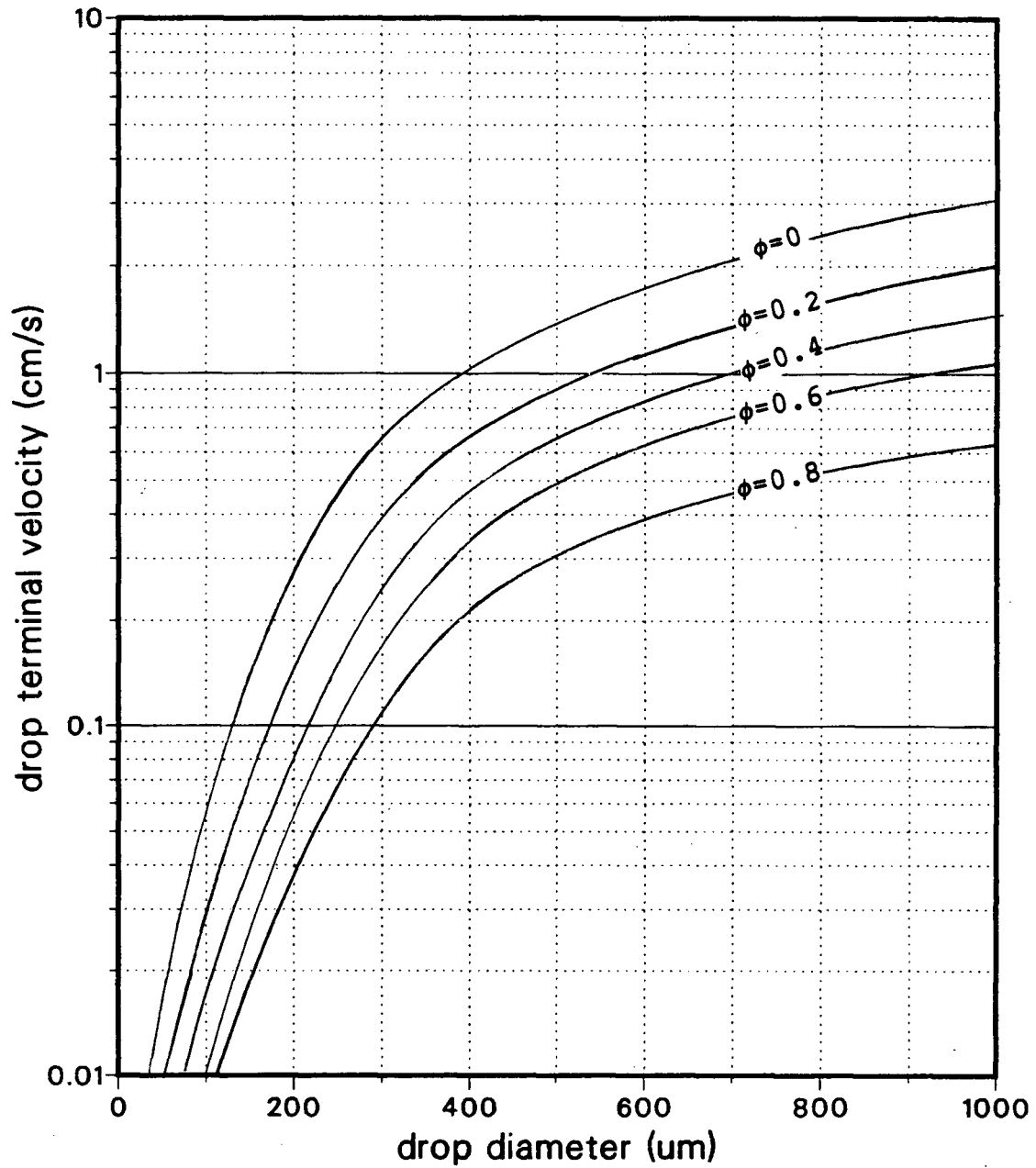


Figure 36. Theoretical terminal drop velocity versus drop diameter for different dispersion concentrations, HSLIX64N-copper phase system, organic continuous operation, 24°C.

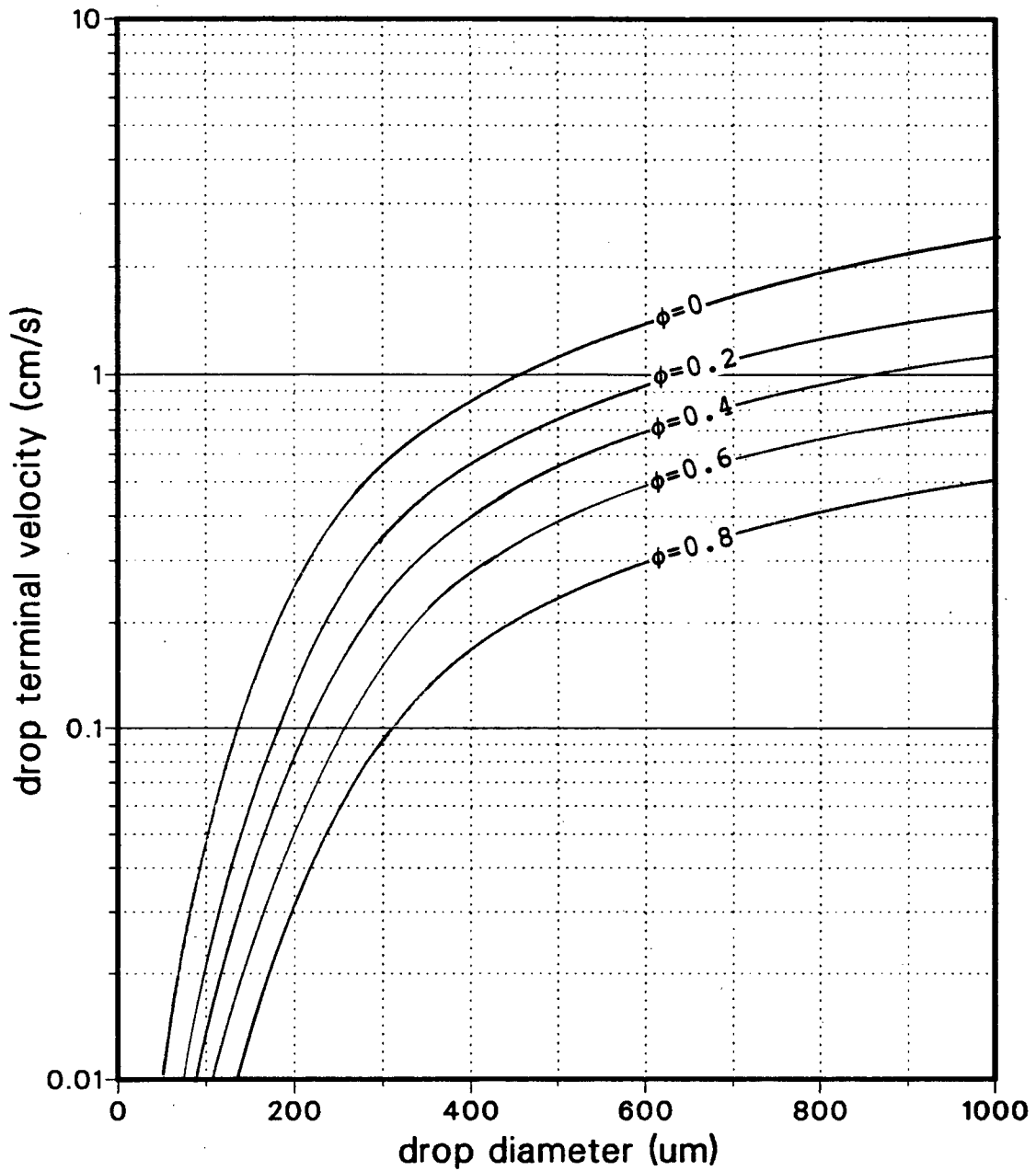


Figure 37. Theoretical terminal drop velocity versus drop diameter for different dispersion concentrations, HSLIX64N-copper phase system, aqueous continuous operation, 24°C.

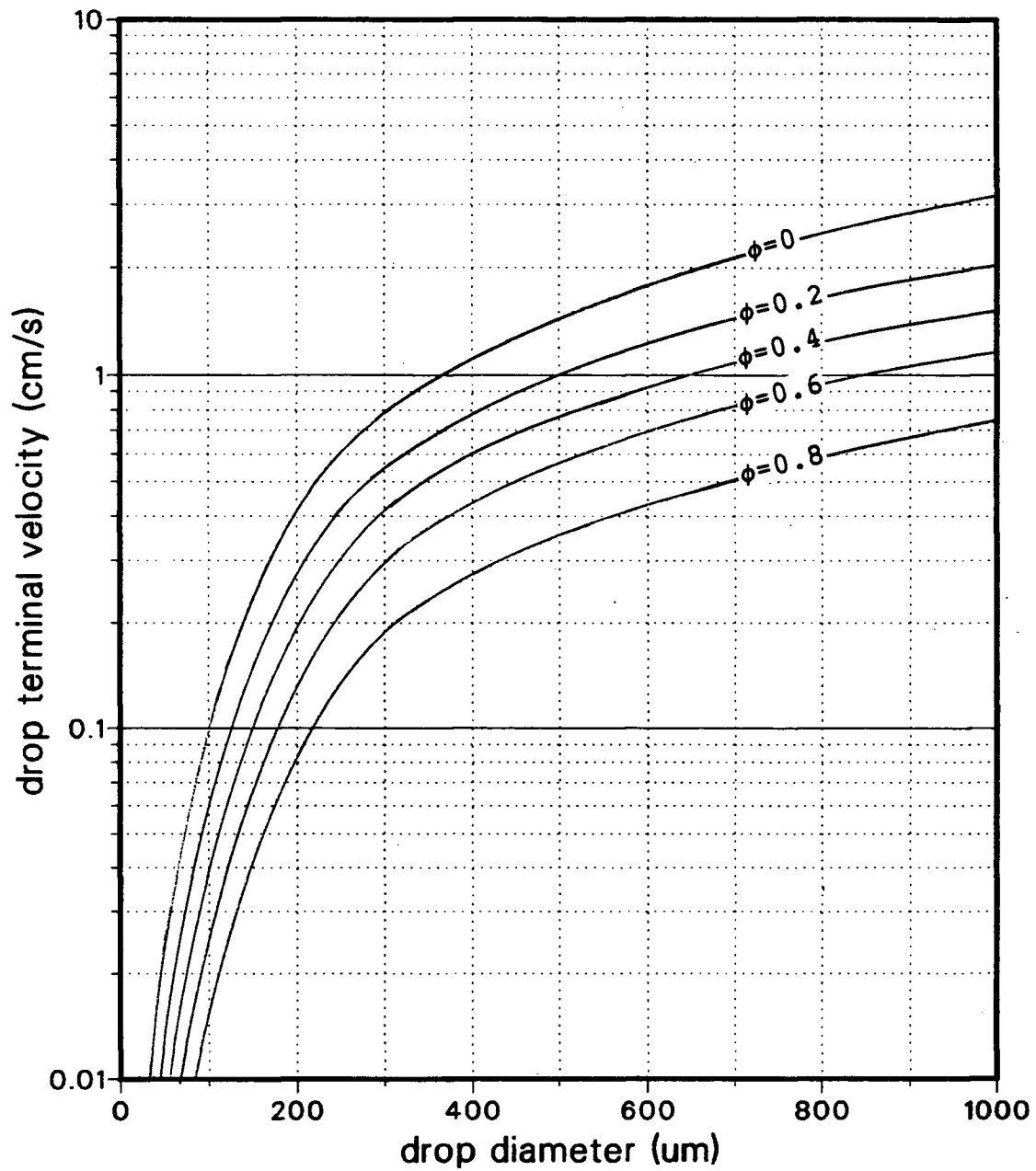


Figure 38. Theoretical terminal drop velocity versus drop diameter for different dispersion concentrations, Key Lake phase system, organic continuous operation, 35°C.

1. Figures 36,37, and 38 illustrate how hindered settling is retarded as drop size decreases (lower terminal velocities).
2. Comparison of Figures 36 and 37 reveals the increased settling velocity associated with aqueous continuous operation, which contributes to the smaller dispersion band thickness expected in this mode of operation.

CHAPTER 8 - SUMMARY AND CONCLUSIONS

An experimental investigation was undertaken to study the factors affecting phase separation in a laboratory scale mixer-settler. Two phase systems were tested:

1. The laboratory prepared HSLIX64N-copper phase system, similar to that used in commercial copper solvent extraction processes.
2. A phase system obtained directly from the uranium extraction circuit of the Key Lake Mining Corporation, Sask., millsite.

From experiments conducted in a specially-constructed, glass-walled, mixer-settler test unit, the following key observations and conclusions were derived.

1. Depending on the phase system, the level of introduction of dispersion into the settler could have a critical effect on the thickness of the dispersion band produced. With the HSLIX64N-copper phase system (both organic and aqueous continuous operation) introduction level had no appreciable effect. However, with the Key Lake system, introducing the dispersion at or near the level of the coalescence front gave a larger ΔH than if the dispersion was introduced elsewhere. This was attributed to the incoming dispersion occupying a portion of the coalescence front, thereby reducing

the effective area of the settler.

2. The scale-up criterion of Ryon (ie. $\Delta H = k(Qd/A)^Y$) was tested by plotting the characteristic curves for different O/A ratios for both phase systems. The relationship provided a good approximation for the $Qd/A - \Delta H$ data obtained. However, the following was observed:

- For the HSLIX64N-copper system, a single characteristic curve could be used to fit the data taken for all O/A ratios, indicating that for this system ΔH depends only on the dispersed phase throughput and not on that of the continuous phase
- For the Key Lake phase system, separate characteristic curves were produced for each O/A ratio, indicating that with this system ΔH depends on both the dispersed and the continuous phase throughput. For a given value of Qd/A , operation with a low dispersed phase concentration gave the thickest dispersion band.

3. Comparison of the estimated dispersion band thickness existing in Key Lake's Krebs mixer-settlers, with the value of ΔH projected from the experimental data, shows that the Krebs mixer-settlers' performance exceeds that predicted from the experimental data. This may be due to the conical pump and superimposed launder features of the Krebs design, as claimed by Krebs.

4. Phase separation is enhanced at higher operating temperatures. This may be attributed primarily to the lower continuous phase viscosity associated with higher temperatures.
5. Within the range tested, mixer impellor speed did not affect the dispersion band thickness, supporting the contention of Ryon that power input does not affect ΔH .
6. From the holdup profile of the dispersion band, it was generally (but not always) possible to distinguish the "dense" and "even" concentration sublayers identified by Barnea and Mizrahi.
 - For the Key Lake phase system the sublayers could be easily identified for all O/A ratios studied.
 - For the HSLIX64N-copper phase system (aq. continuous) the sublayers were also clearly distinguishable. However, for organic continuous operation at high O/A ratios, it was not possible to distinguish the two. The holdup decreased uniformly, nearly linearly, from the coalescence front to the settling front. In these cases, the results closely correspond to those of Gondo and Kusonoki (1969) who found that, regardless of the concentration of the settler feed, the average holdup in the dispersion band was constant at roughly 0.55.
7. Microscopic examination of the mixer-settler dispersion (Key Lake system) revealed the existence

of double dispersions; that is, drops within drops. This would be expected to increase continuous phase losses and may account for the higher than anticipated organic losses being experienced by Key Lake Mining Corp.

8. Determination of the average drop size of the dispersion, for the Key Lake system, showed that the O/A ratio can dramatically affect the average drop size produced. The average drop size of concentrated dispersions was considerably greater than that of more dilute dispersions. This provides an explanation for the separate characteristic curves obtained for different O/A ratios with this phase system.

Because of the opacity of the HSLIX64N-copper phase system, no drop size data could be obtained for this system. However, since a single characteristic curve could be used to fit the data for all phase ratios, it may be inferred that the nature of the HSLIX64N-copper phase system is such that the O/A ratio does not change the dispersion drop size distribution to the extent necessary to noticeably shift the characteristic curve.

9. The average dispersion drop size was shown to decrease somewhat with increasing impellor speed. The effect was most pronounced for dilute dispersions. Since it had also been observed that, for $O/A=1.5$, impellor speed did not shift the characteristic curve

appreciably, it was concluded that the change in drop size was not substantial enough to significantly affect phase separation.

10. The drop size profile for the Key Lake dispersion band allowed a distinction between the dense and even concentration sublayers to be made. In the even concentration sublayer, occupying 80-90% of the band, the average drop size was approximately constant throughout. However, near the coalescence front the mean drop diameter increases sharply, identifying the dense concentration sublayer.

As indicated by the variations in behavior of the two phase systems, there does not appear to be a simple, universally applicable model of dispersion band structure, or of the separation mechanism in a deep layer settler. It was possible to extend the "dense concentration-even concentration" sublayer concept to most, but not all cases. Similarly, although the scale-up criterion of Ryon appears to have considerable merit, the different effect of phase ratio on the $Qd/A-\Delta H$ relationship for the two phase systems, illustrates the unpredictability of the behavior of different phase systems. Phase separation in a mixer-settler is a complicated process which remains to some extent unpredictable and not fully understood. It is likely that design of settlers will continue to depend on empirical data taken for each specific phase system.

NOMENCLATURE

A	horizontal cross-sectional area of settler	L^2
C_D	drag coefficient	
$C_{D\phi}$	modified drag coefficient	
d	drop diameter	L
D	diameter of cylindrical horizontal settler	L
g	gravitational constant	ML/T^2
h	distance from coalescence front	L
ΔH	dispersion band thickness	L
k	experimental constant (equation 1)	
N	impellor speed (rpm)	$1/T$
O/A	org./aq. volume ratio	
Q	total dispersion flowrate = $Q_c + Q_d$	L^3/T
Q_c	continuous phase flowrate	L^3/T
Q_d	dispersed phase flowrate	L^3/T
Re	Reynolds number	
Re_ϕ	modified Reynolds number	
U_ϕ	relative velocity between drops and continuous phase	L/T
V	dispersion band volume	L^3
y	experimental constant (equation 1)	
γ	interfacial tension	M/T^2
μ	viscosity	M/LT
μ_c	continuous phase viscosity	M/LT

μ_d	dispersed phase viscosity	M/LT
μ_ϕ	effective dispersion viscosity	M/LT
ν	kinematic viscosity	L ² /T
ρ	density	M/L ³
ρ_c	continuous phase density	M/L ³
ρ_d	dispersed phase density	M/L ³
ϕ	holdup of dispersed phase	

REFERENCES

- Bailes, P.J., J.C. Godfrey, and M.J. Slater. Designing Liquid-Liquid Extraction Equipment. The Chemical Engineer, July 1981, pp. 331-333.
- Barnea, E.. Liquid/Liquid Contacting-Art or Science? Part II. Design Methods for Mixer Settlers. Hydrometallurgy, 5 (1980), pp. 127-147.
- Barnea, E.. Flooding Conditions in a Deep-Layer Liquid/Liquid Settler. Trans. I. Chem. E., 56 (1978), pp. 73-76.
- Barnea, E. and J. Mizrahi. Separation Mechanism of Liquid/Liquid Dispersions in a Deep Layer Gravity Settler-Part I. Trans. Instn. Chem. Engrs., 53 (1975), pp. 61-69.
- Barnea, E. and J. Mizrahi. Separation Mechanism of Liquid/Liquid Dispersions in a Deep Layer Gravity Settler-Part II. Trans. Instn. Chem. Engrs., 53 (1976), pp. 70-74.
- Barnea, E. and J. Mizrahi. Separation Mechanism of Liquid/Liquid Dispersions in a Deep Layer Gravity Settler-Part III. Trans. Instn. Chem. Engrs., 53 (1976), pp. 75-82.
- Barnea, E. and J. Mizrahi. Separation Mechanism of Liquid/Liquid Dispersions in a Deep Layer Gravity Settler-Part IV. Trans. Instn. Chem. Engrs., 53 (1976), pp. 83-92.
- Central Scientific Company. The Ring Method for Surface and Interfacial Tensions with the Cenco-duNouy Tensiometers. Bulletin 101.
- Davies, G.A., G.V. Jeffreys, F. Ali. Design and Scale Up of Gravity Settlers. The Chemical Engineer. London, no. 243, Nov. 1970, pp. 378-385
- Davies, G.A. et al.. The Formation of Secondary Droplets in a Dispersion at a Phase Boundary. Can. J. Chem. Engng., 48 (1970), pp. 328-329.
- DeMent, E.R. and N. Lynn. The Liquid Ion Exchange Process. TMS-AIME Short Course, New Orleans, Louisiana, Feb. 16-18, 1979. Selection of Equipment and Materials: A Special Workshop on Hydrometallurgical Plant Design. pp. 9.1-9.18.
- Flett, D.S. Some Recent Developments in the Application of Liquid Extraction in Hydrometallurgy. The Chemical Engineer, July 1981, pp. 321-324.
- Flett, D.S., D.N. Okuhara, and D.R. Spink. Solvent Extraction of

- Copper by Hydroxyoximes. J. Inorg. Nucl. Chem., 35 (1973), pp. 2471-2487.
- Gardner, S.A. and G.C.I. Warwick. Pollution-free Metallurgy: Copper via Solvent Extraction. E/MJ-April 1971, pp. 108-110.
- Glasser, A., D.R. Arnold, A.W. Bryson, and A.M.S. Vieler. Aspects of Mixer Settler Design. Minerals Science Engineering, v. 8, no. 1, (1976), pp. 23-44.
- Godfrey, J.C., C. Hanson, M.J. Slater, and S. Tharmalingam. Studies of Entrainment in Mixer-Settlers. AIChE Symposium Series, v.74, no. 173. Fundamental Aspects of Hydrometallurgical Processes, 1978, pp. 127-133.
- Golob, J., and R. Modic. Coalescence of Liquid/Liquid Dispersions in Gravity Settlers. Trans. I. Chem. Eng., 55 (1977), pp. 207-211.
- Gondo, S., and K. Kusonoki. A New Look at Gravity Settlers. Hydrocarbon Processing, Sept. 1969, pp. 209-210.
- Groothuis, H., and F.S. Zuiderweg. Influence of Mass Transfer on Coalescence of Drops. Chemical Engineering Science, 12 (1960), pp. 288-289.
- Hanson, C. Handbook of Solvent Extraction. John Wiley and Sons., 1983.
- Hanson, C. Recent Advances in Liquid-Liquid Extraction. Pergamon Press Ltd., 1971.
- Hill, E.C., D.A. Evans, and I. Davies. The Growth and Survival of Micro-organisms in Aviation Kerosene, J. Inst. Petrol., v. 53, no. 524, (1967), pp. 280-284.
- Hudson, M.J. An Introduction to Some Aspects of Solvent Extraction Chemistry in Hydrometallurgy. Hydrometallurgy, 9 (1982), pp. 149-168.
- Jeffreys, G.V., G.A. Davies, and K. Pitt. Rate of Coalescence of the Dispersed Phase in a Laboratory Mixer-Settler Unit: Part I, A. I. Ch. E. Journal, 16 (1970), pp. 823-831.
- Johnstone, R.E., and M.W. Thring. Pilot Plants, Models, and Scale-up Methods in Chemical Engineering. McGraw Hill, 1957.
- Keeney, M.E., and K. Osseo-Asare. Thermal Stability of LIX63 Oxime. Hydrometallurgy, 12 (1984), pp. 255-265.
- Kordosky, G.A.. The Chemistry of Metals Recovery Using LIX®

- Reagents. General Mills Chemicals Inc. (Henkel Corporation), 1979.
- Lewis, I.E.. Design of Mixer-Settlers to Achieve Low Entrainment and Reduce Capital Costs. Proceedings. International Solvent Extraction Conference ISEC71, Toronto, Sept. 1977, pp. 325-333.
- Lott, J.B., G.I. Warwick, and J.B. Scuffham. Design of Large Scale Mixer Settlers. Trans. Soc. Min. Engrs., AIME, 252 (1972), pp. 27-35.
- MacKay, G.D.M., and S.G. Mason. The Marangoni Effect and Liquid/Liquid Coalescence. Nature, 191 (1961), pp. 191-191.
- Manchanda, K.D., and D.R. Woods. Significant Design Variables in Continuous Gravity Decantation. Industrial and Engineering Chemistry. Process Design and Development., vol. 7, no. 2 (1968), pp. 182-187.
- McClary, M.J., and G.A. Mansoori. Factors Affecting the Phase Inversion of Dispersed Immiscible Liquid-Liquid Mixtures. AIChE Symposium Series no. 173, volume 74 (1978), pp. 134-139.
- McGarr, H.J.. Liquid Ion-Exchange Recovers Copper from Wastes and Low Grade Ores. E/MJ, October 1970, pp. 79-81.
- Merritt, R.C.. The Extractive Metallurgy of Uranium Colorado School of Mines Research Institute. (1971).
- Mizrahi, J., and E. Barnea. Compact Settler Gives Efficient Separation of Liquid/Liquid Dispersion. Process Engineering, Jan. 1973, pp. 60-65.
- Murray, D.J.. Equipment Development in Solvent Extraction. (1979). p. 367.
- Neven, M., and L. Gormely. Design of the Key Lake Leaching Process. Twelfth Annual Hydrometallurgical Meeting, Uranium '82. Toronto, Canada. Aug 29-Sept 1, 1982.
- Neven, M., R. Steane, and J. Becker. Arsenic Management and Control at Key Lake. CIM Metallurgical Society, Hydrometallurgy Section. Fifteenth Annual Hydrometallurgical Meeting (Proceedings). Vancouver, Canada, Aug. 18-22, 1985, pp. 6.1-6.21.
- Oldshue, J.Y., and A.T. Gretton. Helical Coil Heat Transfer in Mixing Vessels. Chem. Eng. Progr., 50 (1954), pp. 615-621.
- Orjans, J.R., C.W. Notebaart, J.C. Godfrey, C. Hanson, and

- M.J. Slater. The Design of Mixer Settlers for the
Zambian Copper Industry. Proceedings. International
Solvent Extraction Conference ISEC77, Toronto, Sept.
1977, pp. 340-346.
- Paatero, E.Y.O.. Determination of the Composition of the
Hydroxyoxime Extractant LIX65N. Hydrometallurgy, 13
(1984), pp. 193-201.
- Pike, F.P., and S.E. Wadhamen. Properties of an Emulsion Band
in a Mixer-Settler Contactor. Proceedings.
International Solvent Extraction Conference ISEC71, The
Hague, 1971, pp. 113-124.
- Rachuk, W. Manual of Radiation Hazards Control at the
University of British Columbia, 1980.
- Rice, N.M.. Recommended Nomenclature for Solvent Extraction
(Liquid-Liquid Distribution). Hydrometallurgy, 7
(1981), pp. 177-199.
- Ritcey, G.M.. Crud in Solvent Extraction Processing-A Review
of Causes and Treatment. Hydrometallurgy, 5 (1980), pp.
97-107.
- Ritcey, G.M., and B.H. Lucas. Diluents and Modifiers - Their
Effect on Mass Transfer and Separation. In Proceedings
of the International Solvent Extraction Conference,
Lyon 1974 (London: Society of Chemical Industry, 1974),
pp. 2437-2481.
- Ryon, A.D., F.L. Daley, R.S. Lowrie. Scale Up of
Mixer-Settlers. Chemical Engineering Progress, vol. 55,
no. 10 (1959), pp. 70-75.
- Scuffham, J.B.. CMS: A Davy McKee Concept. The Chemical
Engineer, July 1981, pp. 328-330.
- Shaw, D.J., Introduction to Colloid and Surface Chemistry.
Butterworth, London, 1980.
- Skelland, A.H.P., W.K. Blake, J.W. Dabrowski, J.A. Ulrich,
and T.F. Mach. Heat Transfer to Coils in Propellor
Agitated Vessels. A.I.Ch.E. Journal, vol. 11, no. 5,
(1955), pp. 951-954.
- Sokal, R.R., and F.J. Rohlf. Biometry. Freeman, 1981.
- Stonner, H.M., and F. Wohler. An Engineer's Approach to a
Solvent Extraction Problem. In: Hydrometallurgy.
Davies, G.A., and J.B. Scuffham (eds.), London, I. Chem.
E. Symp. Series, no. 42, 1975, pp. 14.1-14.11.
- Treybal, R.E.. Liquid Extraction, McGraw Hill, New York,

1963.

Urban, M.R.. Factors Affecting the Formation of the Dispersed Phase in Liquid-Liquid Systems. M.Sc. Thesis, Johannesburg, University of the Witwatersrand, 1972.

Warwick, G.I., J.B. Scuffham, and J.B. Lott. Considerations in the Design of Large Scale Solvent Extraction Plants for the Recovery of Metals. Proceedings. International Solvent Extraction Conference, The Hague ISEC71, 1971, pp. 1373-1385.

Whewell, R.J., H.J. Foakes, and M.A. Hughes. Degradation in Hydroxyoxime Solvent Extraction Systems., Hydrometallurgy, 7 (1980), pp. 7-26.

APPENDIX I - PLOTS OF CHAPTER 7

Figure 14. Time for dispersion band thickness to achieve steady-state after introduction of dispersion into settler (HSLIX64N-copper phase system).

Settler operating condition	Time (min)	Dispersion Band thickness (cm)
1. Organic continuous operation	0	0
O/A ratio=0.67	1	5.
$Q_d/A=2.43 \text{ m}^3/\text{m}^2/\text{hr}$	3	12.5
Area=0.22 m^2	7	17.5
	13	22.
	18	24.5
	23	26.
	28	27.5
2. Organic continuous operation	0	0
O/A ratio=1.91	1	5.5
$Q_d/A=1.91 \text{ m}^3/\text{m}^2/\text{hr}$	2	7.5
Area=0.22 m^2	4	9.
	6	9.5
	11	10.5
	21	11.5
	31	12.5
	40	13.5
	49	14.
3. Organic continuous operation	0	0
O/A ratio=1.5	2	10.5
$Q_d/A=2.90 \text{ m}^3/\text{m}^2/\text{hr}$	5	15.3
Area=0.22 m^2	6	18.5
	9	23.5
	13	27.
	17	28.5
	22	31.
	36	31.
	56	30.
4. Organic continuous operation	0	0
O/A ratio=1.5	4	1
$Q_d/A=0.77 \text{ m}^3/\text{m}^2/\text{hr}$	8	1.5
Area=0.36 m^2	15	1.4
	20	1.5
5. Aqueous continuous operation	0	0
O/A ratio=0.67	9	4.5
$Q_d/A=2.44 \text{ m}^3/\text{m}^2/\text{hr}$	15	6.2
Area=0.13 m^2	22	7.2
	30	7.3
	37	7.4
6. Aqueous continuous operation	0	0
O/A ratio=1.5	10	12.
$Q_d/A=3.22 \text{ m}^3/\text{m}^2/\text{hr}$	13	14.5
Area=0.22 m^2	18	14.5
	25	16.
	30	16.
	38	16.

Figure 18. Dispersion band thickness versus specific settler flow of dispersed phase (effect of O/A ratio and settler area), HSLIX64N-copper system, organic continuous operation, 24°C, 300rpm.

test no.	O/A ratio	Settler area (m**2)	Organic flow (l/min)	Aqueous flow (l/min)	Qd/A (m**3/m**2/hr)	ΔH (cm)
1	0.67	.22	4.7	7.0	1.91	10.8
2	0.67	.22	7.1	10.5	2.87	24.
3	0.67	.22	6.0	8.9	2.43	27.
4	0.67	.22	4.7	7.0	1.91	13.9
5	0.67	.22	4.5	6.8	1.86	14.5
6	0.67	.22	5.5	8.0	2.20	25.
7	0.67	.22	4.9	7.2	1.97	18.
8	0.67	.22	3.9	6.0	1.64	14.
9	0.67	.36	8.7	13.0	2.15	13.3
10	0.67	.36	12.7	18.9	3.14	31.
11	0.67	.36	4.8	7.1	1.18	4.9
12	0.67	.36	6.7	10.0	1.66	10.5
13	0.67	.36	10.7	16.0	2.65	30.0
14	0.67	.36	4.5	6.7	1.11	7.
15	0.67	.36	5.7	8.5	1.41	11.
16	0.67	.36	7.9	11.8	1.96	18.
17	1.5	.13	8.8	5.9	2.76	27.
18	1.5	.13	3.8	2.5	1.17	6.5
19	1.5	.22	9.9	6.6	1.80	10.5
20	1.5	.22	14.4	9.6	2.62	19.5
21	1.5	.22	15.9	10.6	2.90	30.0
22	1.5	.22	3.8	2.5	0.68	3.5
23	1.5	.22	7.1	4.7	1.28	7.0
24	1.5	.36	8.8	5.9	0.97	4.3
25	1.5	.36	19.5	13.0	2.15	12.0
26	1.5	.36	13.8	9.2	1.52	8.0
27	1.5	.36	23.5	15.7	2.60	20.0
28	1.5	.36	10.5	7.0	1.16	6.5
29	1.5	.36	18.4	12.3	2.04	14.5
30	1.5	.36	7.2	4.9	0.82	4.2
31	1.5	.36	15.0	10.0	1.66	12.0
32	1.5	.36	19.9	13.3	2.22	21.
33	3.0	.13	13.8	4.6	2.16	19.5
34	3.0	.13	8.5	2.9	1.35	9.0
35	3.0	.22	16.5	5.5	1.50	8.8
36	3.0	.22	24.0	8.0	2.20	23.5
37	3.0	.22	12.0	4.2	1.15	6.0
38	3.0	.22	14.4	4.8	1.31	9.0
39	3.0	.36	15.9	5.3	0.88	3.5
40	3.0	.36	20.0	6.6	1.10	5.4
41	3.0	.36	14.1	4.7	0.78	2.8
42	3.0	.36	24.1	8.0	1.33	6.3
43	3.0	.36	14.4	4.8	0.80	4.0
44	3.0	.36	18.0	6.0	1.00	5.0
45	3.0	.36	21.0	7.0	1.20	6.5

Figure 19. Dispersion band thickness versus specific settler flow of dispersed phase (effect of O/A ratio and settler area), HSLIX64N-copper system, aqueous continuous operation, 24°C, 300rpm.

Test no.	O/A	Settler area (m**2)	Organic flow (l/min)	Aqueous flow (l/min)	Qd/A (m**3/m**2/hr)	ΔH (cm)
1	0.33	.13	4.6	13.9	2.17	6.9
2	0.33	.13	6.0	18.0	2.77	12.
3	0.33	.22	4.6	13.9	1.26	2.8
4	0.33	.22	5.7	17.1	1.55	5.
5	0.33	.22	6.6	19.5	1.80	6.
6	0.33	.22	5.1	15.3	1.39	3.5
7	0.33	.36	5.5	16.4	0.91	1.8
8	0.33	.36	5.1	15.3	0.85	1.1
9	0.33	.36	6.2	18.6	1.03	1.5
10	0.33	.36	7.5	22.5	1.25	2.5
11	0.33	.36	4.7	14.1	0.77	0.7
12	0.67	.13	4.4	6.6	2.03	4.0
13	0.67	.13	5.3	7.9	2.44	7.4
14	0.67	.13	6.1	9.1	2.81	10.0
15	0.67	.13	7.1	10.6	3.28	14.7
16	0.67	.13	7.1	10.6	3.28	15.0
17	0.67	.13	8.0	12.0	3.69	21.0
18	0.67	.22	4.9	7.3	1.33	3.3
19	0.67	.22	6.0	9.0	1.64	3.5
20	0.67	.22	8.0	11.9	2.18	6.3
21	0.67	.22	10.1	15.1	2.75	12.5
22	0.67	.22	11.5	17.2	3.14	16.
23	0.67	.22	13.3	19.8	3.64	25.
24	0.67	.22	14.7	22.1	4.01	32.5
25	0.67	.36	4.5	6.7	0.81	1.1
26	0.67	.36	5.8	8.6	0.95	1.7
27	0.67	.36	7.2	10.7	1.18	3.1
28	0.67	.36	8.8	13.1	1.48	3.6
29	0.67	.36	13.2	19.7	2.22	6.3
30	1.5	.13	4.2	2.8	1.97	5.5
31	1.5	.13	6.6	4.4	3.05	10.
32	1.5	.13	7.0	4.7	3.23	12.5
33	1.5	.13	7.6	5.1	3.52	21.5
34	1.5	.13	8.0	5.3	3.69	19.0
35	1.5	.13	9.5	6.3	4.39	33.
36	1.5	.22	12.6	8.4	3.43	25.
37	1.5	.22	4.2	2.8	1.15	2.8
38	1.5	.22	7.0	4.7	1.92	5.7
39	1.5	.22	8.8	5.7	2.35	7.0
40	1.5	.22	10.0	6.7	2.73	13.
41	1.5	.22	12.0	7.9	3.27	19.5
42	1.5	.36	4.6	3.2	0.85	1.5
43	1.5	.36	7.2	4.8	1.21	4.4
44	1.5	.36	16.0	11.0	2.71	12.5
45	1.5	.36	7.3	4.9	1.21	3.2
46	1.5	.36	5.1	3.4	0.85	1.5
47	1.5	.36	4.2	2.8	0.70	.8
48	1.5	.36	9.4	6.3	1.56	3.7
49	1.5	.36	13.1	8.7	2.18	8.5
50	1.5	.36	10.6	7.1	1.77	5.0

Figure 20. Dispersion band thickness versus specific settler flow of dispersed phase (effect of O/A ratio and settler area), Key Lake phase system, organic continuous operation, 35°C, 300rpm.

Test no.	O/A	Settler area (m**2)	Organic flow (l/min)	Aqueous flow (l/min)	Qd/A (m**3/m**2/hr)	ΔH (cm)
1	.67	.13	4.0	6.1	2.95	24.5
2	.67	.13	4.6	6.8	3.19	32.
3	.67	.22	5.3	7.8	2.13	8.
4	.67	.22	4.8	7.3	1.99	8.
5	.67	.22	5.7	8.6	2.35	13.
6	.67	.22	6.3	9.4	2.56	15.5
7	.67	.22	7.0	10.5	2.86	19.8
8	.67	.22	8.1	12.1	3.30	26.5
9	.67	.36	9.3	14.0	2.33	15.
10	.67	.36	11.3	17.0	2.83	18.
11	.67	.36	12.3	18.7	3.12	28.
12	.67	.36	6.8	10.2	1.75	5.
13	.67	.36	8.7	13.0	2.17	9.5
14	.67	.36	5.2	7.8	1.30	3.
15	1.5	.13	7.5	5.0	2.34	12.
16	1.5	.13	8.1	5.4	2.53	14.5
17	1.5	.13	9.1	6.3	2.95	27.
18	1.5	.13	6.8	4.5	2.10	9.5
19	1.5	.13	8.6	5.7	2.67	19.5
20	1.5	.22	12.0	8.0	2.18	11.
21	1.5	.22	7.9	5.3	1.45	3.7
22	1.5	.22	9.1	6.0	1.64	5.5
23	1.5	.22	15.0	10.0	2.73	20.
24	1.5	.22	7.1	4.7	1.28	3.3
25	1.5	.22	16.5	11.0	3.00	30.
26	1.5	.36	8.4	5.6	0.93	2.0
27	1.5	.36	14.2	9.0	1.50	5.2
28	1.5	.36	20.2	13.5	2.25	13.
29	1.5	.36	22.0	14.7	2.45	16.
30	1.5	.36	13.0	8.0	1.33	4.
31	1.5	.36	17.4	11.6	1.93	8.5
32	3.0	.13	13.7	4.6	2.11	17.
33	3.0	.13	15.9	5.3	2.48	27.
34	3.0	.13	15.0	5.0	2.36	22.
35	3.0	.13	15.5	5.2	2.39	20.5
36	3.0	.13	17.3	5.8	2.67	31.
37	3.0	.22	13.5	4.5	1.23	4.5
38	3.0	.22	15.9	5.3	1.45	7.
39	3.0	.22	18.0	6.0	1.64	9.5
40	3.0	.22	21.3	7.1	1.94	18.
41	3.0	.22	24.0	8.0	2.18	20.
42	3.0	.36	19.2	6.4	1.07	3.
43	3.0	.36	21.6	7.3	1.22	5.
44	3.0	.36	13.5	4.5	0.75	1.7
45	3.0	.36	17.4	5.8	0.97	2.2

Figure 21. Dispersion band thickness versus specific settler flow of dispersed phase (effect of operating temperature), HSLIX64N-copper phase system, organic continuous operation, 300rpm.

Test no.	O/A ratio	Settler area (m**2)	Organic flow (l/min)	Aqueous flow (l/min)	Qd/A (m**3/m**2/hr)	ΔH (cm)
Temperature = 24°C:						
1	1.5	.36	8.8	5.9	0.97	4.3
2	1.5	.36	19.5	13.0	2.15	12.0
3	1.5	.36	13.8	9.2	1.52	8.0
4	1.5	.36	23.5	15.7	2.60	20.0
5	1.5	.36	10.5	7.0	1.16	6.5
6	1.5	.36	18.4	12.3	2.04	14.5
7	1.5	.36	7.2	4.9	0.82	4.2
8	1.5	.36	15.0	10.0	1.66	12.0
9	1.5	.36	19.9	13.3	2.22	21.
10	1.5	.22	9.9	6.6	1.80	10.5
11	1.5	.22	14.4	9.6	2.62	19.5
12	1.5	.22	15.9	10.6	2.90	30.0
13	1.5	.22	3.8	2.5	0.68	3.5
14	1.5	.22	7.1	4.7	1.28	7.0
15	1.5	.13	8.8	5.9	2.76	27.
16	1.5	.13	3.8	2.5	1.17	6.5
Temperature = 35°C:						
17	1.5	.13	6.9	4.6	2.16	6.8
18	1.5	.13	10.1	6.7	3.14	16.5
19	1.5	.13	12.0	8.0	3.75	28.5
20	1.5	.22	6.9	4.6	1.26	4.1
21	1.5	.22	10.1	6.7	1.83	6.1
22	1.5	.22	13.4	8.9	2.43	10.5
23	1.5	.22	17.7	11.8	3.22	16.5
24	1.5	.36	12.0	8.0	1.33	4.8
25	1.5	.36	16.5	11.0	1.82	6.6
26	1.5	.36	20.1	13.9	2.31	9.4
27	1.5	.36	7.5	5.0	0.83	2.1
28	1.5	.36	6.9	4.6	0.77	1.5

Figure 22. Dispersion band thickness versus specific settler flow of dispersed phase (effect of impellor speed), HSLIX64N-copper phase system, organic continuous operation, 24°C.

Test no.	Impellor speed (rpm)	O/A ratio	Settler area (m**2)	Organic flow (l/min)	Aqueous flow (l/min)	Qd/A (m**3/m**2/hr)	ΔH (cm)
1	250	1.5	.36	7.5	5.0	0.83	3.5
2	250	1.5	.36	12.0	8.0	1.32	6.5
3	250	1.5	.36	13.6	9.0	1.95	11.5
4	250	1.5	.36	15.1	10.0	2.15	12.5
5	300	1.5	.36	8.8	5.9	0.97	4.3
6	300	1.5	.36	19.5	13.0	2.15	12.0
7	300	1.5	.36	13.8	9.2	1.52	8.0
8	300	1.5	.36	23.5	15.7	2.60	20.0
9	300	1.5	.36	10.5	7.0	1.16	6.5
10	300	1.5	.36	18.4	12.3	2.04	14.5
11	350	1.5	.36	10.1	6.7	1.11	5.7
12	350	1.5	.36	15.7	10.4	1.75	11.0
13	350	1.5	.36	22.5	15.0	2.48	19.5
14	350	1.5	.36	13.8	9.2	1.52	8.5

Figure 23. Dispersion band thickness versus specific settler flow of dispersed phase (effect of impellor speed), HSLIX64N-copper phase system, aqueous continuous operation, 24°C.

Test no.	Impellor speed (rpm)	O/A ratio	Settler area (m**2)	Organic flow (l/min)	Aqueous flow (l/min)	Qd/A (m**3/m**2/hr)	ΔH (cm)
1	250	0.67	.22	4.4	6.6	1.19	3.0
2	250	0.67	.22	7.6	11.3	2.07	7.5
3	250	0.67	.22	10.5	15.7	2.86	12.0
4	250	0.67	.22	14.7	22.1	4.01	26.0
5	300	0.67	.22	4.9	7.3	1.33	1.3
6	300	0.67	.22	6.0	9.0	1.64	3.5
7	300	0.67	.22	8.0	11.9	2.18	6.3
8	300	0.67	.22	10.1	15.1	2.75	12.5
9	300	0.67	.22	11.5	17.2	3.14	16.0
10	300	0.67	.22	13.3	19.8	3.64	25.0
11	300	0.67	.22	14.7	22.1	4.01	32.5
12	350	0.67	.22	6.2	9.3	1.70	4.3
13	350	0.67	.22	8.2	12.2	2.23	7.5
14	350	0.67	.22	11.0	16.4	3.00	15.0
15	350	0.67	.22	14.7	22.1	4.01	24.5

Figure 24. Dispersion band thickness versus specific settler flow of dispersed phase (effect of impellor speed), Key Lake phase system, organic continuous operation, 35°C.

Test no.	Impellor speed (rpm)	O/A ratio	Settler area (m**2)	Organic flow (l/min)	Aqueous flow (l/min)	Qd/A (m**3/m**2/hr)	ΔH (cm)
1	250	1.5	.22	12.8	8.5	2.32	11.
2	250	1.5	.22	12.0	8.0	2.18	10.
3	250	1.5	.22	7.0	4.7	1.28	3.3
4	250	1.5	.22	15.1	10.1	2.80	21.
5	300	1.5	.22	12.0	8.0	2.18	11.
6	300	1.5	.22	7.9	5.3	1.45	3.7
7	300	1.5	.22	9.1	6.0	1.64	6.
8	300	1.5	.22	9.1	6.0	1.64	5.5
9	300	1.5	.22	15.0	10.0	2.73	20.
10	300	1.5	.22	7.0	4.7	1.28	3.3
11	300	1.5	.22	16.1	10.8	3.00	30.
12	350	1.5	.22	7.4	5.0	1.36	3.5
13	350	1.5	.22	15.9	9.9	2.68	19.5
14	350	1.5	.22	13.3	8.9	2.45	16.

Figure 25. Holdup profiles within dispersion band, HSLIX64N-copper phase system, organic continuous operation, 24°C, 300rpm.

Operating condition	Distance, h, of sampling point from coalescence front (cm)	$h/\Delta H$	Local holdup
1. Mixer holdup=0.3 H=26 cm Settler area=.36 m**2	2.5	0.1	0.75
	5.0	0.2	0.70
	7.5	0.29	0.65
	10.0	0.39	0.60
	12.5	0.49	0.58
	13.0	0.5	0.60
	15.5	0.59	0.54
	16.0	0.62	0.55
	18.0	0.69	0.40
	20.5	0.78	0.37
	23.5	0.9	0.34
	25.5	0.98	0.31
2. Mixer holdup=0.4 H=30 cm Settler area=0.22 m**2	2.5	0.08	0.77
	5.0	0.17	0.70
	5.0	0.17	0.75
	7.5	0.25	0.67
	10.0	0.33	0.62
	10.0	0.33	0.64
	12.5	0.42	0.59
	15.0	0.50	0.58
	17.5	0.58	0.56
	20.0	0.66	0.45
	22.5	0.75	0.47
	25.0	0.83	0.41
3. Mixer holdup=0.5 H=26 cm Settler area=0.36 m**2	2.5	0.10	0.82
	5.0	0.19	0.74
	7.5	0.29	0.67
	10.0	0.39	0.63
	12.5	0.48	0.60
	15.0	0.58	0.56
	17.5	0.67	0.53
	20.0	0.77	0.51
	22.5	0.87	0.50
	25.0	0.96	0.22
4. Mixer holdup=0.6 H=27 cm Settler area=0.22 m**2	2.5	0.09	0.81
	4.0	0.15	0.77
	5.0	0.19	0.72
	7.5	0.27	0.65
	9.0	0.33	0.66
	10.0	0.37	0.65
	11.0	0.41	0.61
	12.5	0.46	0.59
	15.0	0.55	0.58
	17.5	0.65	0.56
	20.0	0.74	0.56
	22.5	0.83	0.58
5. Mixer holdup=0.7 H=28 cm Settler area=0.22 m**2	2.5	0.09	0.83
	5.0	0.18	0.81
	7.5	0.27	0.76
	9.0	0.33	0.69
	10.0	0.36	0.67
	11.0	0.40	0.70
	12.5	0.45	0.70
	15.0	0.54	0.71
	18.0	0.65	0.70
	20.0	0.71	0.70
	22.5	0.80	0.71
	25.0	0.89	0.66
6. Mixer holdup=0.8 H=25.5 cm Settler area=0.22 m**2	26.5	0.95	0.68
	1.0	0.04	0.92
	2.5	0.10	0.88
	5.0	0.20	0.85
	7.5	0.29	0.84
	10.0	0.39	0.83
	12.5	0.49	0.82
	15.0	0.59	0.79
	17.5	0.69	0.78
	22.5	0.88	0.76
	24.0	0.94	0.75

Figure 26. Holdup profiles within dispersion band, HSLIX64N-copper system, aqueous continuous operation, 24°C, 300rpm.

Operating condition	Distance, h, of sampling point from coalescence front (cm)	$h/\Delta H$	Local holdup
1. Mixer holdup=0.32 H=33 cm Settler area=.13 m**2	.5	0.02	0.53
	3.0	0.09	0.38
	5.5	0.17	0.37
	8.0	0.24	0.35
	10.5	0.32	0.38
	15.5	0.47	0.35
	16.0	0.49	0.35
	18.0	0.55	0.35
	20.5	0.62	0.35
	23.0	0.70	0.36
	25.5	0.77	0.35
	28.0	0.85	0.34
	30.5	0.92	0.34
	3.0	0.09	0.60
	5.5	0.16	0.50
2. Mixer holdup=0.40 H=33 cm Settler area=.22 m**2	8.0	0.24	0.43
	10.5	0.32	0.45
	13.0	0.39	0.44
	15.5	0.47	0.44
	20.5	0.62	0.44
	21.5	0.65	0.43
	23.0	0.70	0.43
	25.5	0.77	0.43
	28.0	0.85	0.44
	30.5	0.92	0.42
3. Mixer holdup=0.52 H=33 cm Settler area=.22 m**2	0.5	0.02	0.56
	3.0	0.09	0.63
	5.5	0.17	0.54
	8.0	0.24	0.57
	10.5	0.32	0.53
	13.0	0.39	0.53
	15.5	0.47	0.53
	20.5	0.62	0.53
	23.0	0.70	0.54
	25.5	0.77	0.54
	28.0	0.85	0.53
	30.5	0.92	0.52
	3.0	0.09	0.59
4. Mixer holdup=0.60 H=33 cm Settler area=.13 m**2	3.0	0.09	0.62
	5.5	0.16	0.62
	10.5	0.32	0.62
	11.0	0.34	0.61
	13.0	0.39	0.62
	15.5	0.47	0.62
	18.0	0.55	0.61
	20.5	0.62	0.61
	23.0	0.70	0.58
	25.5	0.77	0.61
	28.0	0.85	0.60
	30.5	0.92	0.59
	2.5	0.08	0.69
5. Mixer holdup=0.70 H=30 cm Settler area=.22 m**2	5.0	0.17	0.71
	7.5	0.25	0.70
	10.0	0.33	0.68
	12.5	0.42	0.68
	15.0	0.50	0.68
	18.5	0.62	0.69
	20.0	0.66	0.70
	22.5	0.75	0.68
	25.0	0.83	0.69
	25.0	0.83	0.69

Figure 27. Holdup profiles within dispersion band, Key Lake phase system, organic continuous operation, 35°C, 300rpm.

Operating condition	Distance, h, of sampling point from coalescence front (cm)	$h/\Delta H$	Local holdup
1. Mixer holdup=0.29 H=29 cm Settler area=.22 m**2	2.5	0.09	0.59
	5.0	0.17	0.51
	7.5	0.26	0.33
	10.0	0.35	0.30
	15.0	0.52	0.28
	20.0	0.69	0.28
	25.0	0.86	0.28
	27.0	0.93	0.25
2. Mixer holdup=0.41 H=30 cm Settler area=.22 m**2	2.5	0.08	0.52
	5.0	0.17	0.49
	7.5	0.25	0.41
	10.0	0.33	0.38
	12.5	0.42	0.41
	15.0	0.50	0.40
	17.5	0.58	0.39
	20.0	0.67	0.39
3. Mixer holdup=0.49 H=25 cm Settler area=.22 m**2	25.0	0.83	0.38
	2.5	0.10	0.67
	5.0	0.20	0.53
	7.5	0.30	0.51
	10.0	0.40	0.46
	12.5	0.50	0.47
	15.0	0.60	0.45
	17.5	0.70	0.42
4. Mixer holdup=0.60 H=27 cm Settler area=.22 m**2	20.0	0.80	0.43
	22.5	0.90	0.40
	2.5	0.09	0.94
	5.0	0.19	0.67
	7.5	0.28	0.60
	10.0	0.37	0.59
	12.5	0.46	0.58
	15.0	0.56	0.58
	17.5	0.65	0.58
	20.0	0.74	0.57
	22.5	0.83	0.56
	25.0	0.93	0.55

Figure 28. Change in arithmetic mean drop size of dispersion sample with time after withdrawal from mixer, Key Lake phase system, organic continuous operation, 35°C, 300rpm.

Sample no.	Operating condition	Time after withdrawal of sample (s)	No. of drops in sample	Mean drop diameter (um)		Standard deviation	
				Arith.	Vol.	Arith.	Vol.
1.	Qd=19.1 l/min O/A = 0.67	10	40	373	399	100	129
		15	33	456	512	166	190
		20	35	445	509	167	254
		30	23	618	766	325	372
2.	Qd=13.2 l/min O/A = 0.67	15	40	372	412	127	145
		20	38	410	469	165	168
		25	45	339	400	147	221
		30	37	460	559	221	305
3.	Qd=14.0 l/min O/A = 1.5	15	39	395	410	78	90
		35	35	448	467	95	102
		50	32	456	499	141	173
4.	Qd=5.0 l/min O/A = 1.5	15	35	412	423	71	71
		30	34	396	415	93	85
		40	34	487	511	110	130
		50	31	471	504	127	156
5.	Qd=5.0 l/min O/A = 3.0	15	51	284	308	92	70
		25	55	302	329	94	98
		35	57	289	310	85	66

Figure 30. Effect of O/A ratio and dispersed phase flowrate on arithmetic mean drop diameter at mixer overflow, Key Lake phase system, organic continuous operation, 35°C, 300rpm.

O/A ratio.	Qd (l/min)	No. of drops in sample	Mean drop diameter (um)		Standard deviation	
			Arith. Vol.		Arith. Vol.	
0.67	13.2	40	372	412	127	144
0.67	19.1	39	427	481	155	202
0.67	19.1	40	373	399	100	130
0.67	11.5	42	365	401	123	155
1.5	5.0	35	412	423	71	71
1.5	9.5	42	394	412	86	95
1.5	14.0	39	392	410	78	90
3.0	5.0	51	284	308	92	70
3.0	5.0	60	253	292	100	105
3.0	5.2	57	273	296	102	79

Figure 32. Effect of impellor speed on arithmetic mean drop diameter at mixer overflow, Key Lake phase system, organic continuous operation, 35°C.

Operating condition	Impellor Speed (rpm)	No. of drops in sample	Mean drop diameter (um)		Standard deviation	
			Arith. Vol.		Arith. Vol.	
1. Qd=13.2 l/min O/A = 0.67	250	32	470	540	184	213
	300	40	372	412	127	144
	350	42	351	364	99	108
2. Qd=9.5 l/min O/A = 1.5	250	40	416	435	104	140
	300	42	394	412	86	95
	350	37	331	348	79	74
3. Qd=13.6 l/min O/A = 3.0	250	46	258	287	94	84
	300	51	284	308	92	70
	300	60	253	392	100	175
	350	42	260	297	103	121

Figure 33. Drop size profile within dispersion band for O/A=0.67, Key Lake phase system, organic continuous operation, 35°C, 300rpm.

Operating conditions:

Qd/A=3.14 m³/m²/hr
 Dispersion band thickness (ΔH)=20 cm
 Area=0.22 m²
 Organic flow=7.8 l/min
 Aqueous flow=11.5 l/min

Sample location	Distance from coalescence front (cm)	$h/\Delta H$	No. of drops in sample	Mean drop diameter (um)		Standard deviation	
				Arith.	Vol.	Arith.	Vol.
1	2	.10	25	472	609	274	321
1	5	.25	36	374	448	171	230
1	11	.55	29	417	499	197	219
1	17	.85	29	371	406	120	117
2	2	.10	28	517	528	74	79
2	5	.25	26	451	469	90	101
2	11	.55	29	415	459	141	156
2	14	.70	30	422	449	148	161
2	17	.85	32	380	438	140	305

Note on sample location:

1. 1/3 distance between settler inlet and end
2. 10 cm from end of settler

Figure 34. Drop size profile within dispersion band for O/A=1.5, Key Lake phase system, organic continuous operation, 35°C, 300rpm.

Operating conditions:

$Q_d/A = 2.50 \text{ m}^3/\text{m}^2/\text{hr}$

Dispersion band thickness (ΔH) = 16 cm

Area = 0.22 m^2

Organic flow = 13.7 l/min

Aqueous flow = 9.2 l/min

Sample location	Distance from coalescence front, h (cm)	$h/\Delta H$	No. of drops in sample	Mean drop diameter (um)	Arith. Vol.	Standard deviation	Arith. Vol.
1	3.0	.20	31	485	528	144	201
1	5.5	.35	33	417	429	691	81
1	6.5	.40	47	344	419	166	221
1	6.5	.40	40	380	408	110	106
1	9.5	.60	44	354	393	123	135
1	13.0	.80	46	307	347	118	125
1	13.0	.80	43	345	367	89	96
1	14.5	.90	38	380	390	69	67
2	1.5	.10	19	641	716	231	241
2	3.0	.20	38	447	470	102	119
2	6.5	.40	34	381	447	154	291
2	10.5	.65	39	396	415	86	102
2	13.0	.80	46	313	338	94	90
2	14.5	.90	36	383	395	66	71
2	15.0	.95	45	284	291	46	44

Note on sample location:

1. 1/3 distance between settler inlet and end
2. 10 cm from end of settler

Figure 35. Drop size profile within dispersion band for O/A=3.0, Key Lake phase system, organic continuous operation, 35°C.

Operating conditions:

Qd/A= 2.40 m³/m²/hr
 Dispersion band thickness (ΔH) =23 cm
 Area=0.13 m²
 Organic flow=15.6 l/min
 Aqueous flow= 5.2 l/min

Sample location	Distance from coalescence front, h (cm)	h/ ΔH	No. of drops in sample	Mean drop diameter (um)		Standard deviation	
				Arith.	Vol.	Arith.	Vol.
1	2	.09	23	466	508	150	135
1	5	.22	45	300	321	84	78
1	10	.43	43	262	275	60	61
1	15	.65	38	325	357	105	113
1	20	.87	48	304	336	101	118
2	1	.05	28	472	541	182	253
2	5	.22	41	361	380	86	84
2	10	.43	42	280	301	80	87
2	15	.65	38	284	305	77	88
2	20	.87	41	309	342	107	104

Note on sample location:

1. 1/3 distance between settler inlet and end
2. 10 cm from end of settler

APPENDIX II - CHARACTERISTIC CURVE STATISTICAL ANALYSIS

Part 1: k and y values for the characteristic curves

Values of the empirical constants, k and y, for the characteristic curves of figures 18-24 were calculated using linear regression and are tabulated below:

Figure	Case	k	y
18	O/A=0.67	5.16	1.64
	O/A=1.5	5.17	1.47
	O/A=3.0	4.77	1.84
	all data pts.	5.01	1.62
19	O/A=0.33	1.61	2.08
	O/A=0.67	1.65	1.91
	O/A=1.5	1.95	1.81
	all data pts.	1.73	1.90
20	O/A=0.67	1.34	2.61
	O/A=1.5	1.92	2.32
	O/A=3.0	2.86	2.42
21	T=24 °C	5.17	1.47
	T=35 °C	2.54	1.63
22	all data pts.	4.68	1.45
23	all data pts.	1.29	2.21
24	all data pts.	1.64	2.48

Part 2: statistical analysis of characteristic curves

In order to determine whether the functional relationships described by two or more regression equations are the same, regression lines were compared using an analysis of covariance procedure.

A preliminary step in this procedure is testing the two (or more) lines for homogeneity of slope. The procedure is described fully elsewhere (Sokal and Rohlf, 1981) and only the results are summarized here, in the form of an anova table. An F ratio (the ratio of one mean square, MS, to another) is used to determine the probability of two variances being from the same population.

The final step is an analysis of covariance (ancova) to test for homogeneity of the intercepts of the regression lines. This step requires that the slopes of the regression lines be equal, as determined in the first step. An F ratio of the appropriate mean square values is calculated and can be used to determine whether the assumption of a single regression line for two sets of data may be accepted or must be rejected.

Comparisons (between the three characteristic curves, taken at three different O/A ratios) were made for;

1. Figure 18 - HSLIX64N-copper phase system, organic continuous.

2. Figure 19 - HSLIX64N-copper phase system, aqueous continuous.
3. Figure 20 - Key Lake phase system, organic continuous.

In this way, it could be determined whether the three characteristic curves for each figure are statistically the same (to a 99% level of confidence).

The final anova and ancova tables for the statistical analysis follow.

1. Figure 18 - HSLIX64N-copper phase system, org. continuous.

a) Comparison of $O/A=0.67$ and $O/A=1.5$.

Anova table (for comparison of slopes)

source of variation	degree of freedom df	sum of squares SS	mean square MS	F ratio
variation among regressions	1	.00536	.00536	.8134
weighted average of deviations from regression	28	.18448	.00659	

$F_{.01(1,28)}=7.64$. Since $F < F_{.01(1,28)}$ we conclude that the two characteristic curves have the same slope.

Ancova table (for comparison of intercepts)

source of variation	df	SS	MS	F
adjusted means	1	.01015	.01015	1.551
error (deviations from a common slope)	29	.18984	.00655	

$F_{.01(1,29)}=7.60$. Since $F < F_{.01(1,29)}$ we conclude that the two characteristic curves have the same intercept.

b) Comparison of $O/A=0.67$ and $O/A=3.0$.

Anova table (for comparison of slopes)

source of variation	df	SS	MS	F
variation among regressions	1	.00483	.00483	.7606
weighted average of deviations from regression	25	.15886	.00635	

$F_{.01(1,25)}=7.77$. Since $F < F_{.01(1,25)}$ we conclude that the two characteristic curves have the same slope.

Ancova table (for comparison of intercepts)

source of variation	df	SS	MS	F
adjusted means	1	.000013	.000013	0.002
error (deviations from a common slope)	26	.16369	.00630	

$F_{.01(1,26)}=7.72$. Since $F < F_{.01(1,26)}$ we conclude that the two characteristic curves have the same intercept.

c) Comparison of $O/A=1.5$ and $O/A=3.0$.

Anova table (for comparison of slopes)

source of variation	df	SS	MS	F
variation among regressions	1	.00244	.00244	6.082
weighted average of deviations from regression	25	.10024	.00401	

$F_{.01(1,25)}=7.77$. Since $F < F_{.01(1,25)}$ we conclude that the two characteristic curves have the same slope.

Ancova table (for comparison of intercepts)

source of variation	df	SS	MS	F
adjusted means	1	.00839	.00839	0.175
error (deviations from a common slope)	26	.12463	.00479	

$F_{.01(1,26)} = 7.72$. Since $F < F_{.01(1,26)}$ we conclude that the two characteristic curves have the same intercept.

2. Figure 19 - HSLIX64N-copper phase system, aq. continuous.

a) Comparison of $O/A=0.33$ and $O/A=0.67$

Anova table (for comparison of slopes)

source of variation	df	SS	MS	F
variation among regressions	1	.00656	.00656	.8482
weighted average of deviations from regression	25	.19330	.00773	

$F_{.01(1,25)} = 7.77$. Since $F < F_{.01(1,25)}$ we conclude that the two characteristic curves have the same slope.

Ancova table (for comparison of intercepts)

source of variation	df	SS	MS	F
adjusted means	1	.00286	.00286	0.372
error (deviations from a common slope)	26	.19986	.00769	

$F_{.01(1,26)} = 7.72$. Since $F < F_{.01(1,26)}$ we conclude that the two characteristic curves have the same intercept.

b) Comparison of $O/A=0.33$ and $O/A=1.5$.

Anova table (for comparison of slopes)

source of variation	df	SS	MS	F
variation among regressions	1	.01777	.01777	2.235
weighted average of deviations from regression	28	.22267	.00795	

$F_{.01(1,28)} = 7.64$. Since $F < F_{.01(1,28)}$ we conclude that the two characteristic curves have the same slope.

Ancova table (for comparison of intercepts)

source of variation	df	SS	MS	F
adjusted means	1	.00866	.00866	1.551
error (deviations from a common slope)	29	.24032	.00829	

$F_{.01(1,29)} = 7.60$. Since $F < F_{.01(1,29)}$ we conclude that the two characteristic curves have the same intercept.

c) Comparison of $O/A=0.67$ and $O/A=1.5$.

Anova table (for comparison of slopes)

source of variation	df	SS	MS	F
variation among regressions	1	.00432	.00432	.5058
weighted average of deviations from regression	35	.30045	.00858	

$F_{.01(1,35)} = 7.31$. Since $F < F_{.01(1,35)}$ we conclude that the two characteristic curves have the same slope.

Ancova table (for comparison of intercepts)

source of variation	df	SS	MS	F
adjusted means	1	.01624	.01624	1.918
error (deviations from a common slope)	36	.30479	.00847	

$F_{.01(1,36)} = 7.31$. Since $F < F_{.01(1,36)}$ we conclude that the two characteristic curves have the same intercept.

3. Figure 20 - Key Lake phase system, org. continuous.a) Comparison of $O/A=0.67$ and $O/A=1.5$.

Anova table (for comparison of slopes)

source of variation	df	SS	MS	F
variation among regressions	1	.00995	.00995	3.478
weighted average of deviations from regression	27	.07725	.00286	

$F_{.01(1,27)} = 7.68$. Since $F < F_{.01(1,27)}$ we conclude that the two characteristic curves have the same slope.

Ancova table (for comparison of intercepts)

source of variation	df	SS	MS	F
adjusted means	1	.01976	.01976	6.346
error (deviations from a common slope)	28	.08720	.00311	

$F_{.01(1,28)} = 7.64$. Since $F < F_{.01(1,28)}$ we conclude that the two characteristic curves have the same intercept.

b) Comparison of $O/A=0.67$ and $O/A=3.0$.

Anova table (for comparison of slopes)

source of variation	df	SS	MS	F
variation among regressions	1	.00449	.00449	1.604
weighted average of deviations from regression	24	.06721	.00280	

$F_{.01(1,24)} = 7.82$. Since $F < F_{.01(1,24)}$ we conclude that the two characteristic curves have the same slope.

Ancova table (for comparison of intercepts)

source of variation	df	SS	MS	F
adjusted means	1	.37302	.37302	130.6
error (deviations from a common slope)	25	.07140	.00286	

$F_{.01(1,25)} = 7.77$. Since $F > F_{.01(1,25)}$ we conclude that the two characteristic curves have different intercepts.

c) Comparison of $O/A=1.5$ and $O/A=3.0$.

Anova table (for comparison of slopes)

source of variation	df	SS	MS	F
variation among regressions	1	.00227	.00227	.9154
weighted average of deviations from regression	30	.07446	.00248	

$F_{.01(1,30)} = 7.56$. Since $F < F_{.01(1,30)}$ we conclude that the two characteristic curves have the same slope.

Ancova table (for comparison of intercepts)

source of variation	df	SS	MS	F
adjusted means	1	.29535	.29535	116.7
error (deviations from a common slope)	28	.07071	.00253	

$F_{.01(1,28)} = 7.64$. Since $F > F_{.01(1,28)}$ we conclude that the two characteristic curves have different intercepts.

Conclusions of statistical analysis.

The statistical analysis shows that for figures 18 and 19 the characteristic curves for the three O/A ratios are the same. However, for figure 20, although data for $O/A=0.67$ and $O/A=1.5$ could be fitted with a single characteristic curve, a separate characteristic curve existed for $O/A=3.0$.

APPENDIX III - ERROR ANALYSIS; GENERAL COMMENTS

The accuracy with which ΔH was measured depended on several factors. When the dispersion feed was dilute, the settling front was not as sharp as when a concentrated dispersion was used. In addition, there was some cycling of the dispersion band thickness with time, especially with thicker dispersion bands. Because of these factors, the error in a ΔH measurement was estimated to vary from a few millimeters (concentrated dispersions with thin dispersion bands) to roughly 2 cm (dilute dispersions with thick dispersion bands).

An additional error source was in determining the flowrate of the phases, since some fluctuations in flowrate occurred and because inaccuracies in reading the rotameters would be expected.

When a particular run was repeated several hours after it had initially been performed, the values of ΔH recorded typically agreed within 5 to 10%.